Jury

Chair	Prof. Dr Maries Van Bael Universiteit Hasselt
Promoter	Prof. Dr Wanda Guedens Universiteit Hasselt
Co-promoter	Prof. Dr Peter Adriaensens Universiteit Hasselt
PhD committee	Prof. Dr Jean-Paul Noben Universiteit Hasselt Prof. Dr Wouter Maes Universiteit Hasselt
Members of the jury	Prof. Dr Dirk Vanderzande Universiteit Hasselt Prof. Dr Serge Muyldermans Vrije Universiteit Brussel Prof. Dr Xaveer Van Ostade Universiteit Antwerpen

“Knowledge is power, but enthusiasm pulls the switch”

Ivern Ball

Table of Contents

Table of Contents i

List of Tables vii

List of Figures xi

List of Abbreviations xvii

Chapter 1: General introduction 1

1.1 Strategies for protein immobilization 4

1.1.1 Non-oriented, non-covalent protein coupling 4

1.1.2 Non-oriented, covalent protein coupling............................. 5

1.1.3 Oriented, non-covalent protein coupling 8

1.1.4 Oriented, covalent protein coupling................................. 10

1.2 Protein engineering techniques for site-specific protein modification 15

1.3 Nanobodies.. 21

1.3.1 Molecular description of a nanobody 21

1.3.2 Applications of nanobodies 22

1.3.3 Nanobody BcII10 23

1.4 Research aims... 24

1.5 Thesis outline... 25

1.6 References 26

Chapter 2: The clickability of site-specifically functionalized maltose binding protein 35

2.1 Introduction 37

2.2 Experimental section 38

2.2.1 Synthesis of a bifunctional linker for EPL.......................... 38

2.2.2 Site-specific alkynation of MBP using EPL 38

2.2.3 Random alkynation of MBP using an EDC/NHS coupling...... 40

2.2.4 Silanization and subsequent carboxylation of silicon substrates 42

2.2.5 CuAAC reaction of alkynated MBP with azide-functionalized biotin 42

2.2.6 Western blotting after MBP biotinylation 42

2.2.7 Covalent CuAAC mediated immobilization of MBP to a silicon substrate via the DIP method 43

2.2.8 Covalent CuAAC mediated immobilization of MBP to a silicon substrate via the DROP method.. 43

2.3 Results & discussion 45

2.3.1 Synthesis of the bifunctional linker 45

2.3.2 Site-specific alkynation of MBP and covalent coupling to azide-functionalized biotin 46

2.3.3 Covalent coupling of MBP to azide functionalized silicon substrates 50

2.4 Conclusions 55

2.5 References 56

Chapter 3: Site-specific protein alkynation by expressed protein ligation using alternative nucleophiles 59

3.1 Introduction... 61

3.2 Experimental section 64

3.2.1 Synthesis of the bifunctional linkers 64

3.2.2 The expression of the MBP-intein-CBD complex 64

3.2.3 Standard protocol for the alkyne functionalization of MBP using EPL 64

3.2.4 Optimization of the pH for alkyne functionalization of MBP using EPL 66

3.2.5 Optimization of the incubation conditions for alkyne functionalization of MBP using EPL 67

3.2.6 The expression of the NbBcII10-intein-CBD complex.......... 67

3.2.7 Functionalization of NbBcII10 using EPL.......................... 67

3.2.8 Click reaction in solution between modified MBP and azide functionalized biotin 68

3.2.9 Western blotting after MBP biotinylation 68

3.2.10 Covalent CuAAC mediated immobilization of MBP to a silicon substrate 68

3.3 Results & discussion 70

3.3.1 Synthesis of the bifunctional linker 70

3.3.2 The effect of MESNA on the EPL process 71

3.3.3 Western blotting after MBP biotinylation 72

3.3.4 Optimization of the reaction conditions for alkyne functionalization of MBP using EPL 74

3.3.5 Functionalization of NbBcII10 using amine-based EPL 81

3.4 Conclusions 84

3.5 References 85

Chapter 4: Cytoplasmic versus periplasmic expression of site-specifically and bioorthogonally functionalized nanobodies using expressed protein ligation 87

4.1 Introduction 90

4.2 Materials and Methods 93

4.2.1 Materials 93

4.2.2 Molecular cloning 93

4.2.3 Expression and extraction of the Nb-intein-CBD fusion protein. 95

4.2.4 Synthesis of the 2-amino-3-mercapto-*N*-(prop-2-yn-1-yl)propanamide bifunctional linker 96

4.2.5 Site-specific alkynation of NbBcII10 by expressed protein ligation 97

4.2.6 SDS-PAGE and electrospray ionization mass spectrometry .. 97

4.2.7 Clickability of NbBcII10-LEY-alkyne using western blot 98

4.2.8 Enzyme-linked immunosorbent assay 98

4.2.9 Surface plasmon resonance analysis 99

4.3 Results and discussion 100

4.3.1 Periplasmic expression 100

4.3.2 Cytoplasmic expression 102

4.3.3 Expressed protein ligation 103

4.3.4 Functionality test of NbBcII10-LEY-alkyne 106

4.4 Conclusions 109

4.5 References 110

Chapter 5: Experimental details 115

5.1 Introduction ... 117
5.2 Random versus site-specific protein functionalization ... 118
5.2.1 Random protein functionalization via an EDC/NHS coupling reaction ... 118
5.2.2 Site-specific protein functionalization via expressed protein ligation ... 119
5.2.3 Native nanobody expression ... 129
5.3 Molecular cloning techniques ... 131
5.3.1 Two-step polymerase chain reaction ... 131
5.3.2 Vector preparation ... 133
5.3.3 Transformation and selection ... 134
5.3.4 Restriction analysis and sequencing ... 135
5.4 Protein characterization techniques ... 136
5.4.1 Western blotting ... 136
5.4.2 Enzyme-Linked Immuno-Sorbent Assay (ELISA) ... 138
5.4.3 Mass spectrometry ... 140
5.4.4 Ellipsometry ... 141
5.4.5 Surface Plasmon Resonance (SPR) ... 143
5.5 References ... 145
Chapter 6: General discussion, conclusions and future perspectives ... 149
6.1 Site-specific functionalization of MBP for covalent and oriented coupling to an azide-functionalized surface ... 151
6.2 The site-specific functionalization of MBP using alternative nucleophiles in the EPL process ... 153
6.3 Cytoplasmic versus periplasmic extraction of site-specifically and bio-orthogonally functionalized nanobodies using expressed protein ligation ... 154
6.4 Future perspectives ... 156
Summary ... 157
Samenvatting ... 161
Publication list & conference contributions ... 165
Dankwoord ... 169

List of Tables

Table 3.1:	pKa values of the conjugate acids from amine-based nucleophiles.	62
Table 3.2:	An overview of the different cleavage buffers (CB) used for EPL.	66
Table 3.3:	Yield of the different functionalization experiments of MBP.	72
Table 4.1:	Overview of the DNA sequences of the different leader sequences used for the periplasmic expression of NbBcII10.	93
Table 4.2:	Overview of the different forward primers used for the attachment of different leader sequences to NbBcII10.	94
Table 4.3:	Affinity constants of the binding between NbBcII10 variants and BcII.	108
Table 5.1:	Gradient for HPCL chomatograpy used for the ESI-MS experiments.	140

List of Figures

Figure 1.1: The four different categories of protein coupling on a solid surface. 4
Figure 1.2: Protein immobilization via the ε-amine group of lysine and a NHS modified substrate. 5
Figure 1.3: Activation of a carboxylic acid using EDC/NHS to facilitate the coupling of a protein using its endogenous amines. 6
Figure 1.4: Immobilization via a free thiol group of the protein and a maleimide functionalized substrate. 7
Figure 1.5: Immobilization via a free thiol group of the protein and a vinyl-sulfon functionalized surface. 7
Figure 1.6: Immobilization via a free thiol group of the protein by thiol-disulfide exchange. 8
Figure 1.7: Immobilization of a protein using its carboxyl side chains. 8
Figure 1.8: Copper(I)-catalyzed alkyne-azide cycloaddition (CuAAC). 11
Figure 1.9: Strain-promoted alkyne-azide cycloaddition (SPAAC). 12
Figure 1.10: Staudinger ligation 12
Figure 1.11: Diels-Alder cycloaddition 13
Figure 1.12: Strain-promoted inverse electron-demand Diels–Alder cycloaddition (SPIEDAC) 13
Figure 1.13: Thiol-ene reaction. 14
Figure 1.14: Oxime ligation. 14
Figure 1.15: The general principle of expressed protein ligation (EPL) 16
Figure 1.16: The sortase A (SrtA) mechanism. 17
Figure 1.17: Self- labeling protein tags mechanism. 18
Figure 1.18: Amber suppression 20
Figure 1.19: Schematic representation of a conventional antibody, a heavy chain only antibody and a nanobody. 21
Figure 1.20: Schematic representation of the sequence organization and folded structure of the VH of a conventional Ab and a VHH. 22
Figure 2.1: The chemical structure of the bifunctional linker 2-amino-3-mercapto-N-(prop-2-yn-1-yl)propanamide 38
Figure 2.2: Site-specific alkynation of MBP using EPL 39
Figure 2.3: The chemical structure of the alkyne NHS ester 2,5-dioxopyrrolidin-1-yl-hex-5-ynoate 40

Figure 2.4:	Biofunctionalization of silicon surfaces with ssA-MBP and rA-MBP/fA-MBP	41
Figure 2.5:	Chemical structure of the azide-functionalized biotin	42
Figure 2.6:	DIP versus DROP method	44
Figure 2.7:	^{13}C NMR spectrum of 2-amino-3-mercapto-N-(prop-2-yn-1-yl)propanamide.	45
Figure 2.8:	Western blotting results for ssA-MBP	47
Figure 2.9:	Electrospray ionization mass spectrometry spectrum of ssA-MBP.	48
Figure 2.10:	Electrospray ionization mass spectrometry spectra of rA-MBP and fA-MBP	49
Figure 2.11:	Real-time surface mass evolution monitored by *in situ* ellipsometry after the CuAAC click reaction between ssA-MBP and an azide functionalized silicon surface.	50
Figure 2.12:	Real time *in situ* monitoring of the surface mass increase during the CuAAC reaction between different variants of alkynated MBP and azide functionalized silicon surfaces	52
Figure 2.13:	The average surface mass increase after a click reaction between different alkynated MBP variants and a silicon surface, measured using ellipsometry.	52
Figure 2.14:	The net surface mass increase after the CuAAC click reaction between ssA-MBP and an azide-functionalized silicon surface using different concentrations of copper and corresponding concentrations of sodium ascorbate and THPTA ([click mix]).	53
Figure 3.1:	Possible side reactions caused by an additional thiol group	61
Figure 3.2:	The chemical structure of α-hydrazine acetyl and alkyl hydrazine functionalities.	63
Figure 3.3:	The chemical structure of the thiol-based bifunctional linker 2-amino-3-mercapto-N-(prop-2-yn-1-yl)propanamide and the amine-based bifunctional linker 2-hydrazinyl-N-(prop-2-yn-1-yl)acetamide.	64
Figure 3.4:	Expressed protein ligation	65
Figure 3.5:	^{13}C NMR spectrum of 2-hydrazinyl-N-(prop-2-yn-1-yl)acetamide.	70

Figure 3.6: Role of MESNA in EPL 71
Figure 3.7: Click reaction of MBP and an azide-functionalized biotin 72
Figure 3.8: Western blot analysis of the click reaction between alkynated MBP and an azide-functionalized biotin 73
Figure 3.9: The effect of pH on hydrolysis of MBP from the chitin column. 74
Figure 3.10: The effect of pH on the nucleophilicity of the bifunctional linker. 75
Figure 3.11: The effect of temperature and incubation time on the thioester bond hydrolysis of MBP cleavage after incubation with RB. 76
Figure 3.12: The effect of temperature and incubation time on the nucleophilic reaction of the amine-based bifunctional linker. 77
Figure 3.13: SDS page and western blot of the results of the CuAAC reaction between azide functionalized biotin and MBP-alkyne modified via EPL using the amine-based bifunctional linker 77
Figure 3.14: ESI-MS of modified MBP 79
Figure 3.15: Ellipsometry of ssA*-MBP 81
Figure 3.16: ESI spectra of modified NbBII10 82
Figure 4.1: Three periplasmic secretion pathways for proteins in E. coli. 91
Figure 4.2: SDS-page profile of the unpurified periplasmic extract after expression 101
Figure 4.3: Scheme of the expressed protein ligation strategy. 103
Figure 4.4: SDS-page profile of the EPL process. 104
Figure 4.5: ESI-MS spectrum of C-terminally, mono-alkynated NbBcII10-LEY. 105
Figure 4.6: Western blot of the click-reaction product between NbBcII10-LEY-alkyne and a biotin-azide derivate. 106
Figure 4.7: (Competitive) ELISA results of the NbBcII10 – BcII antigen binding 107
Figure 4.8: SPR sensorgrams of the BcII antigen binding study of NbBcII10-His$_6$, NbBcII10-LEY-alkyne and NbBcII10-HLC. 109
Figure 5.1: The ECS/NHS mechanism of the reaction between the ε-amine of a lysine side chain and 2,5-dioxopyrrolidin-1-yl-hex-5-ynoate. 118
Figure 5.2: Overview of the different vector constructs used for EPL. 120

Figure 5.3: Schematic overview of the components of the pTXB1 vector. 121
Figure 5.4: Schematic overview of the components of the pMXB10 vector. 122
Figure 5.5: Induction of protein expression in BL21(DE3) and Lemo21(DE3) *E. coli* cells. 124
Figure 5.6: Cytoplasmic (a) versus periplasmic (b) extraction of proteins. 126
Figure 5.7: Synthetic pathway of 2-amino-3-mercapto-N-(prop-2-yn-1-yl)propanamide 128
Figure 5.8: Synthetic pathway of 2-hydrazinyl-N-(prop-2-yn-1-yl)acetamide 129
Figure 5.9: Overview of the different vectors used for native NbBcII10 expression in this thesis. 130
Figure 5.10: Polymerase chain reaction. 131
Figure 5.11: Attachment of the leader sequence to NbBcII10 using two-step PCRs 132
Figure 5.12: Restriction sites *NdeI* and *LguI* (*SapI*). 133
Figure 5.13: Schematic representation of the digestion and ligation process. 134
Figure 5.14: Western blotting: protein transfer from the gel to the PVDF membran. 136
Figure 5.15: Colorimetric protein detection using western blotting. 137
Figure 5.16: Western blotting using biotin. 138
Figure 5.17: Schematic representation of the ellipsometry principle 139
Figure 5.18: Schematic representation of the ellipsometer as used in this thesis. 141
Figure 5.19: Schematic representation of the direct ELISA, indirect ELISA and competition ELISA concept. 142
Figure 5.20: The principle of surface plasmon resonance 143

List of Abbreviations

AAP	3-azido-1-aminopropane
Abs	antibodies
AP	alkaline phosphatase
BCIP/NTB	bromo-4-chloro-3-indolyl-phosphate/nitro blue tetrazolium
B-PER	bacterial protein extraction reagent
BSA	bovine serum albumin
CB	cleavage buffer
CBD	chitin binding domain
CDI	carbodiimide
CDR	complementary determing regions
CH	heavy chain constant domain
CL	light chain constant domain
CuAAC	copper(I)-catalyzed alkyne-azide cycloaddition
DCC	*N,N'*-dicyclohexyl carbodiimide
DCM	dichloromethane
DNA	deoxyribonucleic acid
DNAse	deoxyribonuclease
dNTP	deoxyribonucleoside triphosphates
dsDNA	double-stranded deoxyribonucleic acid
DTT	dithiothreitol
E. coli	Escherichia coli
EDC	*N*-(3-dimethylaminopropyl)-*N′*-ethylcarbodiimide hydrochloride
EDTA	ethylenediaminetetraacetic acid
ELISA	enzyme-linked immunosorbent assays
EPL	expressed protein ligation
fA-MBP	fully alkynated maltose binding protein
HCAb	heavy chain only antibody
H-chain	heavy chain
HEPES	4-(2-hydroxyethyl)-1-piperazineethanesulfonic acid
His_6	hexahistidine
IMAC	immobilized metal ion affinity chromatography
IPTG	isopropyl β-D-1-thiogalactopyranoside
LB	luria broth
L-chain	light chain
LH	light chain variable domain
MBP	maltose binding protein

MESNA	sodium 2-sulfanylethanesulfonate
Nb	nanobody
NbBCII10	nanobody against the BCII10 antigen
NHS	*N*-hydroxysuccinimide
NMR	nuclear magnetic resonance
OD	optical density
PBS	phosphate buffered saline
PCR	polymerase chain reaction
pI	isoelectric point
POI	protein of interest
pvdf	polyvinylidene fluoride
rA-MBP	random alkynated maltose binding protein
RB	running buffer
rpm	revolutions per minute
SAM	self-assembled monolayers
SdAb	single domain antibody
SDS	sodium dodecyl sulfate
SDS-PAGE	sodium dodecyl sulfate-polyacrylamide gel electrophoresis
SPR	surface plasmon resonance
ssA*-MBP	site-specific alkynated maltose binding protein using CB7
ssA-MBP	site-specific alkynated maltose binding protein
ssDNA	single-stranded deoxyribonucleic acid
TBST	tris buffered saline tween
TBTA	tris(benzyltriazolylmethyl)amine
TCEP	tris(2-carboxyethyl)phosphine
TES	Tris-EDTA-Sucrose
TFA	trifluoroacetic acid
THPTA	tris(3-hydroxypropyltriazolylmethyl)amine
TMS-EDTA	*N*-(trimethoxysilylpropyl)-ethylenediaminetriacetate trisodium salt
UV-Vis	Ultraviolet–visible
VH	heavy chain variable domain
VHH	variable domain of heavy chain of HCAb

Chapter 1

General introduction

In modern health care and biotechnology, the need for innovative bioactive materials is continuously increasing. These materials are of great use for *in vivo* applications such as controlled drug delivery (1, 2), contrast labels for imaging (3, 4) and surface modification of implants (5, 6), as well as for *ex vivo* diagnostic applications, e.g. biosensors (7-10). In these kinds of bioactive materials, surface functionalization plays an important role (11). This thesis focuses on biosensing applications but the used principles can easily be applied for other advanced biomedical applications.

The controlled immobilization of proteins on solid surfaces is a critical step in the development and miniaturization of biosensing systems. In order to be able to respond to the demand of high reproducibility, sensitivity and selectivity, a covalent and oriented coupling of proteins to the biosensing surfaces is necessary. As discussed later in this chapter, the currently used immobilization strategies allow either an oriented or a covalent coupling, but not the combination of both.

Therefore, this thesis focuses on the site-specific modification of proteins using expressed protein ligation for the incorporation of a bioorthogonal functionality (i.e. not present in biological systems) that can be used as a unique handle to couple covalently these proteins to complementary functionalized surfaces in an oriented manner. This way, the active site of the protein is always available which increases the recognition sensitivity and selectivity and is in particularly interesting for early diagnostic applications.

In addition, biosensing surfaces are mostly coated with monoclonal antibodies. These antibodies display several disadvantages, such as their bulky size and complex architecture (12). For this reason, the use of nanobodies (Nbs) is investigated in this thesis.

1.1 Strategies for protein immobilization

Over the years, many possible strategies for protein coupling were developed. Some of these strategies are based on covalent couplings, other on non-covalent couplings. Depending on the used strategy, the proteins are coupled in an oriented or non-oriented way on the surface. This results in four different categories, as represented in Figure 1.1.

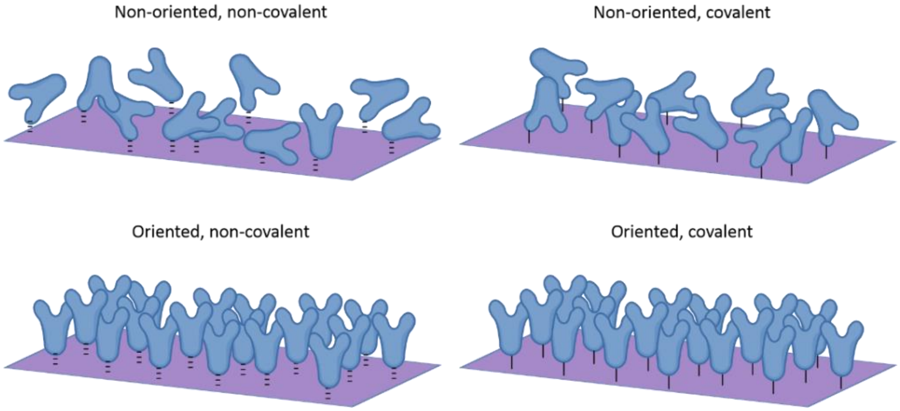

Figure 1.1: The four different categories of protein coupling on a solid surface.

1.1.1 Non-oriented, non-covalent protein coupling

Most standard procedures for the immobilization of proteins are based on non-covalent and non-specific adsorption. The most inexpensive and straightforward method is physical adsorption (physisorption) (13, 14). This method makes use of the weak interactions between the protein and the surface, e.g. van der Waals interactions, hydrophobic interaction, hydrogen bonds and electrostatic interactions (11, 13). The coupling can be done by simply submerging the substrate into a protein solution and incubating it for some time to let adsorption occur. Afterwards, the surface is rinsed to remove all unbound proteins (15). The biggest advantages of this technique are the simplicity and the possibility to reuse surfaces by simply breaking the weak interactions between the protein and the surface (16). One of the biggest disadvantages, on the other hand, is that the bonds are non-covalent, meaning that the adsorbed proteins tend to detach from the surface (15, 17), which makes this technique not suitable for the development of long-life biosensors. Another disadvantage is the disordered orientation of the proteins on the surface, which leads to several drawbacks such as conformational changes (that influence the protein activity) and a reduced accessibility of the functional site of the protein. The conformational changes are not only dependent on the protein properties (e.g. size, stability, surface charge, etc.), but also on surface properties like the type of surface, hydrophobicity, etc.. In addition, coupling conditions such as pH, temperature and buffer solutions also play a role in conformational changes (18).

Despite these disadvantages, physical adsorption is still a commonly used technique for protein immobilization on polystyrene microplate surfaces in enzyme-linked immunosorbent assays (ELISA) and in more sophisticated applications like protein couplings on polymer surfaces for surface plasmon resonance (SPR) (19), as described in Chapter 2.

1.1.2 Non-oriented, covalent protein coupling

To avoid that the immobilized protein leaches from the surface, an alternative is necessary for the commonly used physical adsorption like for instance a covalent coupling between mutually reactive chemical groups, one on the surface and one on the protein. To protect the protein from denaturation, not every chemical reaction is possible. The reaction has to be achievable in physiological conditions, in aqueous buffer and at neutral pH. Most covalent couplings are performed using the endogenous functional groups from the amino acid side chains of the protein. The most commonly used endogenous groups are amines, thiols and carboxylic acids (17, 20, 21). Amines and thiols are both good nucleophiles that can react with complementary groups on the surface. Carboxylic acids on the other hand can be activated to make them reactive towards nucleophiles on the surface. Important to note is that this kind of chemical reactions is of course not only applicable for surface functionalization but also for the coupling of probes and tags to proteins (22).

Amine chemistry. The ε-amine group of lysine is the most used side chain for the covalent attachment of proteins to a surface. Lysines are present in most proteins and frequently located on the outside of the protein (23, 24), which makes them reachable for coupling reactions.

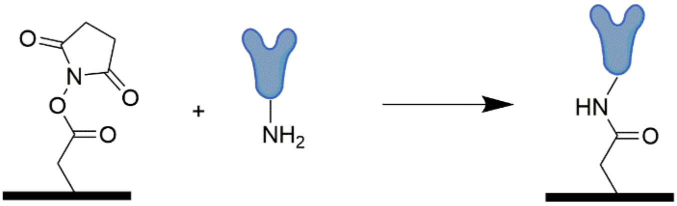

Figure 1.2: Protein immobilization via the ε-amine group of lysine and a NHS modified substrate.

Moreover, lysines are very reactive towards electrophiles without any additional activation and generate a stable bond (24). N-hydroxysuccinimide (NHS) esters are commonly used agents to react with the amine groups of the lysines in proteins, resulting in a stable peptide bond (Figure 1.2)(25).

NHS is also often used as a activating reagent for carboxylic acids in combination with 1-ethyl-3-(3-dimethylaminopropyl)carbodiimide (EDC). Activated esters react with amines to form amides (26, 27) as shown in Figure 1.3.

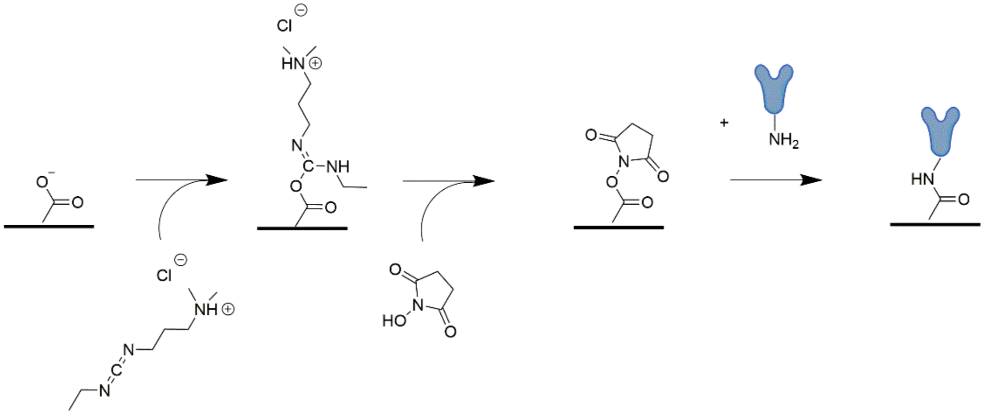

Figure 1.3: Activation of a carboxylic acid using EDC/NHS to facilitate the coupling of a protein using its endogenous amines.

Important to note in this reaction is the fact that EDC esters are rather unstable in aqueous solutions, resulting in the deactivation of the ester before the introduction of the protein (27).

Thiol chemistry. Besides amines, thiol groups are interesting for protein coupling to surfaces. Thiol groups are very nucleophilic, especially at a pH below 9 (pK_a cysteines ~ 8), when the amine groups of lysine are protonated (pK_a ~ 10.5). Free cysteine groups are quite rare in natural proteins because they mostly appear as oxidized disulfide bridges. This makes free cysteine groups interesting for immobilization on a surface because the orientation is less random and it is easy to predict which cysteine(s) will react. This results in a less random orientation (28). When there are no free cysteines available in the protein, an extra cysteine group can be inserted at a specific location in the protein by site-directed mutagenesis. Nevertheless, the introduction of an additional free cysteine group gives rise to several side reactions, as discussed in Chapter 4.

Thiol groups are most commonly coupled to maleimide functionalities because this reaction is highly specific and efficient (Figure 1.4). The disadvantage of this coupling is that the protein must be maintained in a reduced form to prevent the formation of disulfide bridges, which will inactivate the cysteines. Therefore, reducing agents such as dithiothreitol (DTT) and Tris(2-carboxyethyl)phosphine (TCEP) are used. However, for the actual reaction, these reducing agents must be removed to avoid competition between the thiol group of the reducing agent and the thiol group of the protein. To avoid reoxidation of the protein's thiol groups, the reaction must be performed directly after the removal of the reducing agents (22).

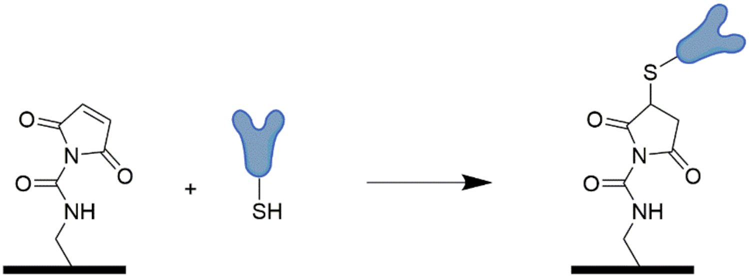

Figure 1.4: Immobilization via a free thiol group of the protein and a maleimide functionalized substrate.

An alternative reaction that can be used to couple a protein using its free thiol group is a reaction with a vinyl-sulfone group (Figure 1.5). This reaction forms a thioether bond and can be performed under mild conditions in aqueous solutions (29) because the vinyl-sulfone groups are stable in water at neutral pH. The disadvantage is that at higher pH, they have the tendency to react with amines and alcohols (30).

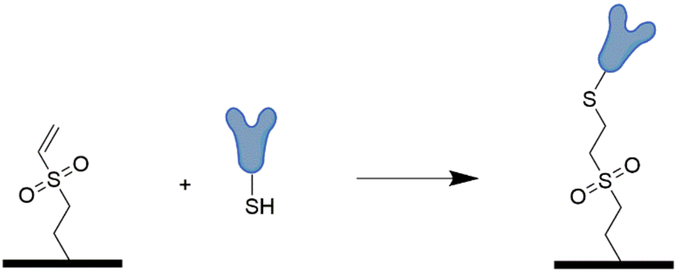

Figure 1.5: Immobilization via a free thiol group of the protein and a vinyl-sulfon functionalized surface.

Because thiol groups tend to form disulfide bridges under oxidative conditions, this property can be used to form a covalent attachment to a substrate functionalized with disulfide probes via a thiol-disulfide exchange Figure 1.6. This reaction is very selective, but the coupling is not resistant to reducing agents such as mercaptoethanol or DTT, which is a major drawback (28, 30).

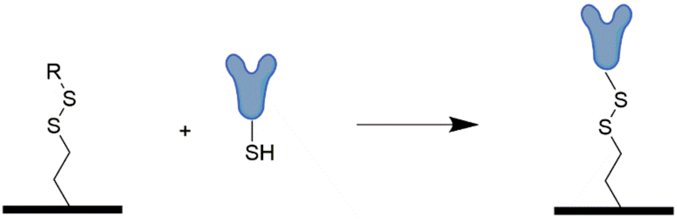

Figure 1.6: Immobilization via a free thiol group of the protein by thiol-disulfide exchange.

Carboxyl chemistry. Protein immobilization using carboxyl chemistry is a very interesting approach because glutamic and aspartic acid constitute a large fraction of the surface exposed amino acids (11). These amino acids can react, together with the C-terminus of the protein, with an amine function to form a peptide bond. The coupling reactions require activation by a carbodiimide (CDI) like EDC or *N,N′*-dicyclohexylcarbodiimide (DCC), as shown in Figure 1.7.

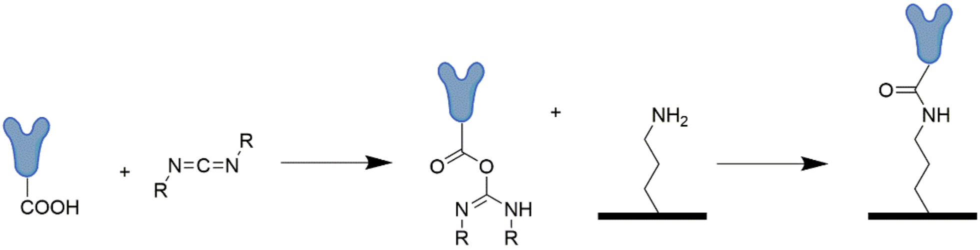

Figure 1.7: Immobilization of a protein using its carboxylic acid side chains. In a first step, the carboxyl group is activated using a carbodiimide. In a second step, a peptide bond is formed between the protein and the amine functionalized surface.

1.1.3 Oriented, non-covalent protein coupling

By using only the endogenous groups of a protein, it is very difficult to have a controlled protein immobilization. This caused an increasing attention to the development of strategies to produce homogeneous and reproducible substrates that can be functionalized with proteins in a controlled way. The easiest way to accomplish this is making use of the affinity between biomolecules. These non-covalent interactions already occur in nature and are very selective. This makes them very useful to control protein alignment on a substrate by site-specifically introducing the selective biological tag into the protein and immobilizing the respective counterpart on the surface. The disadvantage of this technique is that the coupling is not covalent so therefore not stable. The most popular affinity interactions for protein immobilization are polyhistidine, peptide epitope tags, biotin-streptavidin interactions or DNA mediated interactions.

Polyhistidine tag. The most commonly used affinity tag for protein modification is the polyhistidine tag, also known as the His_6 tag. This method is based on the affinity of histidine with divalent metal ions such as Ni^{2+} (or Cu^{2+}, Zn^{2+}) and was originally used for immobilized metal ion affinity chromatography (IMAC) but can also be useful for the immobilization of proteins on a Ni^{2+} coated surface (31, 32). In this approach, a His_6 tag is recombinantly added to the protein, in most cases at the C- or N-terminus of the protein but it has been reported to work on other accessible locations in proteins as well (33). By incubating the protein on a metal treaded substrate, the His_6 tag will interact with the surface and form a site-specific binding with the protein. The interaction is easily reversible by adding competitive ligands such as imidazole or histidine, metal chelators like ethylenediaminetetraacetic acid (EDTA) or by changing the pH (34). This property is very useful when reusability of the surface is important but is a big disadvantage in terms of stability.

Peptide epitope tags. An epitope is the part of the antigen that is recognized by an antibody (35). Epitopes can be any kind of molecule, but most of them are short peptides. By using recombinant techniques, the genetic sequence of these peptides can be fused to the gene coding for the protein of interest (POI). To successfully use peptide epitopes for protein coupling, a few requirements must be met. First of all, the added maker may not interfere with the native protein folding. Secondly, the peptide epitope needs to be water soluble and exposed to the surface of the protein. Finally, the peptide epitope should be suitable for a mild affinity procedure (36). Similar to His_6 tags, these peptides can be introduced in any available place in the protein, but mostly at the C- or N-terminus. Theoretically, the possibilities are limitless, but there are a few commonly used epitopes.

A *FLAG-tag* (Asp-Tyr-Lys-Asp-Asp-Asp-Asp-Lys) is a highly charged, and therefore highly soluble, octapeptide (37). The used vectors and antibodies are widely spread and commercially available (38). Tyr was placed in position 2, flanked by charged amino acids, because aromatic amino acids are the major factor in antigen-antibody interactions, especially in polar environments. The hexapeptide Lys-Asp-Asp-Asp-Asp-Lys increases the hydrophilicity (36). Due to this hydrophilic character, the FLAG-tag is most likely located on the surface of the tagged protein, which is ideal for oriented immobilization. The *Myc-tag* (Gly-Gln-Lys-Leu-Ile-Ser-Glu-Glu-Asp-Leu-Asn) is an 11 amino acid peptide with an affinity to the anti-c-myc antibody (39). The sequence can be recombinantly coupled to the C-or N-terminus of the POI without loss of affinity towards the antibody (40). Besides its use in protein purification, immunochemical reagents and protein detection (31, 40), the tag has also been used for protein immobilization (41).

Biotin-streptavidin interaction. Another high affinity interaction used for protein immobilization is the biotin-streptavidin interaction. Here, a biotinylated protein is bound to a (strept)avidin coated surface. Because of the low dissociation constant of the interaction (10^{-15} M), the bond between the protein and surface is almost irreversible. Protein biotinylation is a straightforward procedure with countless *in vivo* or *in vitro* procedures available. Biotinylation can be easily verified by means of western blotting. For some applications, e.g. SPR, streptavidin-coated sensor chips are commercially available. The biotin-streptavidin binding is resistant to extreme pH values and temperatures, making the interaction very stable, which has advantages in e.g. surface regeneration without loss of the biotinylated protein (42).

Other potential couplings. Besides the commonly used His_6 tag, peptide epitopes and biotin-streptavidin interaction, numerous other affinity-based immobilization tags are reported, for instance the binding between gluthathione-S-transferase (GST) and gluthathione, the binding of antibodies to protein A or protein G via the Fc-region, maltose-binding protein with maltose, chitin binding protein with chitin, etc (18, 43, 44). In addition, DNA mediated conjugation is frequently used. Here, artificial nucleic acids are added to the protein. This approach is very interesting because it is easy to design and prepare a sequence and Watson-Crick base paring has a very high specificity. The disadvantage is that there is still a need for site-specific coupling of the DNA to the proteins (45, 46).

For some applications, non-covalent protein coupling can be interesting due to the possible reuse of the surface. Nevertheless, for a lot of applications, the instability of the bond is a major disadvantage. Unfortunately, oriented covalent couplings are in most cases more complex and often require advanced protein engineering techniques, which will be discussed later. An intermediate solution for this problem can be a two-step procedure during which the protein is first directed and oriented on the surface using affinity tags, followed by a covalent coupling of the already coupled protein to the surface resulting in an oriented and covalent coupling (47).

1.1.4 Oriented, covalent protein coupling

In order to couple a protein on a substrate in a covalent and oriented way, it is necessary to introduce a unique chemical group at a site-specific location. Because, when using the endogenous amino acids of the protein, this amino acid has to be present only once at the surface of the protein (at the target location), and the protein mixture cannot contain any other proteins with the same endogenous amino acids to avoid unwanted protein binding. The presence of a unique and site-specific functional group would make it possible to couple proteins to a functionalized surface in a selective manner. Nevertheless, the unique group should ideally be bioorthogonal, meaning that it can react in physiological conditions, it is not present in nature and cannot cross-react with other protein on endogenous amino acids (48).

One of the mostly used bioorthogonal chemistries for protein coupling is the so-called click chemistry. A click reaction is a highly selective reaction that can be performed using mild reaction conditions, it is insensitive to oxygen and water, water can be used as a solvent and it can form a stable product in physiological conditions (30, 49, 50). Several click chemistries are already applied in terms of protein coupling, for instance copper or ring-strain catalyzed azide-alkyne cycloadditions, Straudinger ligations, Diels-Alder cycloadditions, thiol-ene additions and oxime formation.

Copper(I)-catalyzed alkyne-azide cycloaddition (CuAAC). The CuAAC reaction (Figure 1.8), also known as the Azide-Alkyne Huisgen Cycloaddition (51), is the most commonly known click reaction. It is a reaction between an alkyne and azide that results in the formation of a 1,2,3-triazole. For the reaction, Cu(I) is necessary as a catalyst (48). Several sources for Cu(I) are possible but most protocols prepare the Cu(I) in situ by the reduction of a Cu(II) salt, for example Copper(II)sulfate, by TCEP or ascorbic acid (1, 5).

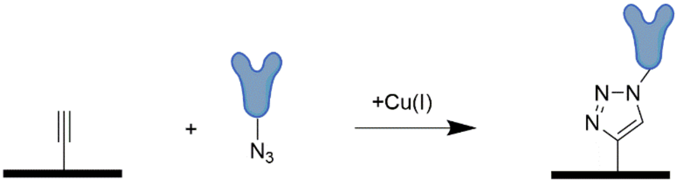

Figure 1.8: Copper(I)-catalyzed alkyne-azide cycloaddition (CuAAC).

The disadvantage is that the use of Cu(I) can be toxic to cells and may cause proteins to precipitate, meaning that it cannot be used for *in vivo* applications and can have limitations for *ex vivo* applications (52, 53).

Strain-promoted alkyne-azide cycloaddition (SPAAC). To avoid any problems due to Cu(I) interacting with the used proteins, Bertozzi et al. (54, 55) reported a copper-free Huisgen cycloaddition. This reaction makes use of the ring strain of a cyclooctyne group in order to increase the efficiency and reaction rate of the Huisgen 1,3-dipolar azide-alkyne cycloaddition without any need of an additional catalyst (Figure 1.9). Over the past decade, this reaction has been significantly improved, resulting in different generations of cyclooctynes with different reaction rates (56).

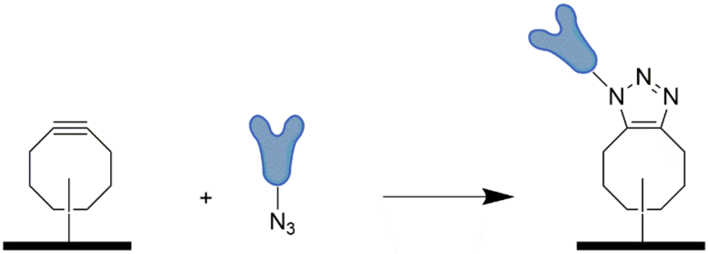

Figure 1.9: Strain-promoted alkyne-azide cycloaddition (SPAAC).

Staudinger ligation. As already proven in CuAAC and SPAAC, azides are a very interesting bioorthogonal chemical group. In a Staudinger reaction, the azides react with triphenylphosphines to produce an aza-ylide (57). In the presence of water, the aza-ylide hydrolyzes spontaneously to yield a primary amine and the corresponding phosphine oxide. The reaction between the phosphine and azide is very fast in water at room temperature, has a high yield and is unreactive towards biomolecules inside or on the cell surface. This makes them ideal for covalent immobilization of proteins on a surface. The only drawback is the instability of the reaction product in water. Saxon et al. solved this by adding an ester group on one of the phosphine’s aryl substituents resulting in the formation of a stable amide bond instead of the amine product of aza-ylide hydrolysis (58) as shown in Figure 1.10.

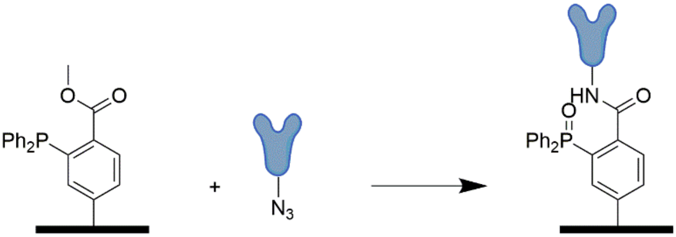

Figure 1.10: Staudinger ligation as described by Saxon et al (58).

Diels-Alder cycloaddition. The Diels-Alder reaction is a cycloaddition between a conjugated diene and a substituted alkene, commonly referred to as the dienophile, into the formation of a substituted cyclohexene. In the reaction shown in Figure 1.11, the dienophile is the maleimide-modified protein that is coupled to a conjugated diene functionalized surface. Diels-Alder cycloadditions have a higher reaction rate and selectivity in water than in organic solvents, which makes them a suitable approach for protein immobilization (11).

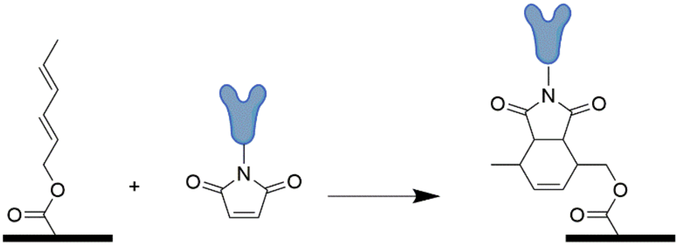

Figure 1.11: Diels-Alder cycloaddition.

Strain-promoted inverse electron-demand Diels–Alder cycloaddition. Besides the SPAAC, another interesting strain-promoted click reaction was developed more recently. The strain-promoted inverse electron-demand Diels–Alder cycloaddition (SPIEDAC) is based on the reaction between 1,2,4,5-tetrazines and strained alkenes and alkynes (Figure 1.12). SPIEDAC is the reaction of choice for *in vivo* studies due to its large rate constant and the absence of toxic by-products. However, the synthesis of 1,2,4,5-tetrazines is complex and can involve volatile reagents (59).

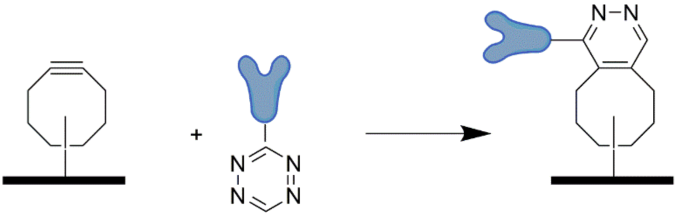

Figure 1.12: Strain-promoted inverse electron-demand Diels–Alder cycloaddition (SPIEDAC).

Thiol-ene reaction. A thiol-ene reaction is the reaction of a thiol group and an alkene by a free radical mechanism that is initiated by a free radical or light (Figure 1.13) and results in the formation of an alkyl sulfide (60). Originally, the thiol-ene reaction was predominantly applied in polymer and material synthesis, but in the recent years also in protein chemistry due to its biocompatible click chemistry properties. Because the reaction has a photoactivatable character, it can be used for surface patterning by means of photo-lithography (61, 62). The disadvantage of the technique is that thiol groups are not bioorthogonal, which results in cross-reaction with other endogenous thiol groups or other proteins.

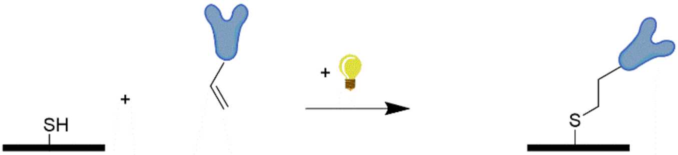

Figure 1.13: Thiol-ene reaction.

Oxime ligation. The oxime ligation is the condensation of an oxyamine or hydrazide with an aldehyde or ketone, which results in a stable oxime linkage (Figure 1.14). The reaction is generally slow (63) and normally proceeds at pH 4-5, making it less suitable for biological systems (64). Nevertheless, the addition of aniline as a catalyst enables a conjugation at neutral pH (65). None of the reagents are naturally present in proteins making it an excellent coupling system for site-specific immobilization of proteins (62, 66).

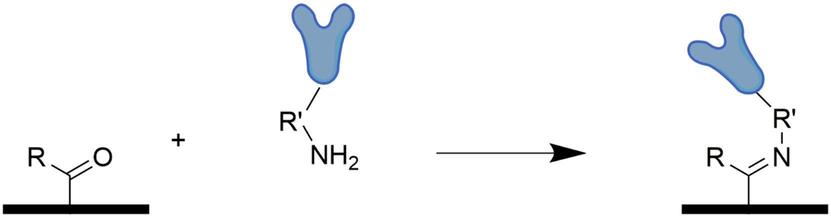

Figure 1.14: Oxime ligation.

1.2 Protein engineering techniques for site-specific protein modification

As described in the previous section, the ideal way to immobilize proteins on a surface is by making use of a covalent and oriented protein coupling with bioorthogonal groups. Over the years, a number of different methods were developed for the introduction of bioorthogonal groups. The most straightforward procedure entails the coupling of small linkers, containing the bioorthogonal group, to the side chain of one of the endogenous amino acids, typically lysine or cysteine. Unfortunately, this method has the same limitations as direct immobilization using this side chains. The protein modification is random and natural amino acids occur most of the time more than once in the protein. This may result in the modification of the protein in its active site or antigen-binding site leading to inactivation of the protein’s recognition properties. This drawback led to the development of different strategies for the site-specific modification of proteins.

Expressed protein ligation. For the post-translational C- or N-terminal modification of proteins, a technique called expressed protein ligation (EPL) can be used (Figure 1.15). EPL is based on the principles of native chemical ligation (NCL) and the natural intein-extein mechanism (48, 67). The POI is recombinantly expressed while fused with a mutated Mxe GyrA intein and a chitin-binding domain (CBD). The mutant intein will facilitate a N,S-acyl shift in the amide bond between the POI and the intein, resulting in a thioester bond. The chitin binding domain is used for purification on a chitin column so after expression, the protein can be immobilized on this column. The POI can be removed from the protein complex by means of a nucleophilic reaction between the thioester bond in the protein and a thiol nucleophile (68, 69). By carefully designing so-called bifunctional linkers that contain, in addition to a nucleophile, a bioorthogonal group, the protein can be C-terminally functionalized using EPL (48, 70). The latter is used in this thesis for the site-specific functionalization of proteins and will be discussed thoroughly in the next chapters.

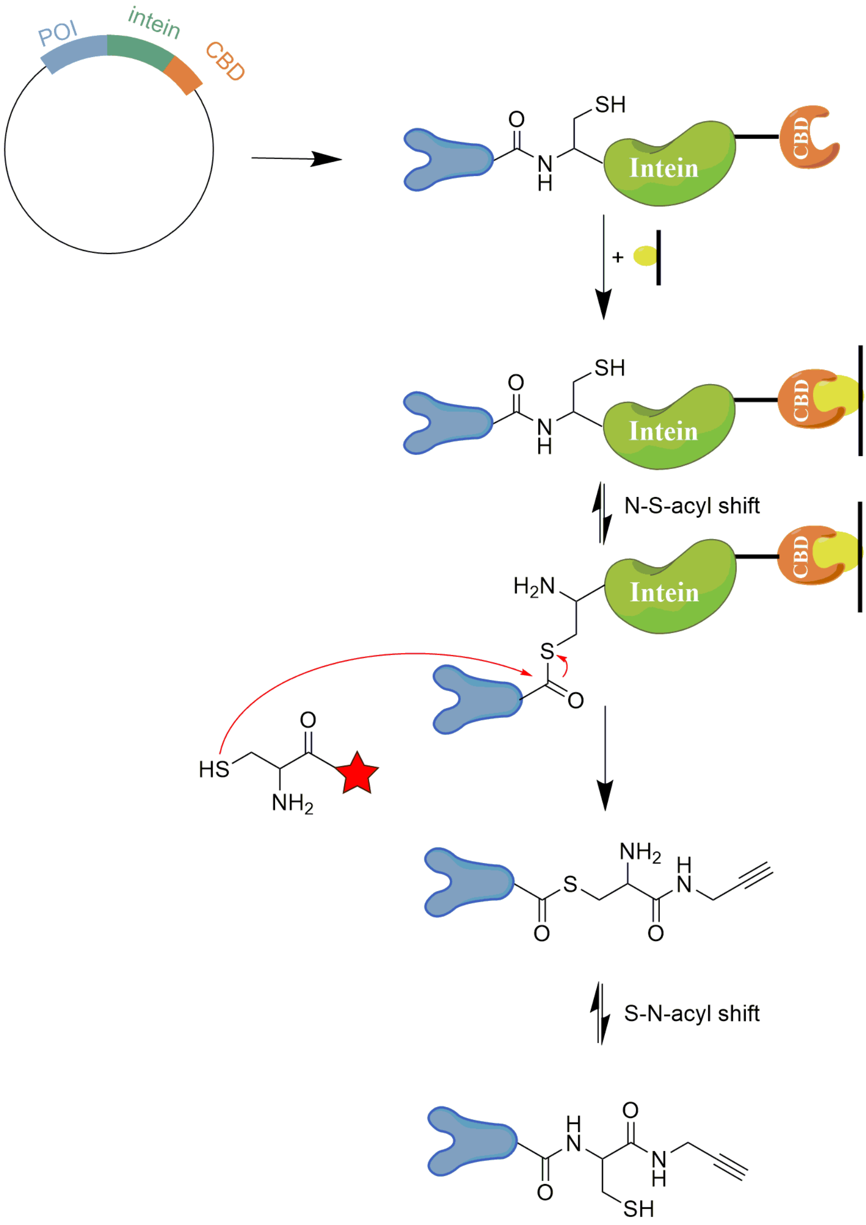
POI
intein
CBD
SH
O
N
H
Intein
CBD
+
N-S-acyl shift
H2N
S
O
HS
NH2
NH2
H
N
O
S-N-acyl shift
H
N
SH

Figure 1.15: The general principle of expressed protein ligation (EPL). The protein of interest (POI) is expressed in combination with intein and a chitin-binding domain (CBD). The intein will facilitate an N,S-acyl shift, resulting in an unstable thioester bond. A bifunctional linker, containing a free thiol group and a bioorthogonal group (★), will react with this thioester bond resulting in the functionalization of the POI and the removal of the POI from the intein-CBD complex.

Enzymatic modification. Another way of post-translationally modifying proteins is the use of an enzyme-based functionalization. The principle is relatively simple. The enzyme will recognize a certain short peptide sequence that has been recombinantly added to the protein, and will covalently modify the protein with small molecules, containing the bioorthogonal group of interest. A very popular example of this kind of modification is the sortase A (SrtA) enzyme. SrtA is a transpeptidase from *Staphylococcus aureus* that is naturally present on the plasma membrane and which catalyzes a cell wall sorting reaction that attaches surface proteins to the cell wall. However, the reaction can also be used for the covalent attachment of a bioorthogonal group near the C-terminus of a protein, as shown in Figure 1.16.

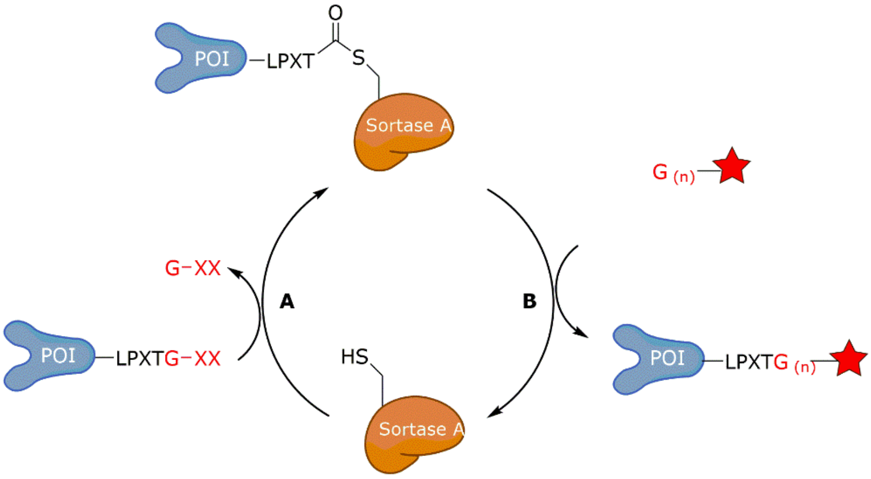

Figure 1.16: The sortase A (SrtA) mechanism. (**A**) SrtA binds to the sortag in the protein of interest (POI). (**B**) Next, a peptide probe, containing a bioorthogonal group (★) and glycine, reacts with the POI-SrtA complex resulting in native SrtA and functionalized POI.

The POI, modified at the C-terminus with the sortase A tag (sortag) LPXTG (were X can be any amino acid), was incubated with SrtA enzyme. The enzyme will cleave the threonine (T) – glycine (G) bond using the thiol group from the cysteine in its active site. This will form an acyl intermediate with threonine in the protein. Next, a peptide probe containing a series of N-terminal glycine residues and a bioorthogonal group is added. This resolves the acyl intermediate and subsequently results in the regeneration of the cysteine in the active site of srtA and in the ligation of the peptide probe with the POI (71, 72). The advantages of the sortA system are the relatively easy expression of the recombinant sortA enzyme, its flexibility towards its substrates and the use of very short peptide sequences on the POI and the target peptide. Besides the coupling of a bioorthogonal group for surface modification, it is also possible to directly add a small molecule like a radiolabel, to the POI (71).

Other enzymes used for the site-specific incorporation of a bioorthogonal group are e.g. biotin ligase (BirA) (73), protein farnesyltransferase (PFTase) (63), transglutaminase (TGase), lipoic acid ligase (LplA), formylglycine-generating enzyme (FGE), etc. (48).

Self-labeling protein tags. A standard enzymatic approach, as discussed in the previous section, consists of 3 components: the POI with a tag, the tag-recognizing enzyme and the enzyme substrate that has to be coupled to the POI. In addition to this approach, another enzyme-based method is possible, i.e. the self-labeling protein tags. This approach comprises two components, a self-labeling protein tag (mostly derived from enzymes) and a substrate. As shown in Figure 1.17, the protein tag binds directly to its substrate (74).

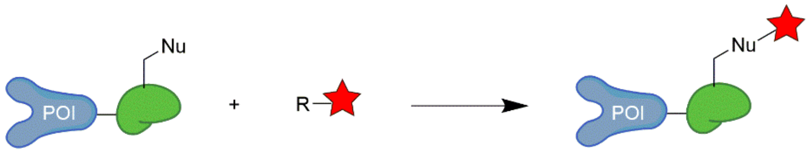

Figure 1.17: Self-labeling protein tags mechanism. The self-labeling protein tag (🟢), that contains a nucleophile (Nu), reacts directly with its substrate (R) that contains the bioorthogonal group (★).

Often used tags are the SNAP-tag, CLIP-tag and HaloTag (72, 74). The disadvantage of this system is that the protein tags are quite large (20-35 kDa) which makes the technique not useful for the immobilization of small proteins.

Auxotrophic expression. Another possibility to site-specifically introduce a bioorthogonal functionality into a protein is by replacing one of the 20 natural amino acids by a structural analogue containing the bioorthogonal functionality, e.g. an azide, through interference with the organism's native translational systems. In these systems, aminoacyl-tRNA synthetases are responsible for the incorporation of amino acids. These enzymes couple amino acids to tRNA. If the natural amino acid is not present in the growth medium and the host organism is auxotrophic, meaning that it is incapable to produce the natural amino acid by itself, the amino acid analogue is incorporated in the genetically encoded position of the natural amino acid (53).

However, the incorporation is residue-specific instead of site-specific, meaning that, if the replaced natural amino acid is present more than once in the protein, the functionality will be integrated multiple times into the protein.

Nonsense suppression. By using so-called genetic code expansion, it is possible to incorporate bioorthogonal functionalities in proteins during the protein translation by means of an unnatural amino acid. To add such an unnatural amino acid to a protein, different components of the biological translation process are necessary:

- A unique codon and corresponding tRNA to recognize this codon
- A unnatural amino acid (containing the bioorthogonal group)
- A new aminoacyl-tRNA synthetase that recognizes the unnatural amino acid and directs it towards the tRNA

These components also need to meet certain criteria. First of all, the unnatural amino acid needs to be metabolically stable and biologically available to be included into the host organism. Secondly, the unnatural amino acid may not be used as a substrate for endogenous synthetases. The same applies for the new codon that may only be recognized by the new tRNA and not by any endogenous tRNA. Finally, the aminoacyl-tRNA synthetase/tRNA pair must be specific for the unnatural amino acid and not crosstalk with the endogenous translational system (75). The natural genetic system comprises 64 unique codons formed by the combination of 4 possible nucleotides. The 20 natural amino acids are encoded by 61 codons, leaving 3 codons that are called the stop codons because they terminate the protein translation process. The stop codons, also called nonsense codons, are TAG (amber), TAA (ochre) and TGA (opal) (76). These stop codons can be used for the site-specific introduction of unnatural amino acids using a technique called nonsense suppression. This technique is based on the fact that only one stop codon is needed for the termination of protein translation meaning that the other two can be reassigned to an additional unnatural amino acid (77). Since the amber stop codon is the least used in both *E. coli* and yeast, this codon is the most frequently used stop codon in nonsense suppression. The use of the amber codon to code for an unnatural amino acid requires a suppressor $tRNA_{CUA}$ and the corresponding aminoacyl-$tRNA_{CUA}$ synthetase, which has evolved to selectively bind the unnatural amino acid to the suppressor $tRNA_{CUA}$ (78). A schematic representation of the amber suppression process is shown in Figure 1.18.

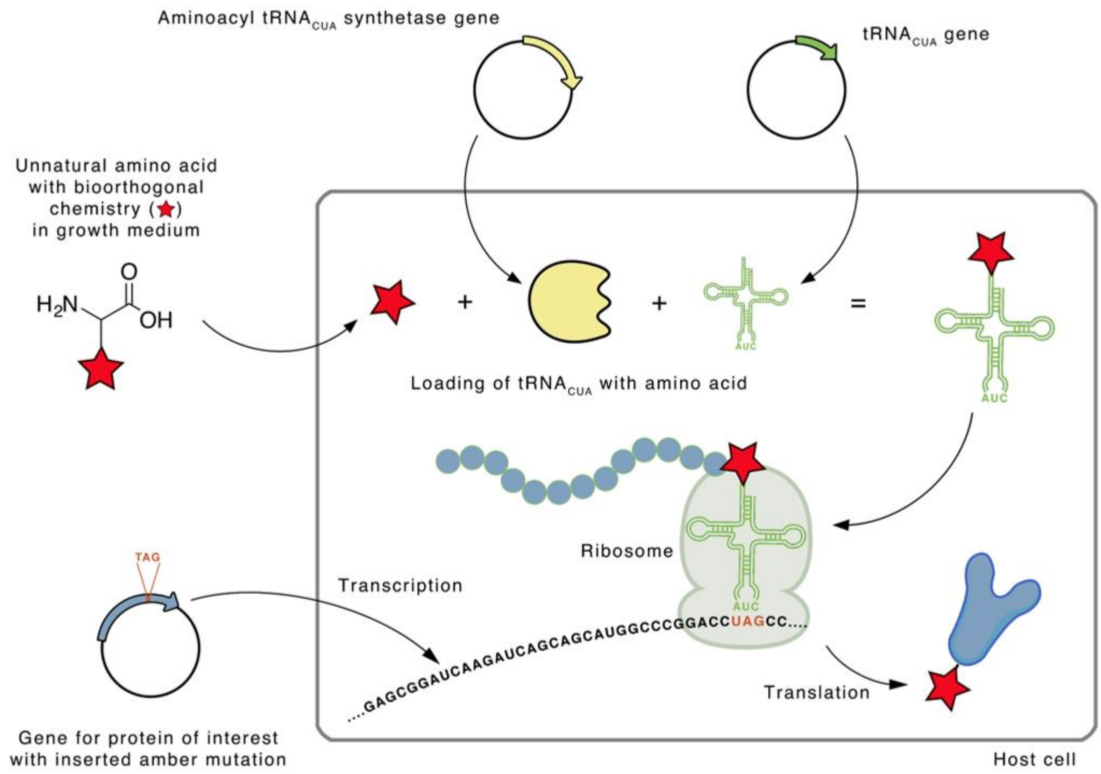
Aminoacyl tRNA$_{CUA}$ synthetase gene
tRNA$_{CUA}$ gene
Unnatural amino acid with bioorthogonal chemistry (★) in growth medium
H_2N
O
OH
+
+
=
AUC
AUC
Loading of tRNA$_{CUA}$ with amino acid
Ribosome
Transcription
TAG
AUC
....GAGCGGAUCAAGAUCAGCAGCAUGGCCCGGACCUAGCC....
Translation
Gene for protein of interest with inserted amber mutation
Host cell

Figure 1.18: Amber suppression (based on (78)). The gene for the POI is mutated with an amber codon (UAG) at the desired site of modification. A mutant aminoacyl-tRNA$_{CUA}$ synthetase recognizes the unnatural amino acid bearing the desired functionality and loads it to the corresponding tRNA$_{CUA}$. This leads to the expression of the POI with the desired functionality at the genetically encoded site.

1.3 Nanobodies

1.3.1 Molecular description of a nanobody

Conventional antibodies (Abs) are made up of two identical heavy chains (H-chain) and two identical light chains (L-chain). Each L-chain consists of two immunoglobulin domains, each H-chain contains four immunoglobulin domains, as shown in Figure 1.19a. The variable domain (V_H and V_L) is located at the N-terminus of every chain. The variable domain contains three hypervariable regions called complementarity determining regions (CDRs) because they form the eventual Ag-binding surface (79). This means that the Ag-binding region, also known as the paratope, comprises six CDR loops, three from each domain.

Certain animal species, Camelidae (camels, dromedaries, etc.), nurse sharks and wobbegong sharks, also have Abs without a light chain in addition to the conventional Abs. These are the so-called heavy chain only antibodies (HCAbs)(80). Besides the lacking light chain, these HCAbs are also devoid of a first constant domain (CH1), which is encoded in the genome but is spliced out during mRNA processing (81). This leads to a paratope that is only formed by the three CDRs in the variable domain of the heavy chain of heavy chain antibodies (VHH). These VHHs can be obtained recombinantly from microbial expression sytems as autonomous single domain antibodies (SdAbs). Such SdAbs, more commonly known and further referred to as nanobodies (Nbs), are the smallest Ab-derived fragments with a fully intact paratope (82). Nbs have a molecular mass of ca. 15 kDa, and a rugby ball shape of approximately 2.5 nm diameter and 4.2 nm in length (83).

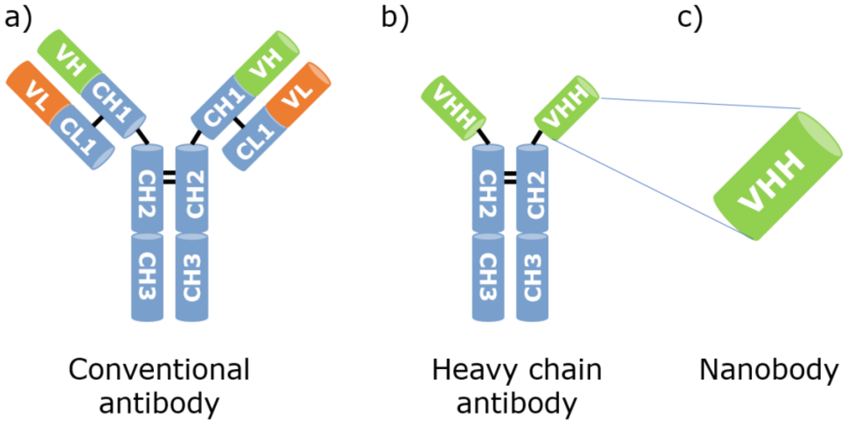

Figure 1.19: Schematic representation of (a) a conventional antibody, (b) a heavy chain only antibody and (c) a nanobody.

As described in Figure 1.20, there are also some structural differences between the VH of a conventional antibody and a VHH (nanobody). The antigen-binding loops of a VHH are longer than in the VH of a conventional antibody. In particular CDR3 of a Nb is longer (84). This increases the antigen-binding surface and compensates for the paratope of the VHH that only has three CDRs compared with the six CDRs in a conventional antibody. In most Nbs, these longer antigen-binding loops are stabilized by a disulfide bridge between CDR1 and CDR3 (85). In the framework-two, four hydrophobic amino acids of the VH are replaced by hydrophilic residues in the VHH(86), which results in a higher solubility of the VHH (87).

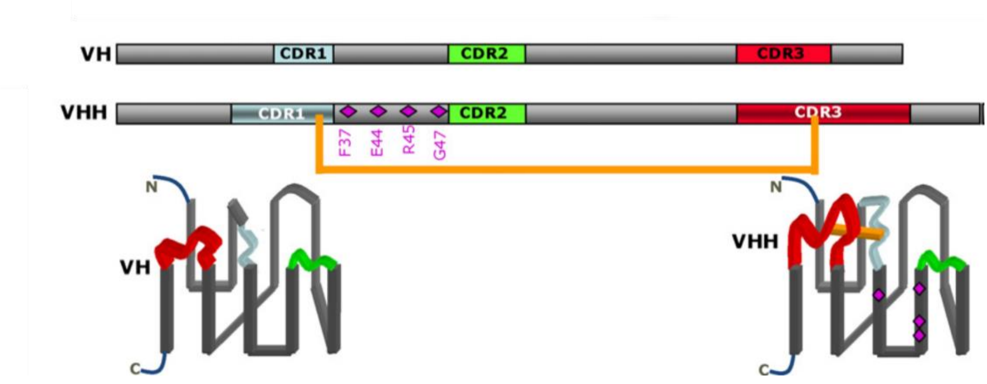

Figure 1.20: Schematic representation of the sequence organization and folded structure of the VH of a conventional Ab and a VHH. Adapted from Muyldermans et al. (88).

In general, the biggest advantage of Nbs is their small size. With a molecular weight of 15 kDa, they are 10 times lighter than conventional antibodies. Therefore, they can bind to epitopes that are hard to reach for conventional antibodies. Furthermore, they have a conserved structure, are economic to produce and easy to express in large quantities in bacteria and yeast. They are encoded by a single gene, facilitating their genetic manipulation, they have a high solubility and they are very stable, also at higher temperatures (12, 80, 89, 90).

1.3.2 Applications of nanobodies

The numerous advantages of Nbs compared to conventional antibodies make them suitable for numerous applications. At the moment, nanobodies are mainly used for diagnostics (biosensor development and *in vivo* imaging), affinity capture and therapeutics.

Diagnostics. For the development of biosensors, were small, robust, highly specific affinity probes are important, Nbs are an interesting asset (83). Nbs can be site-specifically functionalized, as further discussed in this thesis, resulting in a covalent and oriented binding with no loss of affinity and specificity (91, 92). Due to the small size of nanobodies, they provide a binding capacity on the surface, which results in a higher sensitivity. By directional immobilization, the immunoreaction occurs very close to the sensor-solution interface, which increases the sensitivity (83). The high stability of Nbs allows rigorous washing and regeneration conditions and increases the shelf life of the biosensor.

In vivo imaging. Due to their small size, Nbs are exceptionally interesting to target probes against antigens in isolated locations such as tumors. They can bind their target with a nanomolar affinity and are relatively easy to generate against a certain antigen (93). In addition to size, stability, low immunogenicity and easy labeling are also factors in favor of the use of Nbs for *in vivo* imaging (83).

Therapeutics. Nbs have a resemblance of ca. 80% with the human VH frameworks. For therapeutic use, nanobodies can be humanized with 95-99% homology by changing a few amino acids in the framework region (80, 90, 94). As a result of their high stability in extreme pH (95, 96) and small size, Nbs can be used for oral treatment (94) with a fast tissue penetration (97) and renal elimination (98). Nbs can be applied to target toxic enzymes (97, 99) or to block certain molecular interactions with application in the treatment of diseases such as cancer (100-102) and inflammatory diseases like rheumatoid arthritis (103).

Affinity capture. Because of their small size and single-domain format, Nbs are suitable reagents for affinity capture. They provide higher capacity binding surfaces and lower non-specific background binding compared to conventional antibodies. Their monovalent mode of binding allows the use of mild elution conditions, which is interesting for sensitive molecules. Nevertheless, the high stability and refolding capacities of nanobodies makes them suitable for harsh and repeated regeneration conditions (83, 104).

1.3.3 Nanobody BcII10

This thesis used a nanobody against β-lactamase, nanobody BcII10 (NbBcII10) as a model for nanobody functionalization using EPL. β-lactamases are enzymes, produced by bacteria that break the four-atom ring of β-lactam antibiotics (e.g. penicillins and cephamycins) (105, 106). NbBcII10 can be very useful in the fight against antibiotic resistance (107), it also has some interesting properties for research on nanobody modification. Saerens et al. (108) discovered that the VHH framework of NbBcII10 could be used as a universal VHH framework. The plasticity of the NbBcII10 framework allows a successful transfer of antigen specificity from a donor VHH (e.g. an unstable nanobody) to the NbBcII10 scaffold. NbBcII10 is the ideal scaffold candidate for such loop transfer due to its good expression levels and its high level of stability.

1.4 Research aims

For the development of bioactive surfaces (in particularly miniaturized surfaces) reproducibility, sensitivity and selectivity are incredibly important. These properties can be achieved by the covalent and oriented coupling of proteins to functionalized surfaces. As discussed previously, the currently used strategies are not capable to fulfill these needs. This thesis aims at the development of site-specific functionalized nanobodies for the covalent coupling on functionalized surfaces in order to obtain a uniform and oriented layer of nanobodies for next generation biosensors. The major research goals are:

i) To achieve a better understanding of the Expressed Protein Ligation (EPL) technique by researching the possibilities to optimize current known protocols for the C-terminal alkynation of Maltose Binding Protein (MBP).

ii) One of the disadvantages of EPL is the introduction of a C-terminal thiol group, which can result in side reactions like dimerization. To avoid these side reactions, an amine-based bifunctional linker for the C-terminal alkynation of MBP will be synthesized.

iii) An in detail study of the covalent coupling by means of a click reaction between MBP and an azide functionalized silicon surface will be performed using ellipsometry. A comparison will be made between random alkynated MBP and site-specific alkynated MBP.

iv) The possibility for a periplasmic extraction of the NbBcII10-intein-chitin binding domain complex needs to be investigated using different approaches: by means of different transportation pathways using different leader sequences, different extraction techniques and different expression hosts.

v) Site-specific alkynation of the nanobody BcII10 (NbBcII10) using the knowledge gained during the site-specific alkynation of MBP and the NbBcII10 extraction study.

vi) After the site-specific alkynation, the clickability of alkynated Nb-BcII10 to an azide functionalized support needs to be examined. The binding activity of NbBcII10 for its original antigen BcII needs to be investigated using ELISA and SPR in order to determine influences of the EPL process and alkynation on the binding capacity of the NbBcII10.

1.5 Thesis outline

This thesis explores the possibility to site-specifically modify proteins for the purpose of surface biofunctionalization for applications in biosensing. By using expressed protein ligation (EPL), an alkyne functionality was site-specific incorporated in the proteins, at the C-terminus. Consequently, the proteins can be coupled to an azide functionalized surface using click-chemistry. This results in a layer of oriented proteins on the surface resulting in a maximal availability of the active site of the proteins. In this thesis, maltose-binding protein (MBP) is used as a proof of concept for the alkynation and covalent coupling using click chemistry. Nanobody BcII10 (NbBcII10) is used as a model Nb for the site-specific Nb alkynation.

In **Chapter 1** existing strategies for protein immobilization are introduced as well as state-of-the-art protein engineering techniques for site-specific protein modification.

As a proof of concept for the site-specific alkynation of proteins, the model protein MBP is used. MBP is a commonly used protein to test EPL approaches because the vector is commercially available and well-documented. **Chapter 2** describes the MBP functionalization and focuses on the coupling of alkynated MBP to azide functionalized silicon surfaces. A study using ellipsometry is performed analyzing the covalent click coupling between MBP and the silicon surface in detail.

One of the disadvantages of EPL is the introduction of a thiol functionality along with the alkyne group. Therefore, a non-thiol-based bifunctional linker was developed and the EPL procedure is optimized, as described in **Chapter 3**.

In **Chapter 4**, different expression strategies are presented to facilitate extraction of the NbBcII10-intein-CBD complex from the periplasmic space. As a valuable alternative, cytoplasmic expression and extraction of the NbBcII10 is investigated and its functionality was evaluated by ELISA and SPR.

In **Chapter 5** the experimental techniques and procedures used in the previous chapters are described in more detail.

Lastly, **Chapter 6** is a general discussion of the research performed in this thesis and presents an outlook for future research.

1.6 References

1. Lallana E, Sousa-Herves A, Fernandez-Trillo F, Riguera R, Fernandez-Megia E. Click Chemistry for Drug Delivery Nanosystems. Pharm Res. 2012;29(1):1-34.
2. Han H, Davis ME. Single-Antibody, Targeted Nanoparticle Delivery of Camptothecin. Mol Pharm. 2013;10(7):2558-67.
3. Broisat A, Hernot S, Toczek J, De Vos J, Riou LM, Martin S, Ahmadi M, Thielens N, Wernery U, Caveliers V, Muyldermans S, Lahoutte T, Fagret D, Ghezzi C, Devoogdt N. Nanobodies Targeting Mouse/Human VCAM1 for the Nuclear Imaging of Atherosclerotic Lesions. Circ Res. 2012;110(7):927-37.
4. De Vos J, Mathijs I, Xavier C, Massa S, Wernery U, Bouwens L, Lahoutte T, Muyldermans S, Devoogdt N. Specific Targeting of Atherosclerotic Plaques in ApoE−/− Mice Using a New Camelid sdAb Binding the Vulnerable Plaque Marker LOX-1. Mol Imag Biol. 2014;16(5):690-8.
5. Nebhani L, Barner-Kowollik C. Orthogonal Transformations on Solid Substrates: Efficient Avenues to Surface Modification. Adv Mater. 2009;21(34):3442-68.
6. Li Q-L, Huang N, Chen C, Chen J-L, Xiong K-Q, Chen J-Y, You T-X, Jin J, Liang X. Oriented immobilization of anti-CD34 antibody on titanium surface for self-endothelialization induction. J Biomed Mater Res A. 2010;94A(4):1283-93.
7. Nguyen H, Park J, Kang S, Kim M. Surface Plasmon Resonance: A Versatile Technique for Biosensor Applications. Sensors. 2015;15(5):10481.
8. Li H, Sun Y, Elseviers J, Muyldermans S, Liu S, Wan Y. A nanobody-based electrochemiluminescent immunosensor for sensitive detection of human procalcitonin. Analyst. 2014;139(15):3718-21.
9. Trilling AK, Beekwilder J, Zuilhof H. Antibody orientation on biosensor surfaces: a minireview. Analyst. 2013;138(6):1619-27.
10. Grieten L, Janssens SD, Ethirajan A, Bon NV, Ameloot M, Michiels L, Haenen K, Wagner P. Real-time study of protein adsorption on thin nanocrystalline diamond. Phys Status Solidi A. 2011;208(9):2093-8.
11. Rusmini F, Zhong Z, Feijen J. Protein Immobilization Strategies for Protein Biochips. Biomacromolecules. 2007;8(6):1775-89.
12. Huang L, Muyldermans S, Saerens D. Nanobodies®: proficient tools in diagnostics. Expert Rev Mol Diagn. 2010;10(6):777-85.
13. Camarero JA. New developments for the site-specific attachment of protein to surface. Biophysical Reviews and Letters. 2006;01(01):1-28.
14. Camarero JA. Recent developments in the site-specific immobilization of proteins onto solid supports. Peptide Science. 2008;90(3):450-8.
15. Spahn C, Minteer SD. Enzyme Immobilization in Biotechnology. Recent Patents on Engineering. 2008;2(3):195-200.
16. Kim D, Karns K, Tia SQ, He M, Herr AE. Electrostatic Protein Immobilization Using Charged Polyacrylamide Gels and Cationic Detergent Microfluidic Western Blotting. Anal Chem. 2012;84(5):2533-40.

17. Novick SJ, Rozzell JD. Immobilization of Enzymes by Covalent Attachment. In: Barredo JL, editor. Microbial Enzymes and Biotransformations. Totowa, NJ: Humana Press; 2005. p. 247-71.
18. Nakanishi K, Sakiyama T, Kumada Y, Imamura K, Imanaka H. Recent Advances in Controlled Immobilization of Proteins onto the Surface of the Solid Substrate and Its Possible Application to Proteomics. Curr Proteomics. 2008;5(3):161-75.
19. Lin P-C, Weinrich D, Waldmann H. Protein Biochips: Oriented Surface Immobilization of Proteins. Macromol Chem Phys. 2010;211(2):136-44.
20. Wu P, Shui W, Carlson BL, Hu N, Rabuka D, Lee J, Bertozzi CR. Site-specific chemical modification of recombinant proteins produced in mammalian cells by using the genetically encoded aldehyde tag. Proceedings of the National Academy of Sciences. 2009;106(9):3000-5.
21. Foley TL, Burkart MD. Site-specific protein modification: advances and applications. Curr Opin Chem Biol. 2007;11(1):12-9.
22. Kim Y, Ho SO, Gassman NR, Korlann Y, Landorf EV, Collart FR, Weiss S. Efficient Site-Specific Labeling of Proteins via Cysteines. Bioconj Chem. 2008;19(3):786-91.
23. Sokalingam S, Raghunathan G, Soundrarajan N, Lee S-G. A Study on the Effect of Surface Lysine to Arginine Mutagenesis on Protein Stability and Structure Using Green Fluorescent Protein. PLoS One. 2012;7(7):e40410.
24. Brady D, Jordaan J. Advances in enzyme immobilisation. Biotechnol Lett. 2009;31(11):1639-50.
25. Wang B, Guo C, Zhang M, Park B, Xu B. High-Resolution Single-Molecule Recognition Imaging of the Molecular Details of Ricin–Aptamer Interaction. The Journal of Physical Chemistry B. 2012;116(17):5316-22.
26. Fischer ME. Amine Coupling Through EDC/NHS: A Practical Approach. In: Mol NJ, Fischer MJE, editors. Surface Plasmon Resonance. Methods in Molecular Biology. 627: Humana Press; 2010. p. 55-73.
27. Pei Z, Anderson H, Myrskog A, Dunér G, Ingemarsson B, Aastrup T. Optimizing immobilization on two-dimensional carboxyl surface: pH dependence of antibody orientation and antigen binding capacity. Anal Biochem. 2010;398(2):161-8.
28. Baslé E, Joubert N, Pucheault M. Protein Chemical Modification on Endogenous Amino Acids. Chem Biol. 2010;17(3):213-27.
29. Masri MS, Friedman M. Protein reactions with methyl and ethyl vinyl sulfones. J Protein Chem. 1988;7(1):49-54.
30. Hermanson GT. Chapter 2 - The Chemistry of Reactive Groups. Bioconjugate Techniques (Second Edition). New York: Academic Press; 2008. p. 169-212.
31. Terpe K. Overview of tag protein fusions: from molecular and biochemical fundamentals to commercial systems. Appl Microbiol Biotechnol. 2003;60(5):523-33.

32. Porath J, Carlsson JAN, Olsson I, Belfrage G. Metal chelate affinity chromatography, a new approach to protein fractionation. Nature. 1975;258(5536):598-9.

33. Ganesana M, Istarnboulie G, Marty J-L, Noguer T, Andreescu S. Site-specific immobilization of a (His)6-tagged acetylcholinesterase on nickel nanoparticles for highly sensitive toxicity biosensors. Biosensors Bioelectron. 2011;30(1):43-8.

34. Bornhorst JA, Falke JJ. [16] Purification of proteins using polyhistidine affinity tags. Methods Enzymol. Volume 326: Academic Press; 2000. p. 245-54.

35. Huang J, Honda W. CED: a conformational epitope database. BMC Immunol. 2006;7(1):1-8.

36. Einhauer A, Jungbauer A. The FLAG™ peptide, a versatile fusion tag for the purification of recombinant proteins. J Biochem Biophys Methods. 2001;49(1–3):455-65.

37. Hopp TP, Prickett KS, Price VL, Libby RT, March CJ, Pat Cerretti D, Urdal DL, Conlon PJ. A Short Polypeptide Marker Sequence Useful for Recombinant Protein Identification and Purification. Nat Biotech. 1988;6(10):1204-10.

38. Schmidt PM, Sparrow LG, Attwood RM, Xiao X, Adams TE, McKimm-Breschkin JL. Taking down the FLAG! How Insect Cell Expression Challenges an Established Tag-System. PLoS One. 2012;7(6):e37779.

39. Evan GI, Lewis GK, Ramsay G, Bishop JM. Isolation of monoclonal antibodies specific for human c-myc proto-oncogene product. Mol Cell Biol. 1985;5(12):3610-6.

40. Sudheer PDVN, Pack SP, Kang TJ. Cyclization tag for the detection and facile purification of backbone-cyclized proteins. Anal Biochem. 2013;436(2):137-41.

41. Wingren C, Steinhauer C, Ingvarsson J, Persson E, Larsson K, Borrebaeck CAK. Microarrays based on affinity-tagged single-chain Fv antibodies: Sensitive detection of analyte in complex proteomes. Proteomics. 2005;5(5):1281-91.

42. Hutsell SQ, Kimple RJ, Siderovski DP, Willard FS, Kimple AJ. High-affinity immobilization of proteins using biotin- and GST-based coupling strategies. Methods Mol Biol. 2010;627:75-90.

43. Hernandez K, Fernandez-Lafuente R. Control of protein immobilization: Coupling immobilization and site-directed mutagenesis to improve biocatalyst or biosensor performance. Enzyme Microb Technol. 2011;48(2):107-22.

44. Berrade L, Garcia AE, Camarero JA. Protein Microarrays: Novel Developments and Applications. Pharm Res. 2011;28(7):1480-99.

45. Niemeyer CM. Semisynthetic DNA–Protein Conjugates for Biosensing and Nanofabrication. Angew Chem Int Ed. 2010;49(7):1200-16.

46. Fruk L, Müller J, Weber G, Narváez A, Domínguez E, Niemeyer CM. DNA-Directed Immobilization of Horseradish Peroxidase–DNA Conjugates on Microelectrode Arrays: Towards Electrochemical Screening of Enzyme Libraries. Chem Eur J. 2007;13(18):5223-31.

47. Mateo C, Fernández-Lorente G, Abian O, Fernández-Lafuente R, Guisán JM. Multifunctional Epoxy Supports: A New Tool To Improve the Covalent Immobilization of Proteins. The Promotion of Physical Adsorptions of Proteins on the Supports before Their Covalent Linkage. Biomacromolecules. 2000;1(4):739-45.
48. Sletten EM, Bertozzi CR. Bioorthogonal Chemistry: Fishing for Selectivity in a Sea of Functionality. Angew Chem Int Ed. 2009;48(38):6974-98.
49. Hein CD, Liu XM, Wang D. Click chemistry, a powerful tool for pharmaceutical sciences. Pharm Res. 2008;25(10):2216-30.
50. Rostovtsev VV, Green LG, Fokin VV, Sharpless KB. A Stepwise Huisgen Cycloaddition Process: Copper(I)-Catalyzed Regioselective "Ligation" of Azides and Terminal Alkynes. Angew Chem Int Ed. 2002;41(14):2596-9.
51. Huisgen R. Proceedings of the Chemical Society. October 1961. Proc Chem Soc. 1961(October):357-96.
52. Kalia J, Raines RT. Advances in Bioconjugation. Curr Org Chem. 2010;14(2):138-47.
53. van Hest JCM, van Delft FL. Protein Modification by Strain-Promoted Alkyne–Azide Cycloaddition. ChemBioChem. 2011;12(9):1309-12.
54. Baskin JM, Prescher JA, Laughlin ST, Agard NJ, Chang PV, Miller IA, Lo A, Codelli JA, Bertozzi CR. Copper-free click chemistry for dynamic in vivo imaging. Proceedings of the National Academy of Sciences. 2007;104(43):16793-7.
55. Agard NJ, Prescher JA, Bertozzi CR. A Strain-Promoted [3 + 2] Azide−Alkyne Cycloaddition for Covalent Modification of Biomolecules in Living Systems. J Am Chem Soc. 2004;126(46):15046-7.
56. Mbua NE, Guo J, Wolfert MA, Steet R, Boons G-J. Strain-Promoted Alkyne–Azide Cycloadditions (SPAAC) Reveal New Features of Glycoconjugate Biosynthesis. ChemBioChem. 2011;12(12):1912-21.
57. Staudinger H, Meyer J. Über neue organische Phosphorverbindungen III. Phosphinmethylenderivate und Phosphinimine. Helv Chim Acta. 1919;2(1):635-46.
58. Saxon E, Bertozzi CR. Cell Surface Engineering by a Modified Staudinger Reaction. Science. 2000;287(5460):2007-10.
59. Horner KA, Valette NM, Webb ME. Strain-Promoted Reaction of 1,2,4-Triazines with Bicyclononynes. Chem Eur J. 2015;21(41):14376-81.
60. Hoyle CE, Bowman CN. Thiol–Ene Click Chemistry. Angew Chem Int Ed. 2010;49(9):1540-73.
61. Jonkheijm P, Weinrich D, Köhn M, Engelkamp H, Christianen PCM, Kuhlmann J, Maan JC, Nüsse D, Schroeder H, Wacker R, Breinbauer R, Niemeyer CM, Waldmann H. Photochemical Surface Patterning by the Thiol-Ene Reaction. Angew Chem. 2008;120(23):4493-6.
62. Chen Y-X, Triola G, Waldmann H. Bioorthogonal Chemistry for Site-Specific Labeling and Surface Immobilization of Proteins. Acc Chem Res. 2011;44(9):762-73.

63. Rashidian M, Song JM, Pricer RE, Distefano MD. Chemoenzymatic Reversible Immobilization and Labeling of Proteins without Prior Purification. J Am Chem Soc. 2012;134(20):8455-67.

64. Milles S, Tyagi S, Banterle N, Koehler C, VanDelinder V, Plass T, Neal AP, Lemke EA. Click Strategies for Single-Molecule Protein Fluorescence. J Am Chem Soc. 2012;134(11):5187-95.

65. Dirksen A, Dawson PE. Rapid Oxime and Hydrazone Ligations with Aromatic Aldehydes for Biomolecular Labeling. Bioconj Chem. 2008;19(12):2543-8.

66. Lempens EHM, Helms BA, Merkx M. Chemoselective Protein and Peptide Immobilization on Biosensor Surfaces. In: Mark SS, editor. Bioconjugation Protocols: Strategies and Methods. Totowa, NJ: Humana Press; 2011. p. 401-20.

67. Muralidharan V, Muir TW. Protein ligation: an enabling technology for the biophysical analysis of proteins. Nat Meth. 2006;3(6):429-38.

68. Chong S, Mersha FB, Comb DG, Scott ME, Landry D, Vence LM, Perler FB, Benner J, Kucera RB, Hirvonen CA, Pelletier JJ, Paulus H, Xu M-Q. Single-column purification of free recombinant proteins using a self-cleavable affinity tag derived from a protein splicing element. Gene. 1997;192(2):271-81.

69. Berrade L, Camarero JA. Expressed protein ligation: a resourceful tool to study protein structure and function. Cell Mol Life Sci. 2009;66(24):3909-22.

70. Lin P-C, Ueng S-H, Tseng M-C, Ko J-L, Huang K-T, Yu S-C, Adak AK, Chen Y-J, Lin C-C. Site-Specific Protein Modification through CuI-Catalyzed 1,2,3-Triazole Formation and Its Implementation in Protein Microarray Fabrication. Angew Chem Int Ed. 2006;45(26):4286-90.

71. Massa S, Vikani N, Betti C, Ballet S, Vanderhaegen S, Steyaert J, Descamps B, Vanhove C, Bunschoten A, van Leeuwen FWB, Hernot S, Caveliers V, Lahoutte T, Muyldermans S, Xavier C, Devoogdt N. Sortase A-mediated site-specific labeling of camelid single-domain antibody-fragments: a versatile strategy for multiple molecular imaging modalities. Contrast Media Mol Imaging. 2016:n/a-n/a.

72. Guimaraes CP, Witte MD, Theile CS, Bozkurt G, Kundrat L, Blom AEM, Ploegh HL. Site-specific C-terminal and internal loop labeling of proteins using sortase-mediated reactions. Nat Protocols. 2013;8(9):1787-99.

73. Prescher JA, Bertozzi CR. Chemistry in living systems. Nat Chem Biol. 2005;1(1):13-21.

74. Hinner MJ, Johnsson K. How to obtain labeled proteins and what to do with them. Curr Opin Biotechnol. 2010;21(6):766-76.

75. Liu CC, Schultz PG. Adding New Chemistries to the Genetic Code. Annu Rev Biochem. 2010;79(1):413-44.

76. Cropp TA, Schultz PG. An expanding genetic code. Trends Genet.20(12):625-30.

77. Strømgaard A, Jensen AA, Strømgaard K. Site-Specific Incorporation of Unnatural Amino Acids into Proteins. ChemBioChem. 2004;5(7):909-16.

78. Steen Redeker E, Ta DT, Cortens D, Billen B, Guedens W, Adriaensens P. Protein Engineering For Directed Immobilization. Bioconj Chem. 2013;24(11):1761-77.

79. Vanlandschoot P, Stortelers C, Beirnaert E, Ibañez LI, Schepens B, Depla E, Saelens X. Nanobodies®: New ammunition to battle viruses. Antiviral Res. 2011;92(3):389-407.

80. Muyldermans S. Single domain camel antibodies: current status. Rev Mol Biotechnol. 2001;74(4):277-302.

81. Nguyen VK, Hamers R, Wyns L, Muyldermans S. Loss of splice consensus signal is responsible for the removal of the entire CH1 domain of the functional camel IGG2A heavy-chain antibodies1. Mol Immunol. 1999;36(8):515-24.

82. Arbabi Ghahroudi M, Desmyter A, Wyns L, Hamers R, Muyldermans S. Selection and identification of single domain antibody fragments from camel heavy-chain antibodies. FEBS Lett. 1997;414(3):521-6.

83. Hassanzadeh-Ghassabeh G, Devoogdt N, De Pauw P, Vincke C, Muyldermans S. Nanobodies and their potential applications. Nanomedicine. 2013;8(6):1013-26.

84. Nguyen VK, Hamers R, Wyns L, Muyldermans S. Camel heavy-chain antibodies: diverse germline VHH and specific mechanisms enlarge the antigen-binding repertoire. EMBO J. 2000;19(5):921-30.

85. Govaert J, Pellis M, Deschacht N, Vincke C, Conrath K, Muyldermans S, Saerens D. Dual Beneficial Effect of Interloop Disulfide Bond for Single Domain Antibody Fragments. J Biol Chem. 2012;287(3):1970-9.

86. Muyldermans S, Atarhouch T, Saldanha J, Barbosa JARG, Hamers R. Sequence and structure of VH domain from naturally occurring camel heavy chain immunoglobulins lacking light chains. Protein Eng. 1994;7(9):1129-35.

87. Conrath K, Vincke C, Stijlemans B, Schymkowitz J, Decanniere K, Wyns L, Muyldermans S, Loris R. Antigen Binding and Solubility Effects upon the Veneering of a Camel VHH in Framework-2 to Mimic a VH. J Mol Biol. 2005;350(1):112-25.

88. Muyldermans S, Baral TN, Retamozzo VC, De Baetselier P, De Genst E, Kinne J, Leonhardt H, Magez S, Nguyen VK, Revets H, Rothbauer U, Stijlemans B, Tillib S, Wernery U, Wyns L, Hassanzadeh-Ghassabeh G, Saerens D. Camelid immunoglobulins and nanobody technology. Vet Immunol Immunopathol. 2009;128(1–3):178-83.

89. Huang L, Reekmans G, Saerens D, Friedt J-M, Frederix F, Francis L, Muyldermans S, Campitelli A, Hoof CV. Prostate-specific antigen immunosensing based on mixed self-assembled monolayers, camel antibodies and colloidal gold enhanced sandwich assays. Biosensors Bioelectron. 2005;21(3):483-90.

90. Vincke C, Loris R, Saerens D, Martinez-Rodriguez S, Muyldermans S, Conrath K. General Strategy to Humanize a Camelid Single-domain Antibody and Identification of a Universal Humanized Nanobody Scaffold. J Biol Chem. 2009;284(5):3273-84.

91. Sukhanova A, Even-Desrumeaux K, Kisserli A, Tabary T, Reveil B, Millot J-M, Chames P, Baty D, Artemyev M, Oleinikov V, Pluot M, Cohen JHM, Nabiev I. Oriented conjugates of single-domain antibodies and quantum dots: toward a new generation of ultrasmall diagnostic nanoprobes. Nanomed Nanotechnol Biol Med. 2012;8(4):516-25.

92. Ta DT, Steen Redeker E, Billen B, Reekmans G, Sikulu J, Noben J-P, Guedens W, Adriaensens P. An efficient protocol towards site-specifically clickable nanobodies in high yield: cytoplasmic expression in Escherichia coli combined with intein-mediated protein ligation. Protein Eng Des Sel. 2015;28(10):351-63.

93. Vaneycken I, D'huyvetter M, Hernot S, De Vos J, Xavier C, Devoogdt N, Caveliers V, Lahoutte T. Immuno-imaging using nanobodies. Curr Opin Biotechnol. 2011;22(6):877-81.

94. Harmsen MM, De Haard HJ. Properties, production, and applications of camelid single-domain antibody fragments. Appl Microbiol Biotechnol. 2007;77(1):13-22.

95. Dumoulin M, Conrath K, Van Meirhaeghe A, Meersman F, Heremans K, Frenken LGJ, Muyldermans S, Wyns L, Matagne A. Single-domain antibody fragments with high conformational stability. Protein Sci. 2002;11(3):500-15.

96. Dumoulin M, Last AM, Desmyter A, Decanniere K, Canet D, Larsson G, Spencer A, Archer DB, Sasse J, Muyldermans S, Wyns L, Redfield C, Matagne A, Robinson CV, Dobson CM. A camelid antibody fragment inhibits the formation of amyloid fibrils by human lysozyme. Nature. 2003;424(6950):783-8.

97. Cortez-Retamozo V, Backmann N, Senter PD, Wernery U, De Baetselier P, Muyldermans S, Revets H. Efficient Cancer Therapy with a Nanobody-Based Conjugate. Cancer Res. 2004;64(8):2853-7.

98. De Groeve K, Deschacht N, De Koninck C, Caveliers V, Lahoutte T, Devoogdt N, Muyldermans S, De Baetselier P, Raes G. Nanobodies as Tools for In Vivo Imaging of Specific Immune Cell Types. J Nucl Med. 2010;51(5):782-9.

99. Baral TN, Magez S, Stijlemans B, Conrath K, Vanhollebeke B, Pays E, Muyldermans S, De Baetselier P. Experimental therapy of African trypanosomiasis with a nanobody-conjugated human trypanolytic factor. Nat Med. 2006;12(5):580-4.

100. Roovers RC, Laeremans T, Huang L, De Taeye S, Verkleij AJ, Revets H, de Haard HJ, van Bergen en Henegouwen MPP. Efficient inhibition of EGFR signalling and of tumour growth by antagonistic anti-EGFR Nanobodies. Cancer Immunol, Immunother. 2007;56(3):303-17.

101. Reichert JM, Valge-Archer VE. Development trends for monoclonal antibody cancer therapeutics. Nat Rev Drug Discov. 2007;6(5):349-56.

102. Van Impe K, Bethuyne J, Cool S, Impens F, Ruano-Gallego D, De Wever O, Vanloo B, Van Troys M, Lambein K, Boucherie C, Martens E, Zwaenepoel O, Hassanzadeh-Ghassabeh G, Vandekerckhove J, Gevaert K, Fernandez LA, Sanders N, Gettemans J. A nanobody targeting the F-actin capping protein CapG restrains breast cancer metastasis. Breast Cancer Res. 2013;15(6):R116.

103. Coppieters K, Dreier T, Silence K, Haard HD, Lauwereys M, Casteels P, Beirnaert E, Jonckheere H, Wiele CVD, Staelens L, Hostens J, Revets H, Remaut E, Elewaut D, Rottiers P. Formatted anti–tumor necrosis factor α VHH proteins derived from camelids show superior potency and targeting to inflamed joints in a murine model of collagen-induced arthritis. Arthritis Rheum. 2006;54(6):1856-66.
104. Verheesen P, ten Haaft MR, Lindner N, Verrips CT, de Haard JJW. Beneficial properties of single-domain antibody fragments for application in immunoaffinity purification and immuno-perfusion chromatography. Biochimica et Biophysica Acta (BBA) - General Subjects. 2003;1624(1–3):21-8.
105. Holten KB, Onusko EM. Appropriate prescribing of oral beta-lactam antibiotics. Am Fam Physician. 2000;62(3):611-20.
106. Shaikh S, Fatima J, Shakil S, Rizvi SMD, Kamal MA. Antibiotic resistance and extended spectrum beta-lactamases: Types, epidemiology and treatment. Saudi J Biol Sci. 2015;22(1):90-101.
107. Conrath KE, Lauwereys M, Galleni M, Matagne A, Frère J-M, Kinne J, Wyns L, Muyldermans S. β-Lactamase Inhibitors Derived from Single-Domain Antibody Fragments Elicited in the Camelidae. Antimicrob Agents Chemother. 2001;45(10):2807-12.
108. Saerens D, Pellis M, Loris R, Pardon E, Dumoulin M, Matagne A, Wyns L, Muyldermans S, Conrath K. Identification of a Universal VHH Framework to Graft Non-canonical Antigen-binding Loops of Camel Single-domain Antibodies. J Mol Biol. 2005;352(3):597-607.

Chapter 2

The clickability of site-specifically functionalized maltose binding protein

---

Part of this chapter is published in:

Vranken T, Steen Redeker E, Miszta A, Billen B, Hermens W, de Laat B, Adriaensens P, Guedens W, Cleij T. In situ monitoring and optimization of CuAAC-mediated protein functionalization of biosurfaces. Sens Actuators B Chem. 2017;238:992-1000. (IF:5,07)

Author contributions: The experimental work in this chapter was mainly performed by Billen B. Vranken T. contributed to the ellipsometry experiments and performed the silanisation and azidification of the silicon surfaces.

2.1 Introduction

The coupling of proteins to solid supports is playing an important role in modern biotechnology (1). In current biotechnological applications, biofunctionalization of substrates is mostly based on a non-oriented coupling of proteins, either by physical adsorption or by random covalent coupling via functional groups of the endogenous amino acid side chains (2). As a result, not all proteins have their active site(s) available for target binding, which can be a disadvantage when aiming for early diagnostics and miniaturization. Nowadays, only a few oriented couplings are reported, mostly based on affinity (3, 4). Attaching a click functionality site-specifically to proteins, however, combines the best of both worlds, i.e. a stable covalent and oriented coupling of the protein to a substrate. Click chemistry is interesting for the biofunctionalization of surfaces due to its bioorthogonal properties. Indeed, click functionalities are not present in nature, meaning that they do not interfere with biological processes, and the reaction can be performed under physiological conditions (5-8). An interesting approach for the site-specific functionalization of proteins with a click group is expressed protein ligation (EPL). This method offers control of the location (C- or N-terminus), the orientation of the protein and the stability of the coupling between the protein and the surface. All of these factors are expected to result in a high degree of reproducibility, sensitivity and specificity.

The most straightforward and well-known example of click chemistry is the copper (I)-catalyzed alkyne-azide cycloaddition (CuAAC) (6). Vranken et al. (2017) already successfully functionalized silicon surfaces with randomly alkynated *Staphylococcus aureus* protein A (SpA) by using CuAAC (9). They optimized the reaction conditions and monitored the reaction using ellipsometry. This confirms that CuAAC is indeed an interesting alternative to other covalent random coupling procedures like EDC/NHS (10) and offers an interesting platform to test the clickability of site-specifically alkynated proteins.

In this study maltose-binding protein (MBP) was used as a model protein to assess the clickability of site-specifically functionalized proteins. MBP is a protein with a molecular mass of ~ 42.5 kDa and the MBP expression vector for EPL (pMXB10) is commercially available and easy to manipulate, resulting in an accessible approach to produce high amounts of reference material. MBP contains 37 lysines, which is ideal for random functionalization as well, making it an ideal model protein as a preparation for nanobody (Nb) functionalization, as described in the next chapters. MBP was site-specifically functionalized with an alkyne group by EPL or randomly alkynated by an EDC/NHS coupling of an alkyne containing NHS ester that was bound to one or several of the 37 lysine groups on MBP. The EPL-modified MBP is supposed to bear only one alkyne functionality at its C-terminus, while the randomly functionalized MBP via EDC/NHS should contain multiple alkyne functionalities at lysine residues at random locations in the protein. Both proteins were subsequently coupled by a CuAAC reaction to an azide-functionalized silicon surface and the reaction was monitored using *in situ* ellipsometry.

2.2 Experimental section

2.2.1 Synthesis of a bifunctional linker for EPL

The synthesis of the bifunctional linker used in the EPL procedure is discussed in the experimental details (Chapter 5). The chemical structure of the linker is shown in Figure 2.1.

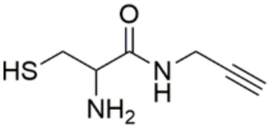

Figure 2.1: The chemical structure of the bifunctional linker 2-amino-3-mercapto-*N*-(prop-2-yn-1-yl)propanamide containing a thiol functionality (left) as a nucleophile and an alkyne click functionality (right) as a bioorthogonal group.

2.2.2 Site-specific alkynation of MBP using EPL

The C-terminal site-specific alkynation of MBP (ssA-MBP) was performed using EPL (11-13). Hereto, the pMXB10 plasmid was transformed in *E. coli* BL21(DE3) cells. The vector encodes for MBP (protein sequence MGRAMDMKTEEGKLVIWINGDKGYNGLAEVGKKFEKDTGIKVTVEHPDKLEEKFPQVAATGDGPDIIFWAHDRFGGYAQSGLLAEITPDKAFQDKLYPFTWDAVRYNGKLIAYPIAVEALSLIYNKDLLPNPPKTWEEIPALDKELKAKGKSALMFNLQEPYFTWPLIAADGGYAFKYENGKYDIKDVGVDNAGAKAGLTFLVDLIKNKHMNADTDYSIAEAAFNKGETAMTINGPWAWSNIDTSKVNYGVTVLPTFKGQPSKPFVGVLSAGINAASPNKELAKEFLENYLLTDEGLEAVNKDKPLGAVALKSYEEELAKDPRIAATMENAQKGEIMPNIPQMSAFWYAVRTAVINAASGRQTVDEALKDAQTNSSSKLGGREFLEY, theoretical pI: 5.1, MW: 42558.3 Da) by making use of the *E. coli* malE gene which is fused in-frame with the Mxe gyrase A intein domain and a chitin binding domain. The *E. coli* cells were grown overnight in Luria Broth (LB) medium, containing 100 µL/mL ampicillin at 37°C. The next day, the cultures were diluted in a larger volume of LB^{amp} and grown at 37°C to an optical density (OD_{600nm}) between 0.5 and 0.6. The protein expression was induced using isopropyl β-D-1-thiogalactopyranoside (IPTG) at a final concentration of 1 mM and an incubation at 37°C for 3 hours after which the bacteria were harvested by centrifugation at 5000 g for 10 min. The bacterial pellet was resuspended in B-PER solution containing 1 U/mL DNAseI. After 15 minutes of incubation at 21°C, the cell suspensions were centrifuged at 4°C for 30 minutes at 15000 g and the supernatant was collected.

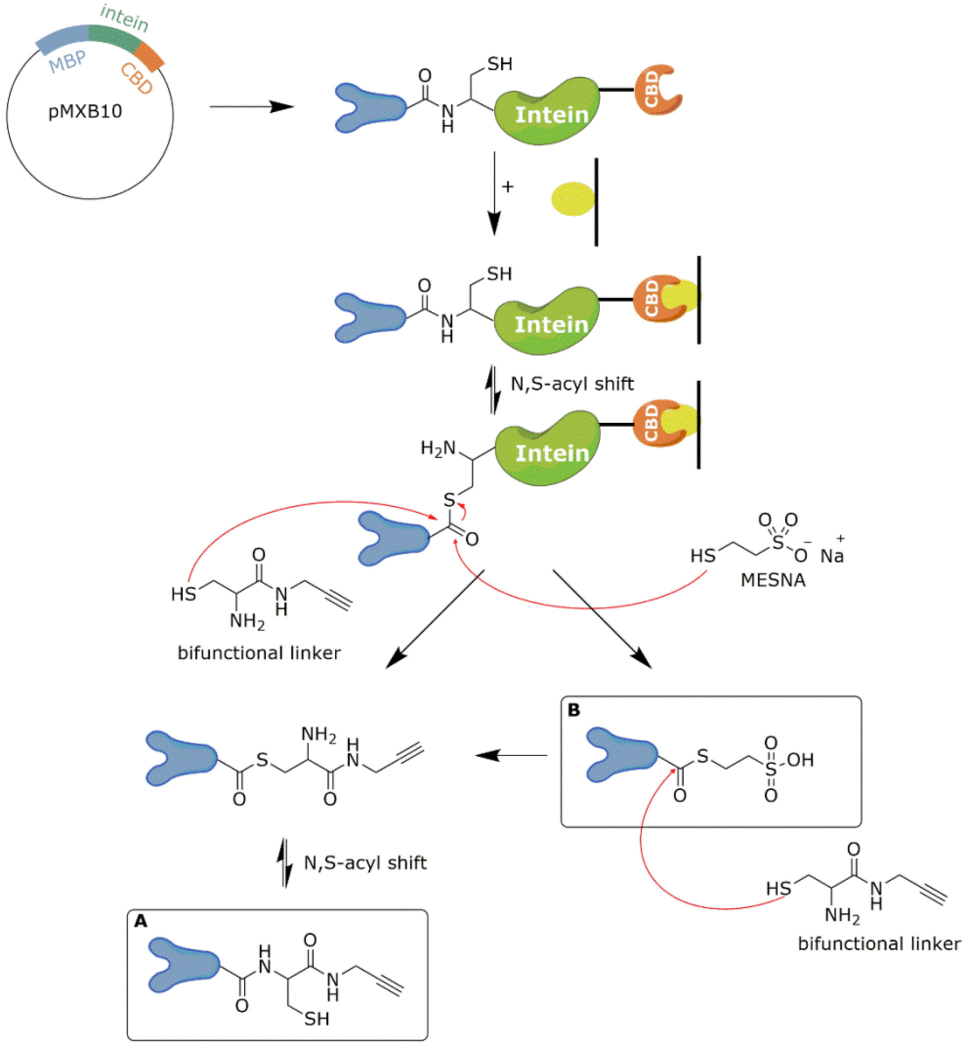

Figure 2.2: Site-specific alkynation of MBP using EPL. The MBP-intein-CBD complex was expressed in *E. coli* BL21(DE3) cells using the pMXB10 vector. After expression, the MBP-intein-CBD protein complex solution was divided in two parts and purified on two separate chitin columns that bind the CBD from the protein complex. Next, the intein will facilitate an N,S-acyl shift of the amide bond between MBP and the intein. The bifunctional linker 2-amino-3-mercapto-*N*-(prop-2-yn-1yl)propanamide reacts with the thioester bond between MBP and the intein, resulting in the splicing of MBP from the column and alkynation of MBP (**A**). To increase the reaction yield, a high concentration of 2-mercaptoethane sulfonate Na (MESNA) was added which also results in a splicing of the column followed by an exchange of MESNA with the bifunctional linker. As a negative control, no bifunctional linker was added resulting in non-alkynated MBP (**B**).

For the purification and functionalization of MBP (Figure 2.2), two separate columns containing chitin beads were equilibrated with 10 column volumes of running buffer (RB; 20 mM HEPES, 500 mM NaCl, 1 mM EDTA, pH 8.5). Afterwards, the bacterial supernatant was devided and slowly added to the columns. One column was incubated with 3 mL of RB supplemented with 1 mM of tris-(2-carboxyethyl)phosphine (TCEP) and 30 mM of 2-mercaptoethane sulfonate Na (MESNA) while a second column was incubated with RB supplemented with 30 mM TCEP, 30 mM MESNA and 1 mM of the bifunctional linker 2-amino-3-mercapto-*N*-(prop-2-yn-1-yl)propanamide.

After overnight incubation at 4°C, both columns were eluted with 3 mL RB. The eluate was further purified by size exclusion chromatography using Sephadex G-25 columns and eluted from the columns with PBS.

The MBP derived from column 1 (non-alkynated MBP) was used as a negative control and later on for the random alkynation experiment (see section 2.2.3) The MBP of the second column was the site-specifically functionalized MBP (ssA-MBP). The proteins were stored at -20°C until further use.

2.2.3 Random alkynation of MBP using an EDC/NHS coupling.

A 5.8-fold molar excess of 2,5-dioxopyrrolidin-1-yl-hex-5-ynoate (Figure 2.3), synthesized as described by Jagadish et al (14) and further referred to as the alkyne NHS ester, was added to a solution of MESNA functionalized MBP in PBS. The alkyne NHS reacts with the ε-amine group of lysine (and the N-terminal amine). Because of the 5.8-fold molar excess of the 2,5-dioxopyrrolidin-1-yl-hex-5-ynoate, 5.8 of the total available lysines were alkynated. There are 37 lysines in MBP so theoretically, this leads to a random alkyne functionalization of maximal 16% of the available lysines (rA-MBP) (15). In addition, a batch of theoretically fully alkynated MBP (fA-MBP) was obtained by adding a 54-fold molar excess of the alkyne NHS ester to a second MBP solution. After 3 hours, both reaction mixtures, containing rA-MBP or fA-MBP were filtered using Zeba micro spin desalting columns. The degree of functionalization was determined using mass spectrometry (see section 5.4.3).

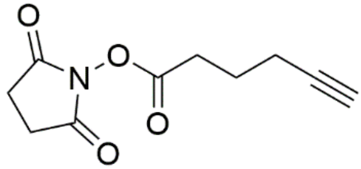

Figure 2.3: The chemical structure of the alkyne NHS ester 2,5-dioxopyrrolidin-1-yl-hex-5-ynoate (14).

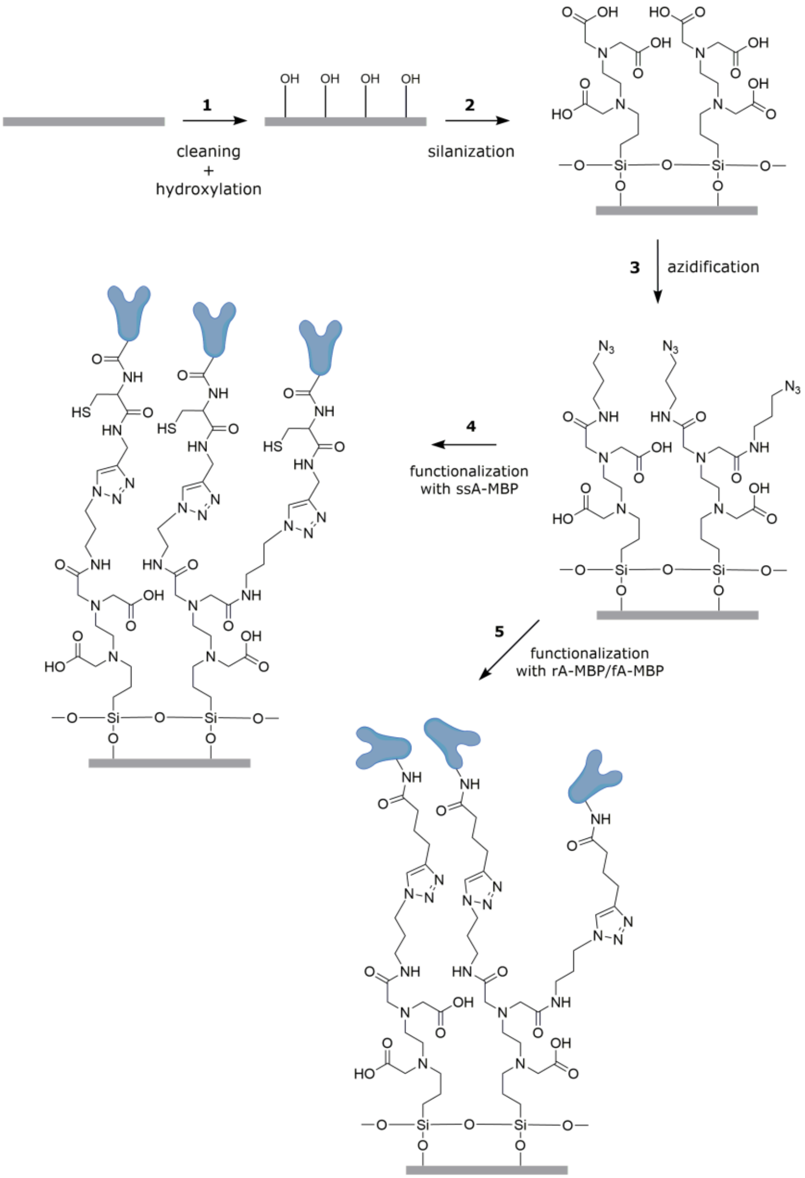
1
cleaning
+
hydroxylation
2
silanization
3
azidification
4
functionalization
with ssA-MBP
5
functionalization
with rA-MBP/fA-MBP

Figure 2.4: Biofunctionalization of silicon surfaces with ssA-MBP and rA-MBP/fA-MBP. First, the surface is cleaned and hydroxylated using piranha, hydrofluoric acid and a potassium dichromate solution (**1**). Next, the surface is silanized and carboxylated using *N*-(trimethoxysilylpropyl)ethylenediaminetriacetate trisodium salt (TMS-EDTA) (**2**) and an EDC/NHS reaction with 3-azido-1-aminopropane (AAP) was performed (**3**) to obtain an azide functionalized surface that is ready for a click reaction. Finally, a click reaction between ssA-MBP (**4**) or rA-MBP/fA-MBP (**5**) was executed and monitored by ellipsometry.

2.2.4 Silanization and subsequent carboxylation of silicon substrates

Prior to carboxylic functionalization, the silicon substrates (0.3x3.2 cm) were cleaned by means of a piranha solution (70:30 H_2SO_4:H_2O_2) during 5 minutes. After repeated rinsing with water, the substrates were dipped in a 6% (v/v) hydrofluoric acid solution in water. Again, the substrates were rinsed repeatedly with water and incubated in a 8% potassium dichromate (w/v) solution in 25% H_2SO_4 (v/v) at 70°C for 30 minutes. After rinsing with water and ethanol, the substrates were dried with nitrogen and ready for silanization (Figure 2.4).

A 10 µL drop of 6% (v/v) *N*-(trimethoxysilylpropyl)ethylenediaminetriacetate trisodium salt (TMS-EDTA) in sodium acetate buffer pH 4.0 was applied on the silicon substrate and incubated at 110°C for 1 hour. Afterwards, the excess TMS-EDTA and sodium acetate were washed away with water resulting in a carboxylated silicon surface.

In a third step, 3-azido-1-aminopropane (AAP), synthesized as described by Hatzakis et al. (16) was coupled to the surface by use of EDC/NHS coupling. The substrates were immersed into a mixture of 0.23 M AAP, 0.2 M EDC and 0.045 M NHS in HEPES buffer (220 mM HEPES, pH 6.8) for 3 hours. Afterwards, the remaining NHS esters were blocked by use of diethylene glycolamine for 45 minutes and rinsed with water. Finally, the slides were dried under a N_2 gas flow.

2.2.5 CuAAC reaction of alkynated MBP with azide-functionalized biotin

To test the clickability of ssA-MBP, the CuAAC reaction was performed in solution. To 200 µL PBS, containing purified ssA-MBP, an excess of azide-functionalized biotin (180 µM, dissolved in DMSO, Figure 2.5), 900 µM TCEP, 90 µM tris(benzyltriazolylmethyl)amine (TBTA, dissolved in DMSO) and 900 µM $CuSO_4$ was added. As a negative control, MESNA-functionalized MBP was used. After 2 hours of shaking at 21°C, the samples were analyzed by western blotting.

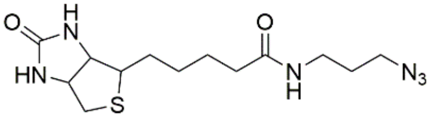

Figure 2.5: Chemical structure of the azide-functionalized biotin (MW=326.4).

2.2.6 Western blotting after MBP biotinylation

To visualize the reaction between ssA-MBP and biotin-azide, western blotting was performed. The reaction product was, without any further purification, boiled with

2x sodium dodecyl sulfate (SDS) sample buffer (125 mM Tris-HCl pH 6.8, 20% glycerol, 4% (w/v) SDS, 0.005% (w/v) bromophenol blue). Afterwards, gel electrophoreses was performed using a 12 % (w/v) acrylamide gel together with a molecular weight marker. After electrophoresis, the proteins were transferred to a polyvinylidene fluoride (pvdf) membrane by means of an overnight western blotting. The next day, the membrane was blocked in Bovine Serum Albumin (BSA) solution in Tris Buffered Saline Tween (TBST) for 2 hours. To visualize the biotinylated MBP, the membrane was incubated with streptavidin alkaline phosphatase (1/1000) in TBST, which will bind the biotinylated MBP, for 1 hour. Finally, the membrane was soaked for a few seconds in a bromo-4-chloro-3-indolyl-phosphate/nitro blue tetrazolium (BCIP/NTB) buffer that will be converted by the alkaline phosphatase on the protein into a purple precipitate visible on the membrane. The reaction is described in detail in Chapter 5.

2.2.7 Covalent CuAAC mediated immobilization of MBP to a silicon substrate via the DIP method

The rA-MBP, fA-MBP and ssA-MBP were coupled to the azide-functionalized silicon surface using CuAAC. To a solution of 1 µM MBP (rA-MBP, fA-MBP or ssA-MBP) in acetate buffer pH 4.0, 0.5 mM $CuSO_4$, 2.5 mM sodium ascorbate and 1 mM tris(3-hydroxypropyltriazolylmethyl)amine (THPTA) was added to a total volume of 400 µl (9). The azide functionalized silicon substrate was submerged in the click solution and the reaction was performed at room temperature during 30 minutes and monitored by *in situ* ellipsometry. Next, the substrates were rinsed with PBS, washing buffer (200 mM dihydrogen sodium phosphate, 200 mM sodium chloride, 150 mM ethylenediaminetetraacetic acid, and 50 mM ethanolamine at pH 7.5) and again PBS. To remove all non-covalently bound MBP, the substrates were incubated in a 0.5% (w/v) SDS solution (dissolved in MilliQ water) in the external incubator outside of the apparatus. The net mass increase was again measured in PBS.

2.2.8 Covalent CuAAC mediated immobilization of MBP to a silicon substrate via the DROP method

A drawback of the DIP method, as discussed in section 2.2.7, is the use of a relatively large volume of protein solution (400 µL) for the functionalization of a small silicon surface. To avoid protein waste, the DROP method was developed (Figure 2.6) that only requires a volume of 30 µL. This way, multiple click conditions can be tested with a reasonable amount of functionalized protein. The disadvantage of this technique is that the click reaction is performed outside the ellipsometer and the reaction cannot be monitored *in situ*.

Similar reagents and concentrations were used as described in section 2.2.7, only the total reaction volume was reduced from 400 µL to 30 µL. In order to test the effect of the click reagents (copper, reducing agent and ligand), the reaction was performed with the same concentration of ssA-MBP (1µM) but with respectively 2, 4, 6, 8 and 10 times more copper, as well as sodium ascorbate and THPTA. A baseline of each substrate was measured before applying the protein-click solution. After a reaction time of 30 minutes, the substrates were again placed in the ellipsometry device and washed with washing buffer and SDS as described in section 2.2.7. The final surface mass increase was measured in PBS and plotted as a function of the click reagents concentration.

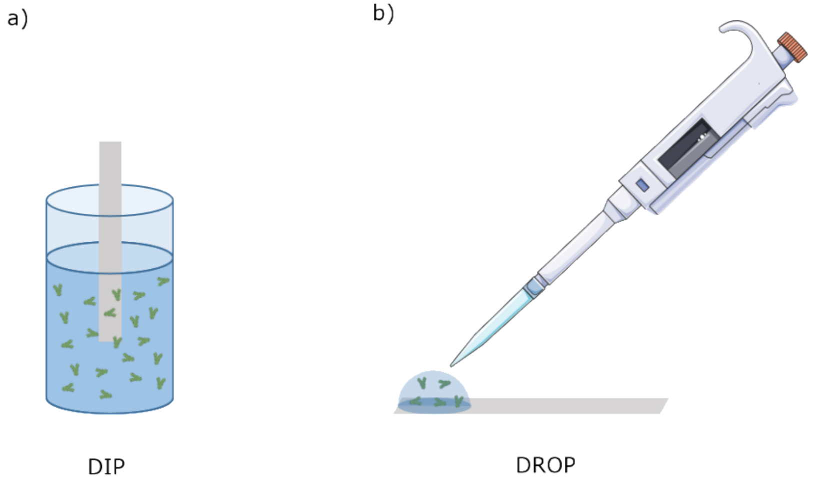

Figure 2.6: DIP versus DROP method. The DIP method (a) makes use of the small cuvettes in the ellipsometry device. The silicon slide is submerged in a large volume of protein-click solution. The DROP method (b) is designed to use less protein by adding a drop of protein-click solution on top of the silicon slide, outside of the ellipsometry device.

2.3 Results & discussion

2.3.1 Synthesis of the bifunctional linker

The synthesis of the bifunctional linker, 2-amino-3-mercapto-*N*-(prop-2-yn-1-yl)propanamide, is discussed in Chapter 5. The end product was analyzed using carbon-13 nuclear magnetic resonance (^{13}C NMR) spectroscopy, as shown in Figure 2.7.

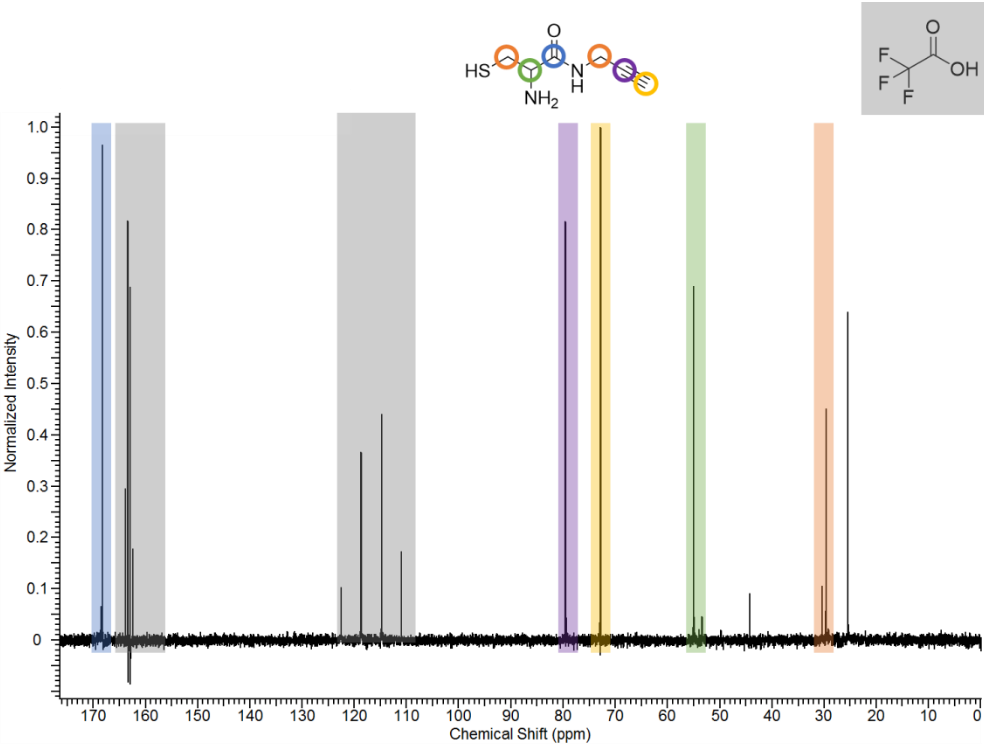

Figure 2.7: ^{13}C NMR spectrum of 2-amino-3-mercapto-*N*-(prop-2-yn-1-yl)propanamide. The trifluoroacetic acid (TFA) used for the deprotection of the Boc functionalities during synthesis is still present in the sample in a ratio of 1:1.6 2-amino-3-mercapto-N-(prop-2-yn-1-yl)propanamide:TFA.

Figure 2.7 shows that the synthesis was successful but that the trifluoroacetic acid (TFA) used during the synthesis for the removal of the protective Boc and trityl groups is still present. After integration of the peaks, a ratio of 1:1.6 2-amino-3-mercapto-*N*-(prop-2-yn-1-yl)propanamide:TFA was determined. Also some remnants of the Boc protection groups can be found in the sample at 44 and 26 ppm.

2.3.2 Site-specific alkynation of MBP and covalent coupling to azide-functionalized biotin

For the C-terminal site-specific alkynation of MBP, the EPL method was used as described in Figure 2.2. MBP was expressed as a complex with intein and a chitin-binding domain. After the expression, a cytoplasmic extraction of the bacteria was performed and the crude extract was divided in two parts and purified on separate chitin columns (column A and B) that bind the chitin binding domain of the protein complex (Figure 2.2, top). After extensive washing of the columns, the chitin resin only contains the MBP-intein-CBD protein complex. On these columns, an intein mediated N,S-acyl shift takes place. This results in a thioester bond between MBP and the intein. This thioester bond creates an unstable spot into the protein complex (Figure 2.2, middle) that is vulnerable for a nucleophilic attack by e.g. a thiol group. One column (column A) was treated with a bifunctional linker containing a thiol and an alkyne group (Figure 2.2, left). The thiol reacts with the carbon of the thioester bond in the protein and releases the protein off the column, containing an alkyne group (ssA-MBP). MESNA is used to increase the yield of the reaction (17-23). Literature indicates that MESNA is responsible for the cleavage of the protein from the intein and the bifunctional linker reacts subsequently with the thioester bond formed by MESNA. Besides MESNA, TCEP is added as a reducing agent. This reaction was performed with a yield of 21.7 mg/L. As a negative control (Figure 2.2, right) the experiment was also performed in the absence of a bifunctional linker (column B). This results in MESNA functionalized MBP (yield: 22.6 mg/L), which will be used for the random functionalization later on in this chapter.

To evaluate whether the ssA-MBP is able to click to an azide functionallity, the CuAAC reaction with azide-functionalized biotin was performed in solution. This is a fast way to find out if the MBP is functionalized with an alkyne function because click reactions in solution are much more straightforward than click reactions on a surface due to the reduced influence of steric hindrance (24) and preconcentration (25). To visualize this reaction, western blotting was used. If the CuAAC reaction succeeded, biotin is present at the C-terminus of MBP. This western blotting makes use of the high affinity of biotin for streptavidin by coupling streptavidin alkaline phosphatase to the biotinylated MBP. By adding BCIP/NTB buffer, a color reaction will appear if alkaline phosphatase (and consequently biotin) is present. This assay is therefore an indirect qualitative proof of the alkynation of MBP. The results of this experiment are visualized in Figure 2.8.

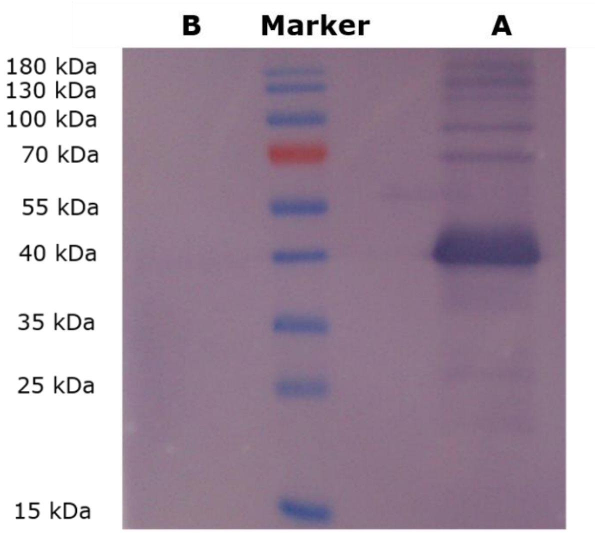

Figure 2.8: Western blotting results for ssA-MBP. The eluens of column B, the negative control, shows no visible bands on the pvdf membrane. The eluens of column A, containing the ssA-MBP shows a clear band around 40 kDa, indicating the presence of an alkyne group on the functionalized MBP.

The blot shows that the modified MBP synthesized in column A, ssA-MBP, contains an alkyne group, that has reacted with the biotin azide. This is a good qualitative indication that the functionalization was successful. Unfortunately, there are also bands visible at higher masses. This indicates the presence of side reactions such as the formation of dimers (band around 80 kDa). Although these bands were not visible on the original SDS-PAGE (data not shown), it indicates that these side reactions concern a small fraction of the modified protein.

To characterize alkynated MBP, randomly and site-specifically, electrospray ionization mass spectrometry (ESI-MS) was used. The theoretical mass of ssA-MBP is 42698.5 Da and the corresponding ESI-MS spectrum is represented in Figure 2.9. A large peak at 42559.4 Da dominates the spectrum. This peak covers a range of more than 50 Da and most probably corresponds to the mass of native MBP (42558.3 Da) or MESNA functionalized MBP without methionine (caused by post-translational modification). Although a peak for ssA-MBP is expected since the result of the western blotting is positive, no ssA-MBP signal is present in the ESI-MS spectrum. It is possible that a small peak for ssA-MBP, without methionine (theoretical mass: 42567.4 Da) is present but not visible due to the large peakt at 42559.4 Da. This means that the amount of ssA-MBP is too low to detect via ESI-MS and probably only a very small percentage of MBP was alkynated.

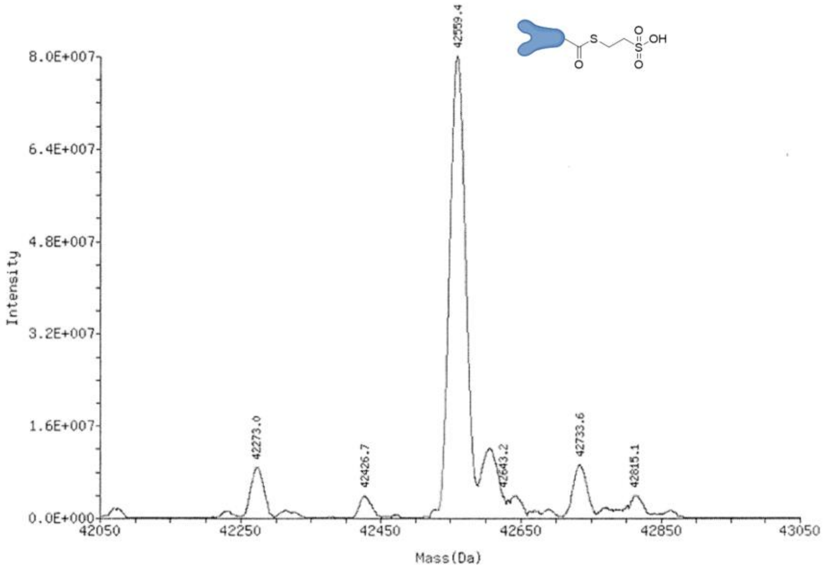

Figure 2.9: Electrospray ionization mass spectrometry spectrum of ssA-MBP. A dominating peak at 42559.4 Da is probably caused by native MBP or MESNA functionalized MBP without methionine.

However, rA-MBP and fA-MBP have a mass of 42682.5 Da, the mass of the MESNA modified protein, plus a mass of 95.1 Da per coupled alkyne functionality. In theory, the maximal amount of coupled alkynes is 5.8 for the rA-MBP and 37 for fA-MBP. The mass spectra are represented in Figure 2.10.

Figure 2.10a shows a small peak at 42560.1 Da which corresponds to the mass of the native MBP meaning that MESNA is not present anymore after the reaction or the N-terminal methionine spliced off due to post-translational modification during expression. Multiple peaks, with a difference of approximately 94 Da are visible in the rest of the spectrum. These peaks correspond with a functionalization degree of one or more alkyne groups. A similar pattern is visible in Figure 2.10b. However, no non-functionalized protein is present here. The minimal amount of functionalization is 4 alkyne groups, the maximum 9. This indicates a large difference in functionalization between the two functionalization conditions used to prepare rA-MBP and fA-MBP. Besides the large peaks, explained above, smaller peaks are visible which are not identified. Nevertheless, the functionalization degree is far from the theoretical maximum of 37, meaning that probably only 9 lysines at the surface of MBP are available for functionalization due to sterical hindrance, polarity, secondary structures and local electrostatic charges in the protein structure.

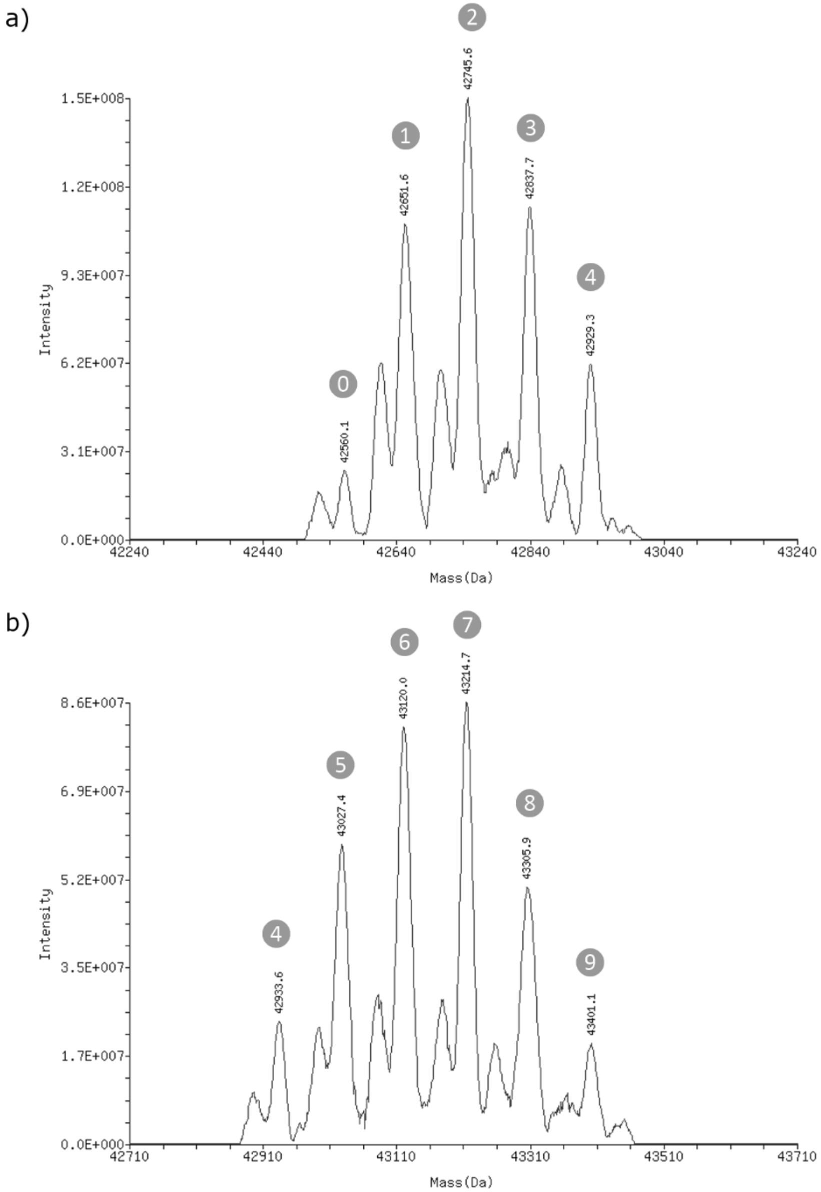

Figure 2.10: Electrospray ionization mass spectrometry spectra of (a) rA-MBP and (b) fA-MBP. rA-MBP, with a theoretical maximum of 5.8 alkyne functionalities, has a functionalization degree between 0 and 4 alkyne groups. The theoretically fully alkynated MBP with a maximum of 37 alkyne groups, has a functionalization degree between 4 and 9 alkyne functionalities. The green numbers indicate the amount of alkyne groups.

2.3.3 Covalent coupling of MBP to azide functionalized silicon substrates

To optimize the CuAAC reaction conditions and to test the specificity of the binding, a first ellipsometry experiment was performed using ssA-MBP and non-alkynated MBP (negative control). The efficiency of the washing steps could also be evaluated in this way. A baseline was recorded (not shown) and a click reaction was performed overnight in an external incubator. The results are plotted in Figure 2.11.

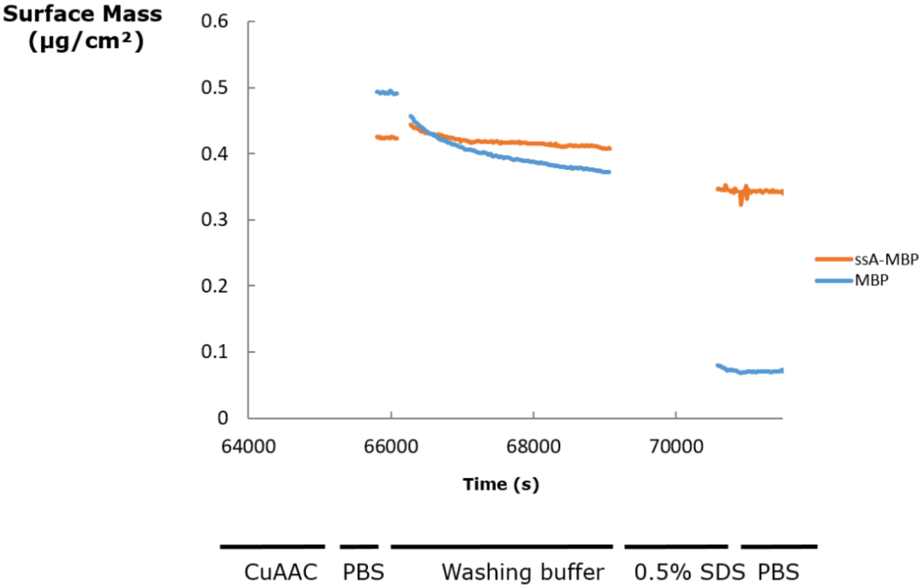

Figure 2.11: Real-time surface mass evolution monitored by *in situ* ellipsometry after the CuAAC click reaction between ssA-MBP and an azide functionalized silicon surface. Non-alkynated MBP was used as a negative control.

After the click reaction, both protein variants (MBP and ssA-MBP) are attached to the silicon substrate. To test if the bond is covalent (only possible for ssA-MBP), the surface was rinsed with PBS and the surface mass was measured in real time by *in situ* ellipsometry. This step only caused a stabilization of the signal but no significant changes. Next, the surface was rinsed with washing buffer to remove proteins from the surface that were physisorbed. Here, a decrease of the surface mass was measured for the non-functionalized protein. The surface mass of the silicon substrate containing ssA-MBP only dropped slightly, indicating that only a minor part of ssA-MBP is adsorbed to the surface. To remove all non-covalently bound proteins from the surface, the substrates were incubated in a 0.5% (w/v) SDS solution for 25 minutes. This will cause denaturation of the proteins and provide them with a negative charge. At pH 4, the charge of the surface will also be negative due to the remaining carboxylic acid groups on the surface (Figure 2.4). The result is that the charge interaction between the protein and the surface is disrupted and all non-covalently bound MBP will detach from the surface. Afterwards, the surfaces were rinsed with PBS. This will stabilize the signal and allow to measure the net surface mass increase caused by the covalently bound MBP. ssA-MBP caused a surface mass increase of 0.32 µg/cm². Still, the non-alkynated MBP caused an increase of 0.06 µg/cm² indicating a certain degree of binding between the protein and the surface that cannot be removed by the washing buffer and SDS treatment. Most likely, this is caused by the fact that MBP precipitates after overnight storage at pH 4 indicating a conformational alteration under influence of pH. To reduce this effect, the reaction time for further experiments was limited to 30 minutes.

Figure 2.12 shows a real time *in situ* monitoring by ellipsometry of the CuAAC click reaction of respectively ssA-MBP, fA-MBP and rA-MBP on three separate silicon substrates. All three alkynated protein species bind to the surface during the CuAAC reaction. After consecutive washing steps with washing buffer, 0.5% (w/v) SDS solution and PBS, respectively, all three protein species remain attached to the surface, indicating that they clicked covalently. As expected, more fA-MBP is bound to the surface than rA-MBP and more rA-MBP than ssA-MBP. This because the probability that the alkyne functionality “meets” an azide group is higher when there are more alkyne functionalities on the protein. As discussed earlier (Figure 2.10), the average degree of functionalization for fA-MBP is 6-7 alkynes, for rA-MBP 2 alkynes and for ssA-MBP only one alkyne. This can explain why the behavior of rA-MBP and ssA-MBP is more or less the same and clearly different from that of fA-MBP. Important to note is that, in comparison to the previous experiment described in Figure 2.11, the mass increase of ssA-MBP is lower in this experiment (0.19 µg/cm² versus 0.36 µg/cm² in the previous experiment). This can be explained by the difference in reaction time. In the previous experiment, the click reaction was performed overnight, while for this experiment it was performed in only 30 minutes. When taking a closer look at the binding curve of fA-MBP, a large bump is seen during the click reaction. The only difference compared with the other samples is the “overload” of alkyne functionalities in the proteins. This over-alkynation probably induces aggregation and/or precipitation of the proteins. It is well known from literature that modification of the lysine functionalities in proteins changes properties like pI and solubility. These changes can be associated with protein aggregation and precipitation (26, 27). With time, these aggregates dissolve slowly and a decrease in surface mass is noticed. The use of washing buffer removes the aggregates and precipitates and shows that a click reaction took place at the surface.

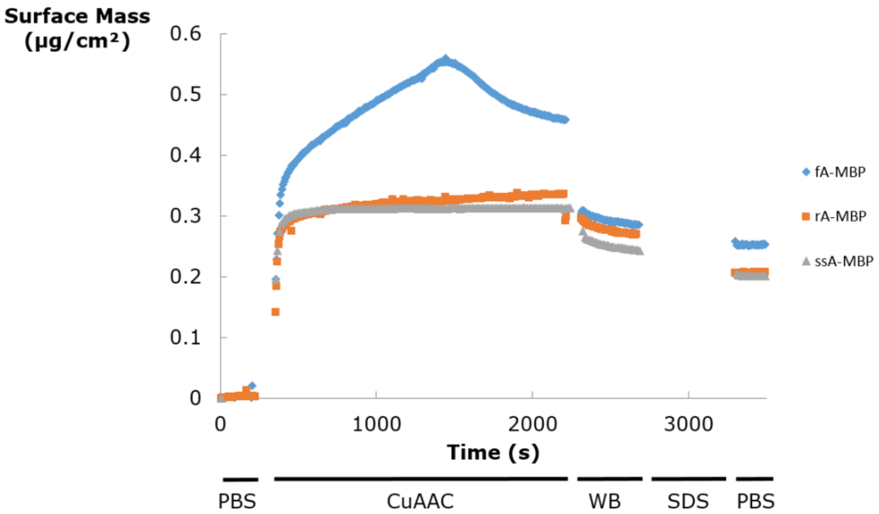

Figure 2.12: Real time *in situ* monitoring of the surface mass increase during the CuAAC reaction between different variants of alkynated MBP and azide functionalized silicon surfaces and subsequent rinsing steps with washing buffer (WB), 0.5% (w/v) SDS and PBS buffer.

To check if there is really a significant difference between the different functionalized species, the experiment was repeated multiple times and the standard deviation was calculated. The results are summarized in Figure 2.13.

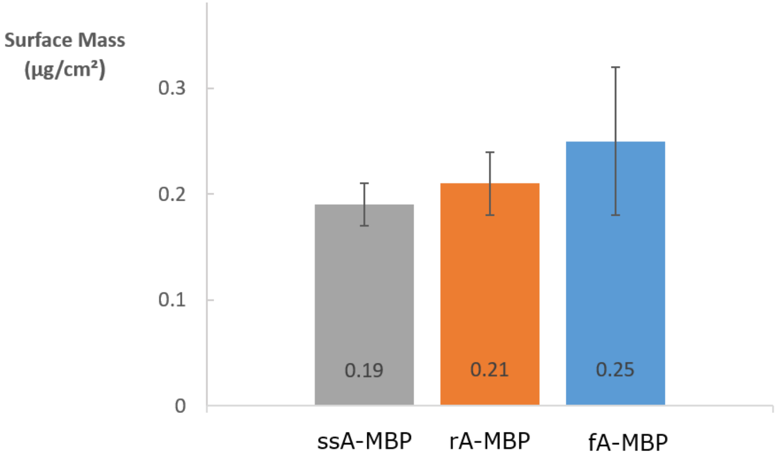

Figure 2.13: The average surface mass increase after a click reaction between different alkynated MBP variants and a silicon surface, measured using ellipsometry. No significant difference can be seen due to the relatively large standard deviation.

The oriented coupling of ssA-MBP led to an average surface mass increase of 0.19 µg/cm² ±0.02 (n=8). The rA-MBP has a similar surface average mass increase of 0.21 µg/cm² ±0.03 (n=3). A slightly higher value was measured for fA-MBP with an average surface mass increase of 0.25 µg/cm ±0.07. These values indicate that it is indeed possible to click alkynated protein to azide functionalized silicon surfaces. Furthermore, this indicates that one single, site-specifically introduced alkyne (ssA-MBP) is enough to create a biofunctionalized surface with a high reproducibility.

In order to reduce the waste of alkynated MBP by reducing the reaction volume, an alternative setup was tested for the click reaction on the silicon surface, the DROP method. Instead of dipping the surface into a vial with the click solution, a drop of click solution was added on the silicon surface as described in Figure 2.6. This method reduces the amount of protein by 92.5%. Unfortunately, due to the horizontal positioning of the silicon substrate in this experiment, real time ellipsometry of the click reaction on the surface was not possible. A baseline of the azide-functionalized silicon substrates was recorded prior to the click reaction and the surface mass was determined after the click reaction and several rinsing steps. This gives the net mass increase on the surface after the different steps.

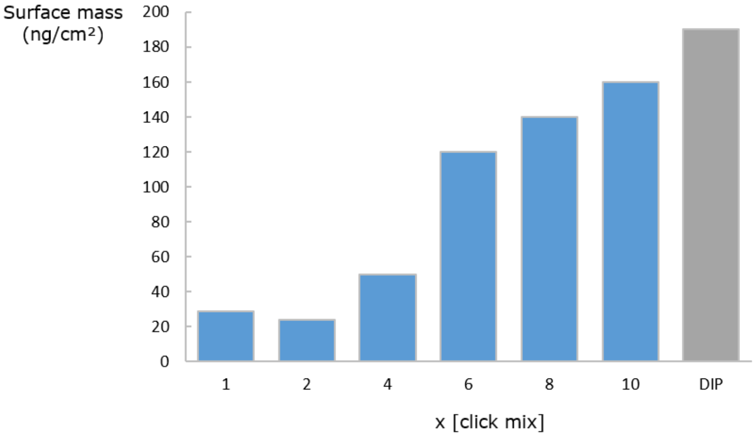

Figure 2.14: The net surface mass increase after the CuAAC click reaction between ssA-MBP and an azide-functionalized silicon surface using different concentrations of copper and corresponding concentrations of sodium ascorbate and THPTA ([click mix]). On the right, the mean surface mass increase using the DIP method is indicated.

Figure 2.14 gives an overview of the effect of the concentration of the click mix, respectively 2, 4, 6, 8 and 10 times more copper sulfate, sodium ascorbate and THPTA, on the surface mass increase, and consequently the click reaction of ssA-

MBP on the silicon surface. A clear trend is visible: the higher the concentration of click mix, the more protein clicks to the surface, especially when using more than 6 times the normal concentration of the click mix. Although the surface mass increase that is reached using the DIP method (Figure 2.14, grey bar) could not be reached using the DROP method and a 10 times higher concentration of click mix is required, it is possible to reach surface masses close to the average surface mass increase using the DIP method, and this by using 92.5% less alkynated protein. This results in a possible alternative for the DIP method that allows to reduce the amount of protein which is sometimes expensive and/or timeconsuming to produce.

2.4 Conclusions

Site-specific protein functionalization resulting in an oriented protein coupling is gaining importance in the field of biosensor development because of the positive effect on reproducibility, sensitivity and specificity. Therefore, CuAAC click chemistry is an interesting tool. As a proof of concept for the clickability of site-specific alkynated proteins, MBP was site-specifically alkynated using EPL (ssA-MBP) and randomly alkynated using EDC/NHS (rA-MBP and fA-MBP).

The expression of the ssA-MBP was successful with a reaction yield of more than 20 mg/L culture. Mass spectrometry could not give a distinctive answer about the amount of successful alkynated protein due to the small mass difference with non-alkynated MBP (MESNA-MBP). The introduction of an alkyne functionality at the C-terminus of MBP (ssA-MBP) was proven by performing a click coupling in solution with azide-functionalized biotin. The successful coupling was visualized using western blotting. This result confirms that MBP was successfully site-specifically alkynated and clickable to a complementary azide functionality.

On the other hand, random functionalization of MBP was illustrated by mass spectrometry by the presence of multiple peaks in the spectrum, each of them illustrating a certain amount of alkynes present on the protein. Finally, ellipsometry showed that all tested MBP variants (rA-MBP, fA-MBP and ssA-MBP) could be coupled to an azide-functionalized surface.

In conclusion, it is assumed that ssA-MBP can be coupled to a azide surface, in a practical amount, resulting in an oriented layer of MBP. By using the DROP method, only a very small amount of site-specifically oriented protein must be used, making it a very cost-efficient way to produce oriented protein surfaces and a promising platform for future biosensor development.

2.5 References

1. Busch K, Tampé R. Single molecule research on surfaces: from analytics to construction and back. Rev Mol Biotechnol. 2001;82(1):3-24.
2. Rusmini F, Zhong Z, Feijen J. Protein Immobilization Strategies for Protein Biochips. Biomacromolecules. 2007;8(6):1775-89.
3. Lin P-C, Weinrich D, Waldmann H. Protein Biochips: Oriented Surface Immobilization of Proteins. Macromol Chem Phys. 2010;211(2):136-44.
4. Trilling AK, Beekwilder J, Zuilhof H. Antibody orientation on biosensor surfaces: a minireview. Analyst. 2013;138(6):1619-27.
5. Sletten EM, Bertozzi CR. Bioorthogonal Chemistry: Fishing for Selectivity in a Sea of Functionality. Angew Chem Int Ed. 2009;48(38):6974-98.
6. Liang L, Astruc D. The copper(I)-catalyzed alkyne-azide cycloaddition (CuAAC) "click" reaction and its applications. An overview. Coord Chem Rev. 2011;255(23–24):2933-45.
7. Bock VD, Hiemstra H, van Maarseveen JH. CuI-Catalyzed Alkyne–Azide "Click" Cycloadditions from a Mechanistic and Synthetic Perspective. Eur J Org Chem. 2006;2006(1):51-68.
8. Nebhani L, Barner-Kowollik C. Orthogonal Transformations on Solid Substrates: Efficient Avenues to Surface Modification. Adv Mater. 2009;21(34):3442-68.
9. Vranken T, Steen Redeker E, Miszta A, Billen B, Hermens W, de Laat B, et al. In situ monitoring and optimization of CuAAC-mediated protein functionalization of biosurfaces. Sens Actuators B Chem. 2017;238:992-1000.
10. Gao Y, Kyratzis I. Covalent Immobilization of Proteins on Carbon Nanotubes Using the Cross-Linker 1-Ethyl-3-(3-dimethylaminopropyl)carbodiimide—a Critical Assessment. Bioconj Chem. 2008;19(10):1945-50.
11. Chong S, Mersha FB, Comb DG, Scott ME, Landry D, Vence LM, et al. Single-column purification of free recombinant proteins using a self-cleavable affinity tag derived from a protein splicing element. Gene. 1997;192(2):271-81.
12. Sletten EM, Bertozzi CR. Bioorthogonal Chemistry: Fishing for Selectivity in a Sea of Functionality. Angewandte Chemie-International Edition. 2009;48(38):6974-98.
13. Noren CJ, Wang J, Perler FB. Dissecting the Chemistry of Protein Splicing and Its Applications. Angew Chem Int Ed. 2000;39(3):450-66.
14. Jagadish B, Sankaranarayanan R, Xu L, Richards R, Vagner J, Hruby VJ, et al. Squalene-derived flexible linkers for bioactive peptides. Bioorg Med Chem Lett. 2007;17(12):3310-3.

15. Duplay P, Bedouelle H, Fowler A, Zabin I, Saurin W, Hofnung M. Sequences of the malE gene and of its product, the maltose-binding protein of Escherichia coli K12. J Biol Chem. 1984;259(16):10606-13.
16. Hatzakis NS, Engelkamp H, Velonia K, Hofkens J, Christianen PCM, Svendsen A, et al. Synthesis and single enzyme activity of a clicked lipase-BSA hetero-dimer. Chem Commun. 2006(19):2012-4.
17. Reulen SWA, Brusselaars WWT, Langereis S, Mulder WJM, Breurken M, Merkx M. Protein−Liposome Conjugates Using Cysteine-Lipids And Native Chemical Ligation. Bioconj Chem. 2007;18(2):590-6.
18. Reulen S, van Baal I, Raats J, Merkx M. Efficient, chemoselective synthesis of immunomicelles using single-domain antibodies with a C-terminal thioester. BMC Biotechnol. 2009;9(1):66-74.
19. Chattopadhaya S, Abu Bakar FB, Yao SQ. Use of Intein-Mediated Protein Ligation Strategies for the Fabrication of Functional Protein Arrays. Methods in Enzymology: Non-Natural Amino Acids. 2009;462:195-223.
20. Ghosh I, Considine N, Maunus E, Sun L, Zhang A, Buswell J, et al. Site-specific protein labeling by intein-mediated protein ligation. Methods Mol Biol. 2011;705:87-107.
21. Johnson ECB, Kent SBH. Insights into the Mechanism and Catalysis of the Native Chemical Ligation Reaction. J Am Chem Soc. 2006;128(20):6640-6.
22. Seyedsayamdost MR, Yee CS, Stubbe J. Site-specific incorporation of fluorotyrosines into the R2 subunit of E. coli ribonucleotide reductase by expressed protein ligation. Nat Protocols. 2007;2(5):1225-35.
23. Hauser PS, Ryan RO. Expressed protein ligation using an N-terminal cysteine containing fragment generated in vivo from a pelB fusion protein. Protein Expression Purif. 2007;54(2):227-33.
24. Hein CD, Liu XM, Wang D. Click chemistry, a powerful tool for pharmaceutical sciences. Pharm Res. 2008;25(10):2216-30.
25. Fischer ME. Amine Coupling Through EDC/NHS: A Practical Approach. In: Mol NJ, Fischer MJE, editors. Surface Plasmon Resonance. Methods in Molecular Biology. 627: Humana Press; 2010. p. 55-73.
26. Walter TS, Meier C, Assenberg R, Au K-F, Ren J, Verma A, et al. Lysine Methylation as a Routine Rescue Strategy for Protein Crystallization. Structure. 2006;14(11):1617-22.
27. Tan K, Kim Y, Hatzos-Skintges C, Chang C, Cuff M, Chhor G, et al. Salvage of Failed Protein Targets by Reductive Alkylation. In: Anderson FW, editor. Structural Genomics and Drug Discovery: Methods and Protocols. New York, NY: Springer New York; 2014. p. 189-200.

Chapter 3

Site-specific protein alkynation by expressed protein ligation using alternative nucleophiles

3.1 Introduction

As described in the previous chapters, the site-specific C-terminal functionalization of proteins with a bioorthogonal group by means of expressed protein ligation (EPL) makes use of a bifunctional linker. This linker contains a functional group that acts as a nucleophile in the reaction with the thioester bond between the protein of interest (POI) and the intein that is formed during the EPL process. The linker further contains a bioorthogonal group, for example an alkyne functionality for click coupling to a complementary azide functionality. In this way, the nucleophilic cleavage of the POI from the intein-CBD complex goes together with its functionalization in the same reaction pathway (1-3). In the standard protocol, a thiol group is used as the nucleophile. In addition, MESNA is commonly used to increase the reaction yield. Literature indicates that by using an excess of MESNA, not only the bifunctional linker is responsible for the splicing of the thioester bond between the POI and the intein, but also MESNA is. This initially results in MESNA functionalized proteins and the nucleophile of the bifunctional linker will react with the newly formed thioester bond. By using this approach, an additional reaction step is introduced (4-9).

Another disadvantage of using thiol-based nucleophiles in EPL is the remaining C-terminal thiol group which can form disulfide bridges with other modified proteins, leading to dimer formation (Figure 3.1a).

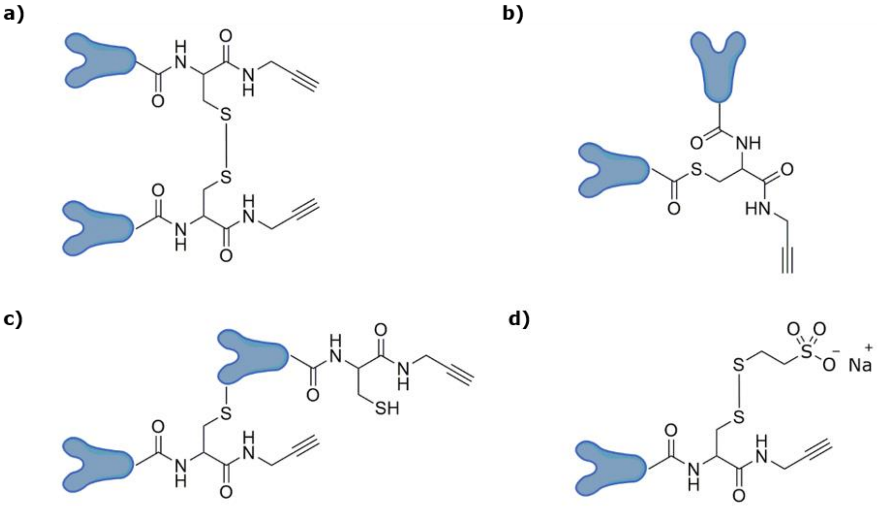

Figure 3.1: Possible side reactions caused by an additional thiol group: the formation of dimers via a disulfide bridge between the additional thiol groups of two modified proteins (**a**), the nucleophilic attack of an introduced cysteine on the thioester bond of a protein-intein-CBD complex which is still on the column (**b**), the formation of a disulfide bridge between an introduced thiol and an endogenous cysteine (**c**) or MESNA (**d**).

It is also possible that during the EPL process, the remaining thiol group attacks the thioester bond of a protein, which is still on the column resulting also in the covalent connection of two proteins (Figure 3.1b). In theory, it is even possible that the thiol group forms a disulfide bridge with a native cysteine of the protein, which results in malformation of the protein (Figure 3.1c). The use of MESNA in the EPL process can also result in the formation of a disulfide bridge between the MESNA and the native cysteine of the protein (Figure 3.1d).

Due to these drawbacks, we investigated the use of bifunctional linkers with alternative nucleophiles for EPL. Kalia et al. (10) investigated the possibility to use nitrogen-based nucleophiles instead of sulfur-based nucleophiles. These nucleophiles will be called in general amine-based nucleophiles in this thesis. In theory, several amine-based nucleophiles are capable to react directly with the thioester bond between the POI and the intein-CBD complex due to their nucleophilicity at neutral pH.

Table 3.1: pKa values of the conjugate acids from amine-based nucleophiles.

Nucleophile	pK_a	Source
CH_3ONH_2	4.60	(11)
$C_2H_5O(O)CCH_2NHNH_2$	6.45	(12)
CH_3NHNH_2	7.87	(13)
$HOCH_2CH_2NH_2$	9.50	(11)

Kalia et al. performed a kinetic study on a chromogenic thioester with different nitrogen-based nucleophiles and concluded that, at neutral pH, α-hydrazine acetyl and alkyl hydrazine functionalities (Figure 3.2) have a much higher nucleophilicity than simple amines and alkoxy amines. This can be explained by the α-effect (10, 14, 15) that increases the nucleophilicity by the presence of an adjacent α-atom (in this case a N-atom) that contains lone pair electrons.Therefore, nitrogen-based nucleophiles might be very suitable as nucleophiles for EPL reactions.

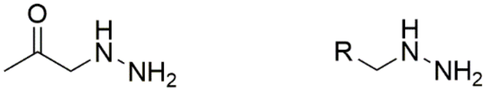

Figure 3.2: The chemical structure of α-hydrazine acetyl (left) and alkyl hydrazine (right) functionalities.

Based on the results of Kalia et al., 2-hydrazinyl-*N*-(prop-2-yn-1-yl)acetamide (Figure 3.3), a bifunctional linker containing an α-hydrazino acetamido group and an alkyne, was synthesized and evaluated for EPL.

To investigate the effect of MESNA in EPL reactions and the possibility to use an amine-based nucleophile instead of a thiol-based nucleophile, maltose-binding protein (MBP, 42 kDa) was used as a model protein. As discussed in Chapter 2, MBP is a well-described protein (16-19) and the vector containing the MBP-intein-CBD construct is commercially available and known as the pMXB10 vector. The EPL reaction was performed in the presence and absence of MESNA. To evaluate the amine-based bifunctional linker, the different conditions in the EPL reaction (pH, temperature, incubation time) were optimized, taking into account that a thioester bond is also sensitive to pH dependent hydrolysis (20). Therefore, a compromise has to be found between the amount of hydrolysis and the amount of site-specific functionalization.

Since the final goal of this thesis is the site-specific functionalization of nanobodies (Nbs), also a nanobody against β-lactamase, called nanobody BcII10 (NbBcII10) was used as a model. The reaction conditions optimized for MBP were applied to this NbBcII10.

3.2 Experimental section

3.2.1 Synthesis of the bifunctional linkers

The full synthesis of both bifunctional linkers (Figure 3.3) is described in Chapter 5. The chemical structure of the end-products is shown in Figure 3.3.

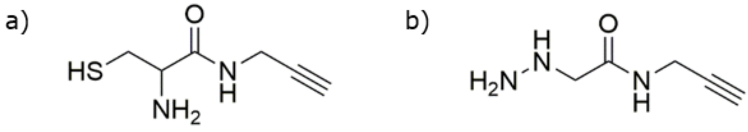

Figure 3.3: The chemical structure of (**a**) the thiol-based bifunctional linker 2-amino-3-mercapto-*N*-(prop-2-yn-1-yl)propanamide and (**b**) the amine-based bifunctional linker 2-hydrazinyl-*N*-(prop-2-yn-1-yl)acetamide.

3.2.2 The expression of the MBP-intein-CBD complex

The pMXB10 plasmid that carries the *E. coli* malE gene fused in frame with the coding region of the Mxe gyrase A intein-chitin binding domain was transformed into competent *E. coli* BL21(DE3) cells. The chitin-binding domain (CBD) was added for purification purposes. An overnight culture was diluted in fresh LB^{amp}, grown at 37 °C and 220 rpm to an optical density (OD_{600nm}) between 0.5 and 0.6. Protein expression was induced by adding IPTG to a final concentration of 1 mM and incubating at 37 °C for 3 hours while shaking. The cells were harvested by centrifugation and resuspended in B-PER solution (containing 1U/mL DNAseI) for cell lysis. The resulting cell suspension was centrifuged and the supernatant was collected for further purification.

3.2.3 Standard protocol for the alkyne functionalization of MBP using EPL

The purification and click functionalization of MBP was done with a column containing chitin beads. The column was equilibrated with 10 column volumes of running buffer (RB; 20 mM HEPES, 500 mM NaCl, 1 mM EDTA, pH 8.5). After equilibration, the cell supernatant was added slowly to the column and drained by gravitational force giving the CBD the chance to bind to the column. Next, the column was washed with 20 column volumes of RB to remove all the non-bonded proteins present in the supernatant (those without a CBD).

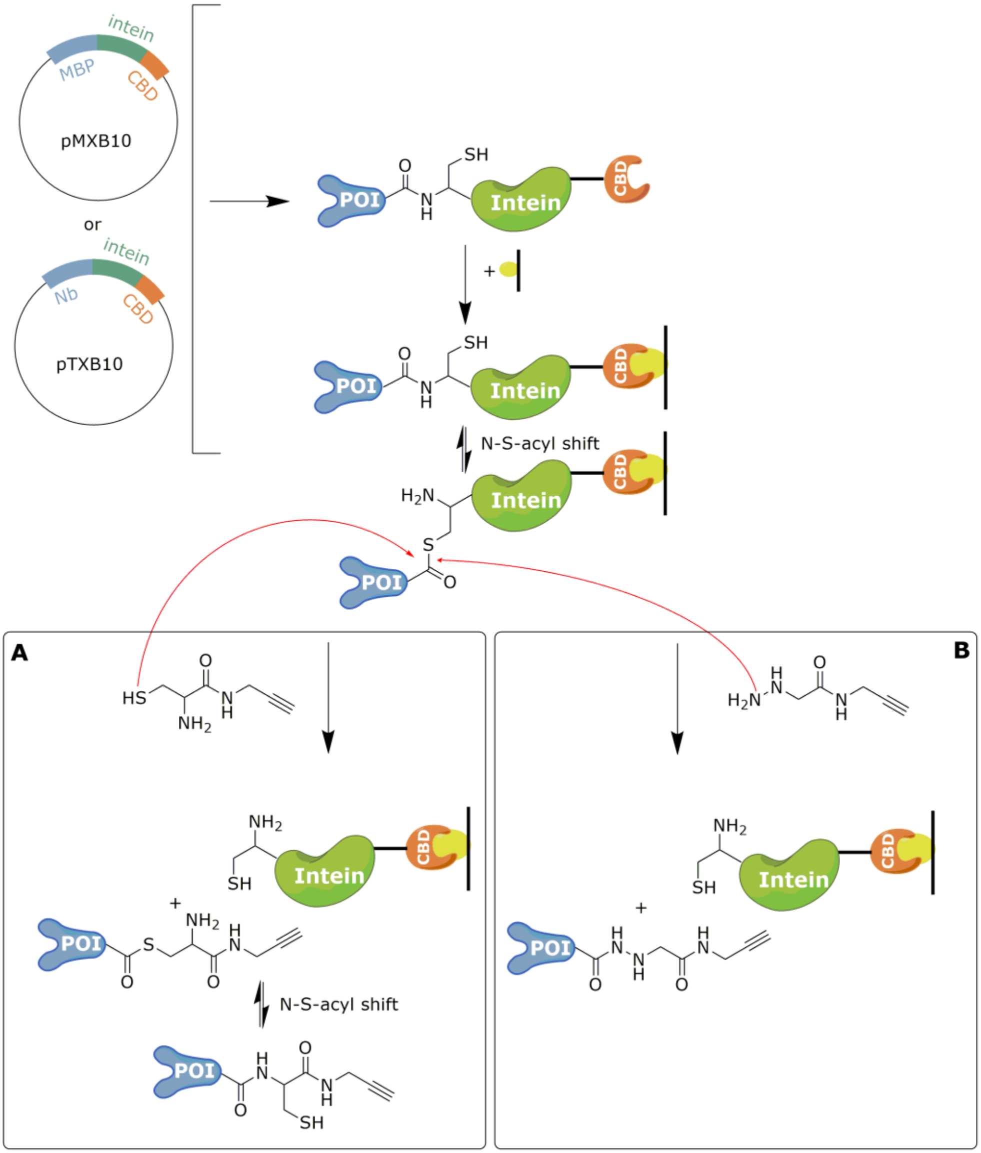
intein
MBP
CBD
pMXB10
or
intein
Nb
CBD
pTXB10
POI
Intein
CBD
SH
+
N-S-acyl shift
H2N
S
O
A
HS
NH2
SH
N-S-acyl shift
B
H2N
+

Figure 3.4: Expressed protein ligation. The proteins of interest (= MBP or NbBcII10) were expressed in their respective vectors in E. coli BL21DE3. After cell extraction, the proteins were purified using a chitin column where the N,S-acyl shift occurs. Classical EPL (pathway **A**) uses a thiol-based bifunctional linker; pathway **B** shows the nucleophilic reaction between an amine-based bifunctional linker and the intein-derived thioester bond of the protein complex.

MBP was eluted and functionalized by rinsing the column with 2 column volumes of cleavage buffer. The cleavage buffers used are summarized in Table 3.2.

Table 3.2: An overview of the different cleavage buffers (CB) used for EPL. All the components were dissolved in running buffer (pH 8.5).

CB1	MESNA*
CB2	MESNA*, TCEP°, 1 mM thiol-based bifunctional linker
CB3	MESNA*, TCEP°, 2 mM amine-based bifunctional linker
CB4	MESNA*, TCEP°, 5 mM amine-based bifunctional linker
CB5	MESNA*, TCEP°, 10 mM amine-based bifunctional linker
CB6	TCEP°, 1 mM thiol-based bifunctional linker
CB7	TCEP°, 2 mM amine-based bifunctional linker
CB8	TCEP°, 5 mM amine-based bifunctional linker
CB9	TCEP°, 10 mM amine-based bifunctional linker

*30 mM; °1 mM

After 16 hours of incubation with the cleavage buffer at 4 °C, the columns were eluted with 1.5 column volume of RB. The proteins were purified by size exclusion chromatography using sephadex G-25 columns and PBS as elution buffer. This protocol is further noted as the standard EPL protocol.

In order to increase the yield of the functionalization reaction, the influence of pH values (pH 6 – 9), incubation time (16 and 40 h) and temperature (4, 21 and 37°C) was tested. The protein concentration was determined with UV-Vis at 280 nm using $\varepsilon_{280\ nm}$ = 66000 $M^{-1}cm^{-1}$.

3.2.4 Optimization of the pH for alkyne functionalization of MBP using EPL

A chitin column, containing the bound MBP-intein-CBD complex prepared as discussed in section 3.2.3 was incubated with RB instead of CB at 4 different pH values (pH 6.0, 7.0, 8.0 and 9.0) for 16 h at 4°C to test the effect of hydrolysis on the MBP-intein-CBD complex. After elution of the samples with RB, the protein concentration in the buffer was determined with UV-Vis spectroscopy at 280 nm. This concentration represents the amount of hydrolyzed, non-functionalized MBP.

To evaluate the effect of pH on the nucleophilic reaction of the bifunctional linkers with the thioester bond between MBP and the intein, the modification of MBP was performed using the standard EPL protocol (section 3.2.3). The columns were incubated with respectively CB6 and CB7. The pH of these cleavage buffers was varied between 6.0 and 9.0. After purification using sephadex G-25 purification columns and PBS, the concentration was measured by UV-Vis spectroscopy at 280 nm.

3.2.5 Optimization of the incubation conditions for alkyne functionalization of MBP using EPL

In addition to the effect of pH, the incubation time and temperature can also influence the amount of non-specific off column splicing by hydrolysis. To test the effect of these parameters, the standard EPL protocol (section 3.2.3) was used. Six conditions were compared by incubating the beads at 4 , 21 and 30°C, for 16 or 40 h with RB instead of CB.

To evaluate the effect of incubation temperature and time on the functionalization reaction, the standard EPL protocol (section 3.2.3) was applied using CB7 for an incubation time of 16 or 40 h and at a temperature of 4 or 21°C.

3.2.6 The expression of the NbBcII10-intein-CBD complex

pTXB1:NbBcII10-LEY-intein-CBD (Construct 7 described in 5.2.2.1), was transformed into competent *E.coli* BL21(DE3) cells. An overnight culture of these cells in LB^{amp} was diluted in a large volume and grown to an OD_{600nm} between 0.5 and 0.6 at 37 °C, 220 rpm. Protein expression (protein sequence NbBcII10-LEY: MQVQLVESGGGSVQAGGSLRLSCTASGGSEYSYSTFSLGWFRQAPGQEREAVAAIASMG GLTYYADSVKGRFTISRDNAKNTVTLQMNNLKPEDTAIYYCAAVRGYFMRLPSSHNFRYW GQGTQVTVSSLEY, theoretical pI: 8.62, MW: 14366.0 Da), cell harvesting and cell lysis were performed as described for MBP (Section 3.2.2).

3.2.7 Functionalization of NbBcII10 using EPL

Purification and modification of NbBcII10 was performed by means of chitin beads. Four columns were packed with 2 mL of 50% chitin slurry and equilibrated with 10 column volumes of RB. The cell supernatant was divided in four equal parts and each part was added slowly to a column and drained by gravitational force. After rinsing with 20 column volumes of RB, NbBcII10 was flushed with 2 column volumes of 4 different cleavage buffers (CB1, CB2 and CB7), one for each of the four columns. Following overnight incubation at 4°C, the columns were eluted by 2 mL RB and the eluents were dialyzed against PBS and concentrated using Amicon® Ultra 2 mL Centrifugal Filters with a molecular weight cut-off of 3 kDa.

In order to test whether higher concentrations of the amine-based bifunctional linker were more efficient for the site-specific modification of NbBcII10, 20 µL of the MESNA-modified NbBcII10 (CB1) was incubated with respectively 50 mM and 100 mM amine-based bifunctional linker for 16 h at 4°C. This way, NbBcII10 could be incubated with very high concentrations of the thiol-based bifunctional linker without using very large amounts of the synthesized linker.

3.2.8 Click reaction in solution between modified MBP and azide functionalized biotin

In order to check whether the ligation was successful, the CuAAC reaction was performed between the modified MBP and an azide-functionalized biotin derivative. This was done by adding an excess of the azide-functionalized biotin derivative (180 µM, dissolved in DMSO, Figure 2.5), 900 µM TCEP, 90 µM TBTA (dissolved in DMSO) and 900 µM $CuSO_4$ to 200 µL of the purified MBP solution (1.82 µM for the samples with MESNA and 0.76 µM for the samples without MESNA) and shaking it at room temperature for 2 hours.

As a negative control, the reaction was performed with non-functionalized MBP (CB1). Additionally, the reaction was executed with alkynated MBP, obtained using CB2, but without the use of copper catalyst.

3.2.9 Western blotting after MBP biotinylation

After the click reaction, as discussed in section 2.2.5, the alkynated MBP is biotinylated. The samples were boiled with 2x SDS sample buffer and loaded on a 12% acrylamide gel for gel electrophoresis (1.5 hour at 120 V) together with a molecular weight marker (ThermoFisher PageRuler™ Prestained Protein Ladder). An overnight western blotting was performed at 20 V to transfer the MBP on a polyvinylidene fluoride (pvdf) membrane. The membrane was blocked in 5% (w/v) Bovine Serum Albumin (BSA) solution in Tris Buffered Saline Tween (TBST) for 2 hours and incubated with streptavidin alkaline phosphatase (1/1000) in TBST for 1 hour. The streptavidin will bind to the biotin. Only the alkynated MBP will have biotin meaning that the streptavidin will only bind to the alkynated MBP. Afterwards, the membrane was soaked in a 5-bromo-4-chloro-3-indolyl-phosphate/nitro blue tetrazolium (BCIP/NTB) buffer for a few seconds until the bands were visible. The full mechanism of this reaction is described in Chapter 5.

3.2.10 Covalent CuAAC mediated immobilization of MBP to a silicon substrate

The silicon substrates were functionalized with 3-azido-1-aminopropane (AAP) as described in Chapter 2.

Site-specifically alkynated MBP (ssA*-MBP, were the * indicates the use of an amine-based biofunctional linker) was produced by EPL using the standard protocol and CB7 as a cleavage buffer. MBP produced by CB1 was used as a negative control. The samples were filtered using size exclusion chromatography (Sephadex G25) and stored in PBS. To a solution of 0.25 µM of ssA*-MBP (diluted in sodium acetate buffer pH 4), 0.5 mM $CuSO_4$, 2.5 mM sodium L-ascorbate and 1 mM THPTA were added. The click reaction was monitored for 90 min by in situ ellipsometry (in duplo). Next, the substrates were washed with PBS, washing buffer and PBS. Finally, the substrates were incubated for 20 minutes in MilliQ water containing 0.5% (w/v) SDS outside of the apparatus. The final mass increase was again measured in PBS.

3.3 Results & discussion

3.3.1 Synthesis of the bifunctional linker

To modify MBP with a C-terminal alkyne group (MBP-alkyne) via the EPL method, two bifunctional linkers were synthesized as described in Chapter 5.

The results of the synthesis of the thiol-based bifunctional linker (2-amino-3-mercapto-*N*-(prop-2-yn-1-yl)propanamide) are already discussed in Chapter 2. Figure 3.5 shows the ^{13}C NMR spectrum of the amine-based bifunctional linker 2-hydrazinyl-*N*-(prop-2-yn-1-yl)acetamide, which showed no significant impurities expect for small amounts of remnants of trifluoroacetic acid (TFA).

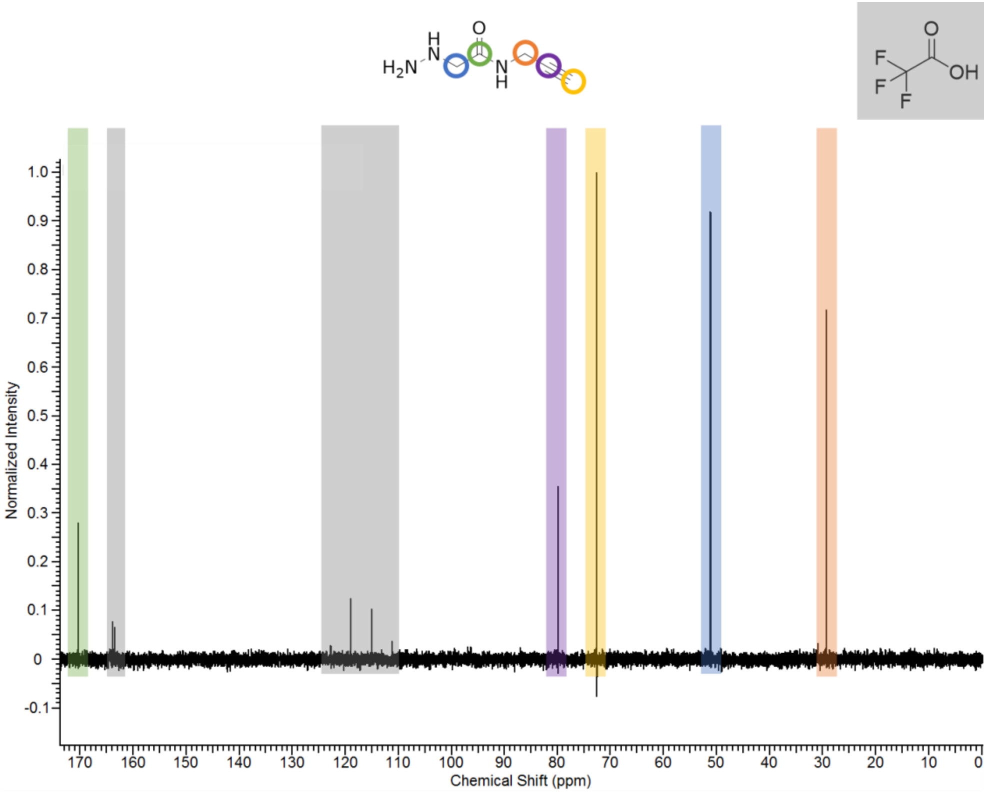

Figure 3.5: ^{13}C NMR spectrum of 2-hydrazinyl-*N*-(prop-2-yn-1-yl)acetamide. Some of the trifluoroacetic acid (TFA) used for the deprotection of the Boc functionality during synthesis was still present.

3.3.2 The effect of MESNA on the EPL process

The classical EPL pathway was already discussed in Chapter 2. In brief, after expression of the MBP-intein-CBD complex and the N,S-acyl shift, a bifunctional linker (thiol or amine based) is added to the column and the nucleophilic part of the bifunctional linkers reacts with the thioester bond at the C-terminus of MBP. As a consequence of this reaction, alkynated MBP is spliced off the column and collected after elution with RB.

In most EPL protocols, MESNA is used to induce the intein-mediated cleavage of the bifunctional linker (CB1-5, Table 3.2) as shown in Figure 3.6. The thiol group of MESNA reacts with the thioester bond of the protein, which results in the cleavage from the chitin column. At the same time, the bifunctional linker can be added as a second nucleophile. This nucleophile reacts with the thioester bond of the MBP-MESNA complex, resulting in C-terminally alkynated MBP.

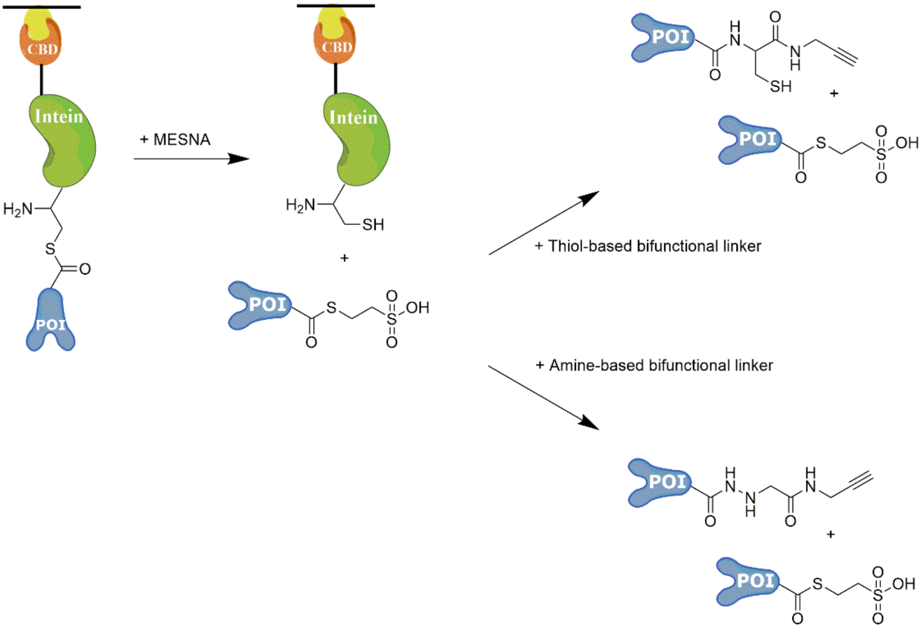
CBD
Intein
H_2N
S
O
POI
+ MESNA
CBD
Intein
H_2N
SH
+
POI
S
O
OH
+ Thiol-based bifunctional linker
+ Amine-based bifunctional linker
POI
H
N
O
SH
+
OH
S
H
N

Figure 3.6: Role of MESNA in EPL: MESNA is used to cleave the protein of interest (POI,) from the column. At the same time, the bifunctional linkers react with the thioester bond of this protein-MESNA complex to form the final alkynated protein.

Literature indicates that the addition of MESNA increases the protein yield after modification (4-9). However, this means that not only the bifunctional linker is responsible for the cleavage from the column but also MESNA (2, 21, 22). In other words, it is possible that besides MBP-alkyne also MBP-MESNA elutes from the column due to the competition of both thiols in case of a thiol-based bifunctional linker. To overcome this problem, the experiment was repeated without the use of MESNA (CB6-9). In this experiment, only the bifunctional linker can cause the cleavage from the column, meaning that only the MBP-alkyne can elute from the column. As expected, the measured yield is lower, around 5 mg/L culture versus 20 mg/L culture for the samples that contain MESNA and thiol-based bifunctional linker as shown in Table 3.3.

Table 3.3: Yield of the different functionalization experiments of MBP by expressed protein ligation in function of the different cleavage buffers.

Cleavage buffer	Yield (mg/L culture)
CB1	22.6
CB2	21.7
CB3	12.6
CB4	9.9
CB5	11.7
CB6	4.5
CB7	4.5
CB8	6.3
CB9	4.5

3.3.3 Western blotting after MBP biotinylation

To test the alkynation by EPL, the eluted protein fraction was coupled to an azide functionalized biotin derivative (Figure 2.5) by a CuAAC reaction. By using this approach, only the modified MBP can react with biotin and as a consequence, only the alkynated MBP can have a biotin label (Figure 3.7).

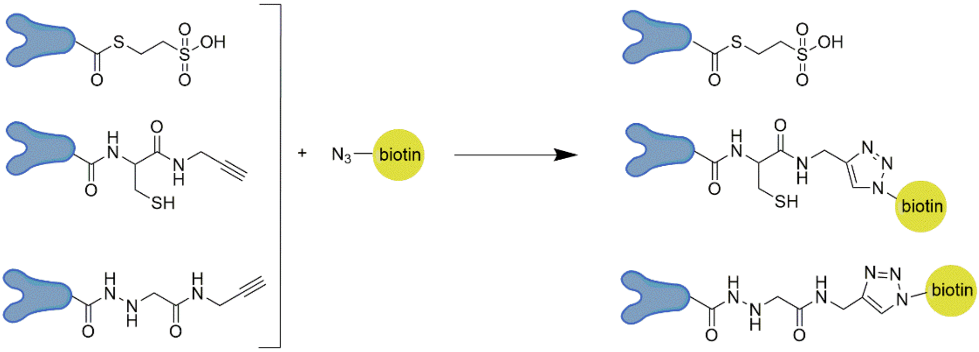

Figure 3.7: Click reaction of MBP ( ) and an azide-functionalized biotin. Only the alkynated protein reacts with the biotin, the MESNA-functionalized protein cannot. This way, the alkyne group can be visualized by western blotting.

The reaction product was separated on a 12% polyacrylamide gel by gel electrophoresis. The proteins were then transferred onto a pvdf membrane for western blotting. After the transfer, streptavidin alkaline phosphatase was added as streptavidin has a large affinity for biotin. Upon adding the substrate BCIP/NTB, an enzymatic reaction starts to take place in which the alkaline phosphatase converts the BCIP/NTB into a purple color, visible on the membrane. The results are shown in Figure 3.8.

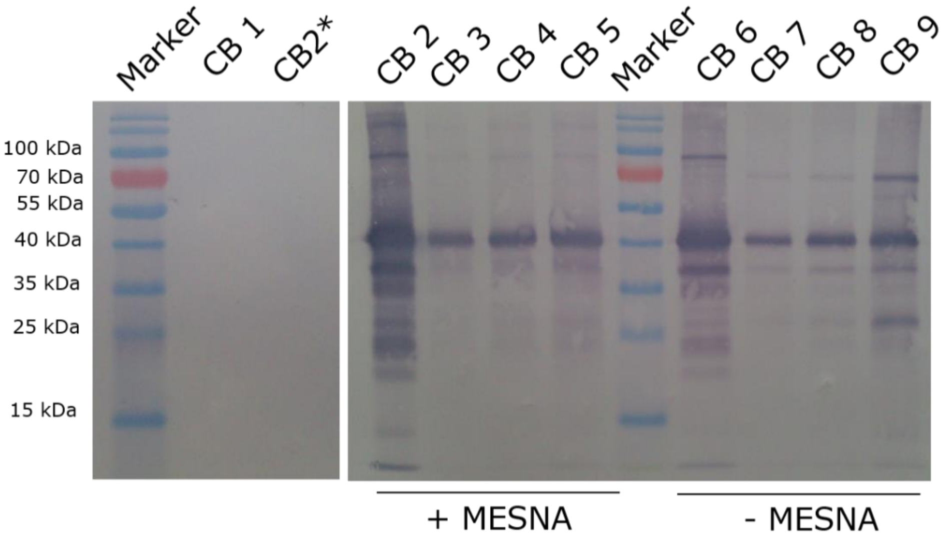

Figure 3.8: Western blot analysis of the click reaction between alkynated MBP and an azide-functionalized biotin. All functionalization conditions showed a band at 42 kDa, indicating the presence of a biotin label. This is an indirect proof of the presence of an alkyne functionalization at the C-terminus of MBP. The negative controls, CB1 (30 mM MESNA) and CB2* (= CB2 without copper catalyst), gave no visible reaction. PageRuler™ Prestained Protein Ladder was used as a marker.

Figure 3.8 shows a biotinylated protein at 42 kDa for all the tested conditions (CB2-CB9). This means that MBP was biotinylated, which is only possible if the alkynation of MBP was successful. The negative controls CB2* (were the click reaction was performed without the copper catalyst) and CB1 showed no visible bands on western blotting. Although this method is not quantitative, there is a visible difference between the different concentrations of the amine-based bifunctional linker. The higher the concentration of the linker, the more intense the band on western blot. In addition, indications are present that MESNA (slightly) increases the degree of functionalization. The high sensitivity of this technique also results in a lot of additional bands on the blotting membrane, especially when a thiol-based bifunctional linker (CB2 and CB6) is used. The origin of these bands is unknown, but these bands are not visible on SDS page (data not shown) meaning that the concentration of these bands is low. Nevertheless, for CB2 and CB6, there is a band visible at 84 kDa, illustrating the formation of dimers. This experiment gives a very good first indication that hydrazines are a possible alternative for thiols as a nucleophile for EPL. Note that this gives no decisive answer to whether all the eluted protein is functionalized. Part of the eluted protein can be the result of hydrolysis of the thioester bound. The impact of hydrolysis versus copper-catalyzed cleavage will be studied in section 3.3.4.

3.3.4 Optimization of the reaction conditions for alkyne functionalization of MBP using EPL

In order to increase the yield of the modification process, several adaptations of the protocol were envisaged. Changes in pH can have an influence on the nucleophilicity of the bifunctional linker due to protonation or deprotonation of the nucleophile. An increase in reaction time and reaction temperature can also affect the yield of the reaction. Nevertheless, these factors can also influence the hydrolysis of the thioester bond. This means that MBP will be spliced off the chitin resin without any functionalization. This results in a mixture of functionalized and native MBP (23, 24).

To investigate the effect of pH on the hydrolysis of MBP from the MBP-intein-CBD complex, the pH of the RB was varied between pH 6 and 9 (Figure 3.9).

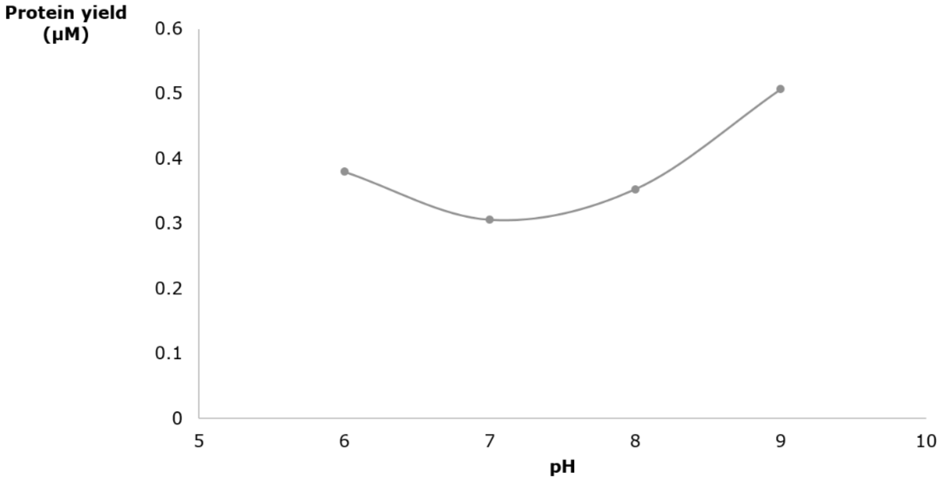

Figure 3.9: The effect of pH on hydrolysis of MBP from the chitin column.

Figure 3.9 indicates that hydrolysis is lowest between pH 7.0 and pH 8.0. The standard pH of RB (HEPES based buffer, pK_a = 7.5) is pH 8.5. However, the bifunctional linkers contain TFA as a by-product from the synthesis, as shown by ^{13}C-NMR. The pH measurements of the cleavage buffers showed that the acid properties of TFA will reduce the pH with approximately 1 unit at a concentration of 1 mM thiol-based bifunctional linker and 2 mM amine-based bifunctional linker. This means that the standard pH of the intein RB (pH 8.5) is the optimal pH (final pH 7.5 due to TFA) and no further optimization is needed to prevent non-specific off column splicing due to buffer pH.

Besides non-specific off column splicing, pH can also affect the nucleophilicity of the bifunctional linker. Hereby, two "extreme" pH's were evaluated.

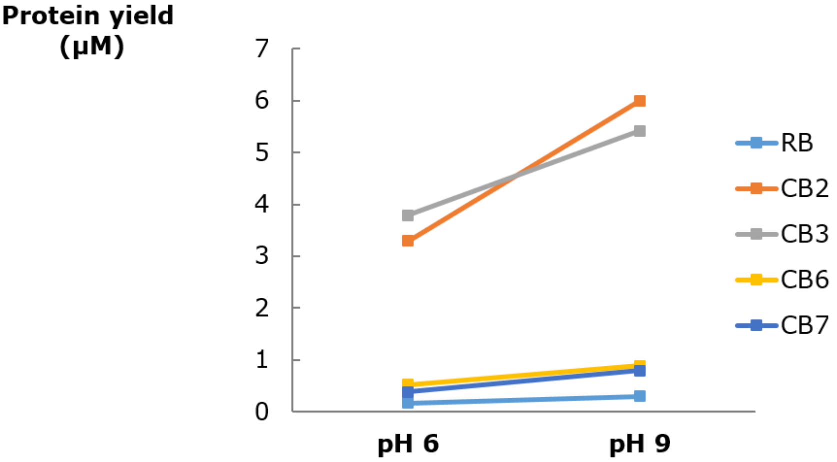

Figure 3.10: The effect of pH on the nucleophilicity of the bifunctional linker. The protein concentration increases when using a higher buffer pH and this for all buffers used.

Figure 3.10 shows that the protein concentration increases as the pH of the buffer increases. This effect seems to be the largest in MESNA (pK_a=9.2) (8) containing cleavage buffers (CB2 and CB3) but also CB6 (thiol-based bifunctional linker) and CB7 (amine-based bifunctional linker) have almost a doubling of the protein concentration. Note that in this experiment the hydrolysis also increased with 43% at higher pH, which is even more than in the previous experiment (Figure 3.9). It can thus be concluded that the increase in protein concentration at pH 9.0 for CB6 and CB7 is partly caused by the increase in hydrolysis and not by MBP functionalization. The effect of pH on the MESNA-based CBs (CB2 and CB3) is significant, as expected based on its pK_a value.

In addition to pH, reaction time and temperature can also influence the hydrolysis of the MBP thioester bond or the efficiency of the nucleophilic reaction between the bifunctional linker and the thioester bond in the MBP-intein-CBD complex.

First, the effect of the RB (pH 8.5) on the thioester bond hydrolysis of MBP from the column was tested as a function of time and temperature.

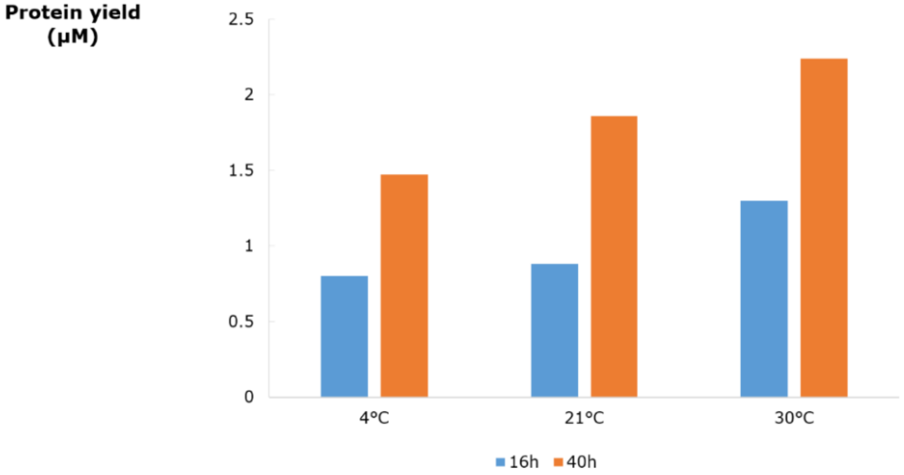

Figure 3.11: The effect of temperature and incubation time on the thioester bond hydrolysis of MBP cleavage after incubation with RB. There is a clear correlation between higher incubation temperatures and longer incubation times and an increasing concentration of hydrolyzed protein.

Figure 3.11 shows that the hydrolysis of MBP from the column increases as a function of temperature. The graph is showing very clearly that long incubation times result in more hydrolysis of MBP from the column, especially at higher temperatures.

The results in Figure 3.12 show a higher protein concentration when the reaction with CB7 is performed at 21 °C. This means that the yield of the nucleophilic reaction increases at higher temperatures. Furthermore, a combination of a higher incubation time with a reaction temperature of 21°C results in a concentration increase of 57%. Unfortunately, this increase in yield corresponds to the increase of hydrolysis of the thioester bond of MBP, as shown in Figure 3.11 (more than double the amount in hydrolysis at 21°C, 40 h compared with 16 h). Note that the absolute values in the different figures cannot be compared because of differences in experimental conditions (other reaction volumes and bacterial cultures), but only the relative ratios.

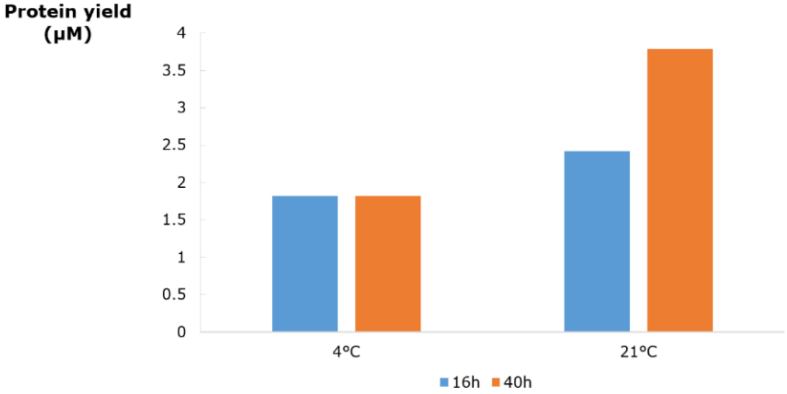

Figure 3.12: The effect of temperature and incubation time on the nucleophilic reaction of the amine-based bifunctional linker (CB7). A higher incubation temperature, especially combined with a longer incubation period, leads to a higher concentration of eluted protein from the column.

To determine whether the increased protein concentration is caused by hydrolysis or by site-specific alkynation, the eluted fraction was treated with an azide-functionalized biotin derivative in a CuAAC reaction.

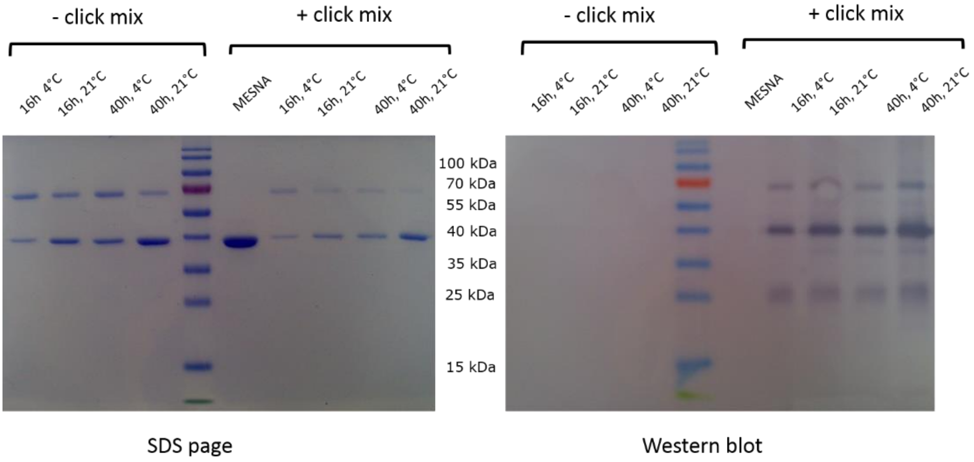
- click mix
+ click mix
16h, 4°C
16h, 21°C
40h, 4°C
40h, 21°C
MESNA
16h, 4°C
16h, 21°C
40h, 4°C
40h, 21°C
100 kDa
70 kDa
55 kDa
40 kDa
35 kDa
25 kDa
15 kDa
- click mix
+ click mix
16h, 4°C
16h, 21°C
40h, 4°C
40h, 21°C
MESNA
16h, 4°C
16h, 21°C
40h, 4°C
40h, 21°C
SDS page
Western blot

Figure 3.13: SDS page (left) and western blot (right) of the results of the CuAAC reaction between azide functionalized biotin and MBP-alkyne modified via EPL using the amine-based bifunctional linker mixture for 2 different incubation times (16 and 40 h) and temperatures (4 and 21°C). All conditions produced alkynated MBP and the intensity of the band increased upon going from 4 to 21°C. MESNA functionalized MBP was used as a negative control.

Figure 3.13 (left) shows that, based on molecular mass, all the reaction conditions result in the elution of MBP. On the left side of the marker, the proteins before the click reaction were loaded; on the right side contains the MBP after the click reaction. MESNA-functionalized MBP was used as a negative control (no alkyne function). Figure 3.13 (right) shows the western blotting result of the eluted proteins. This blot indicates that a click reaction took place between the eluted protein and the azide-functionalized biotin derivative. For the negative control, i.e. the proteins before the click reaction (- click mix), no bands were observed. Although it is difficult to quantify this with western blotting, a trend is visible that a higher incubation temperature and longer incubation time does not only give a higher total protein yield (Figure 3.12), but also a higher amount of alkynated MBP in comparison to the other samples.

In order to evaluate the modification quantitatively, ESI-MS was used. The theoretical mass of alkynated MBP produced via EPL using the amine-based bifunctional linker is 42667.4 Da and in case of hydrolysis 42558.3 Da. As a control, MESNA-functionalized MBP was used giving a theoretical mass of 42682.5 Da. Figure 3.14a shows that MESNA-functionalized MBP gives a mass of 42557.7 Da, meaning that the MESNA functionality is hydrolised after the reaction or the N-terminal methionine is removed during expression. The sample modified with CB3 (Figure 3.14b), containing MESNA and amine-based bifunctional linker, gives a mass similar to the mass measured with CB1 meaning that most of the MBP is hydrolised and there is no effect of the amine-based bifunctional linker visible in the spectrum. MESNA is such a strong nucleophile that there is no significant effect of the amine-based bifunctional linker. Figure 3.14c shows a large peak of 42430.6 Da, corresponding to pure MBP without N-terminal methionine (theoretical mass of 42427.1 Da). This means that the resulting MBP is mainly arising from hydrolysis and not from EPL and support the theory that the peak in Figure 3.14a is MESNA functionalized MBP. Nevertheless, Figure 3.8 shows that there was a click reaction. So probably, a small percentage is modified resulting in the absence of a clear peak on the mass spectrometry spectrum. Higher concentrations of the amine-based bifunctional linker gave similar results.

a)

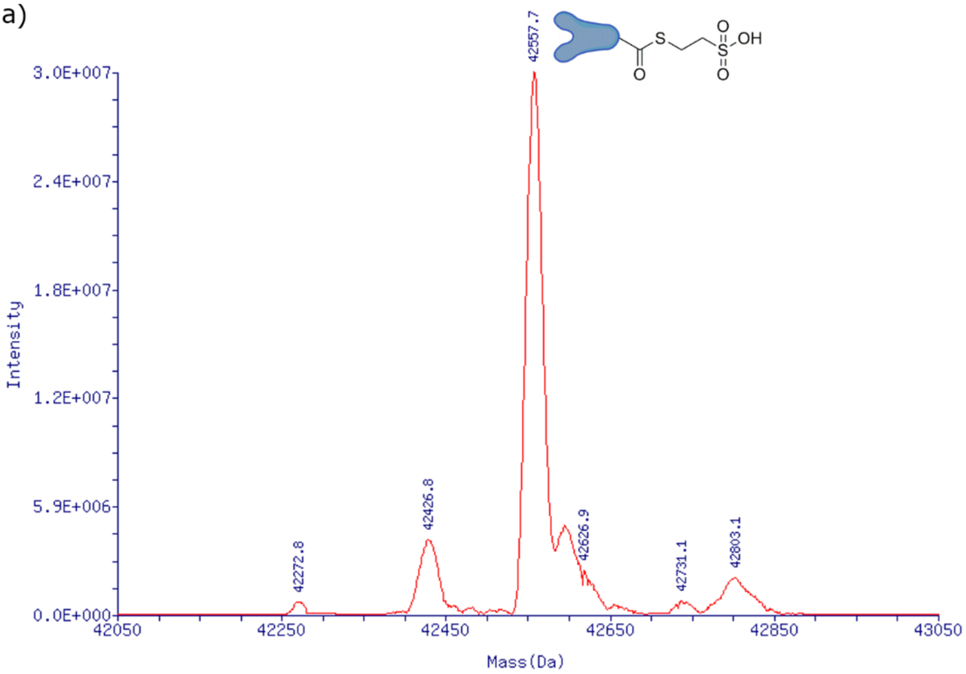
42557.7
S
O
OH
S
O
O
O
3.0E+007
2.4E+007
1.8E+007
1.2E+007
5.9E+006
0.0E+000
Intensity
42272.8
42426.8
42626.9
42731.1
42803.1
42050
42250
42450
42650
42850
43050
Mass(Da)

b)

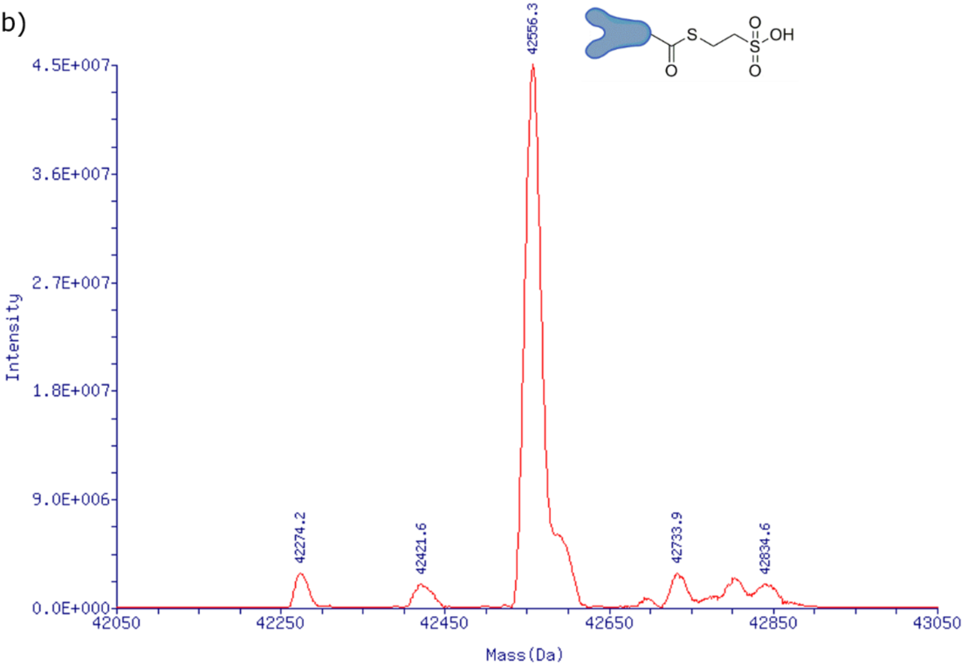
42556.3
S
O
OH
S
O
O
O
4.5E+007
3.6E+007
2.7E+007
1.8E+007
9.0E+006
0.0E+000
Intensity
42274.2
42421.6
42733.9
42834.6
42050
42250
42450
42650
42850
43050
Mass(Da)

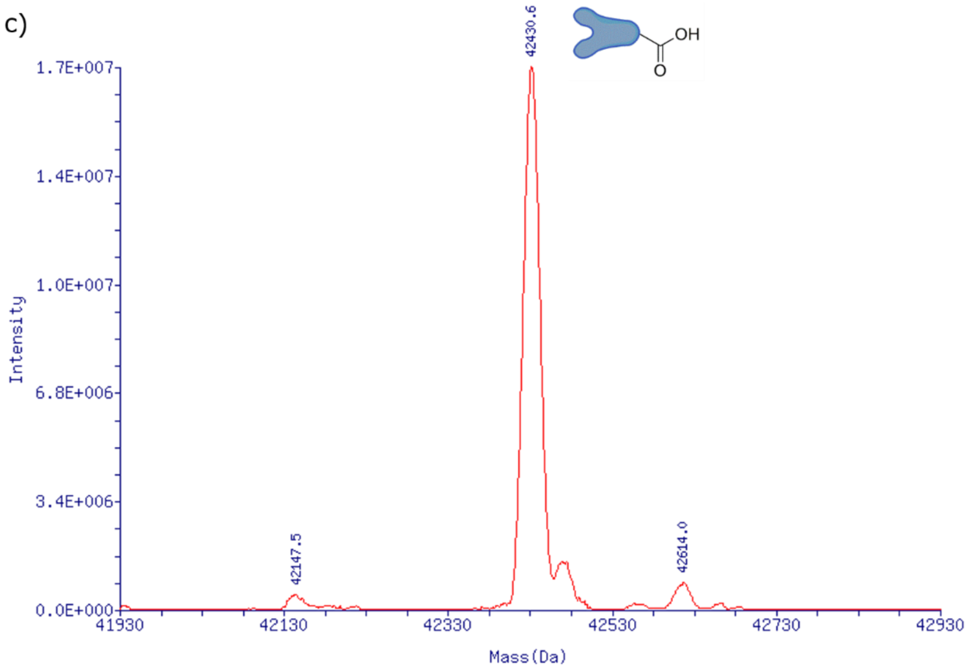

Figure 3.14: ESI-MS of MBP modified with CB1 (a), CB3 (b) and CB7 (c). CB1 only contained MESNA as a nucleophile and was used as a control. CB3 contains MESNA and the amine-based bifunctional linker but only MESNA functionalization is visible in the spectrum. CB7 contains only the amine-based bifunctional linker as a nucleophile but only hydrolyzed MBP was detected.

The ellipsometry experiment shown in Figure 3.15 shows a real time monitoring of the click reaction on an azide-functionalized surface (0-3000 sec, in duplicate). Several washing steps were performed (3000-6500 sec) to remove all of the non-covalently bound protein. After these washing steps, ssA*MBP stays on the surface with a mass increase of 0.14 μg/cm² for ssA*MBP (a) and 0.15 μg/cm² for ssA*MBP (b). This is only possible when there is an alkyne group on the MBP.

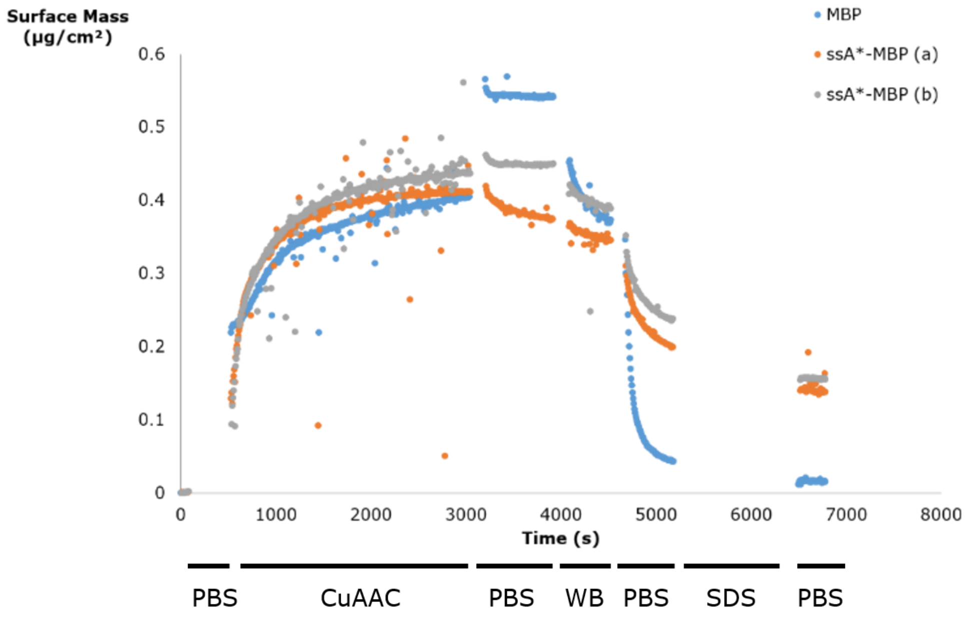

Figure 3.15: Ellipsometry of ssA*-MBP (in duplicate). There is a significant mass increase after several washing steps compared with the non-functionalized MBP, indicating a covalent coupling.

3.3.5 Functionalization of NbBcII10 using amine-based EPL

In order to exclude any protein-specific problems, amine-based EPL was performed with NbBcII10 using CB1 and CB7. This modification was directly tested by ESI-MS as shown in Figure 3.16. The expected mass of NbBcII10-alkyne, produced using the amine-based bifunctional linker, is 14465 Da. If the modification was not successful and only hydrolysis of the thioester bond occurred, a peak at 14366 is expected. As a control, MESNA-functionalized NbBcII10 was used giving an expected mass of 14490 Da.

These spectra show that functionalization with MESNA using EPL is successful for NbBcII10. Nevertheless, reaction with the amine-based bifunctional linker 2-hydrazinyl-*N*-(prop-2-yn-1-yl)acetamide results in pure NbBcII10 by hydrolysis and not in clearly alkynated NbBcII10. Note that the peaks 14486 and 14504 are caused by contamination of the ESI-MS column by the MESNA functionalized NbBcII10 experiment. This result is similar as obtained earlier for MBP, excluding any protein specific problems of protein alkynation by amine-based EPL.

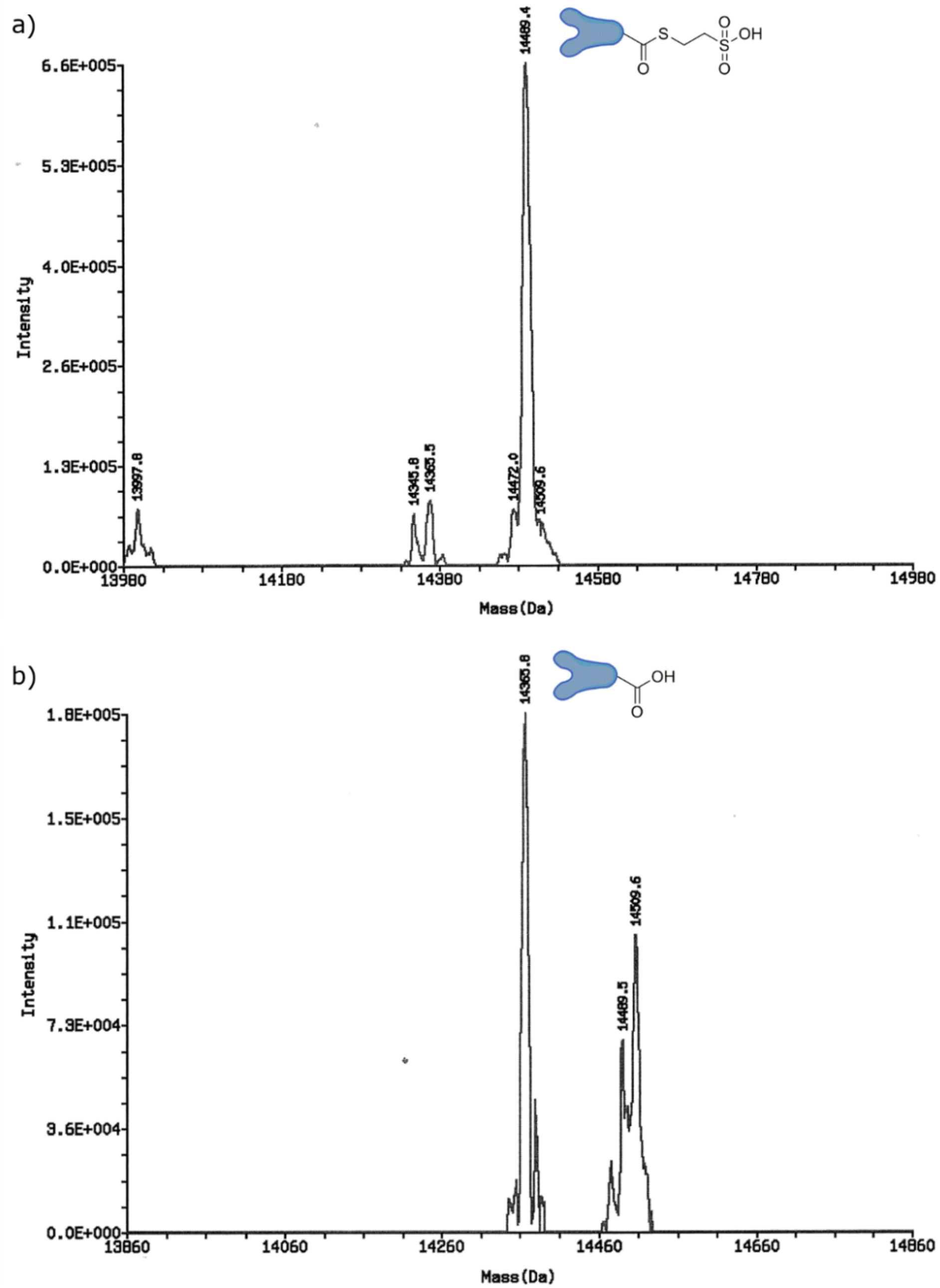

Figure 3.16: ESI spectra of NbBII10 modified by using CB1 (a), CB7 (b). Note that spectrum b still contains impurities from a previous experiment.

Further literature research also indicated that thiols are, 10 years after the publication of Kalia et al., still the most commonly used nucleophiles for EPL. Marshall et al. (25) use the technique for functionalization of proteins in yeast surface display. They described the expression of single chain antibodies and GFP in complex with intein on the surface of yeast. EPL was performed directly on the yeast cells using a hydrazine bifunctional linker or MESNA. A 500 mM concentration of amine-based bifunctional linker and an incubation time of 3 days was necessary to get 20 % of the yield when using 50 mM of MESNA during 45 minutes. This indicates that they also had to use extreme conditions to perform EPL using a hydrazine bifunctional linker. Unfortunately, there is no mass spectrometry evidence of their functionalization, only western blotting of a biotin coupling as showed in this study. These finding combined with the results of this study indicate that amine-based bifunctional linkers are no worthy alternative for thiol-based bifunctional linkers.

3.4 Conclusions

EPL is a suitable technique for the C-terminal modification of MBP. Currently, mainly thiol-based nucleophiles are used for EPL. The disadvantage of this approach is the introduction of an additional cysteine, resulting in disulfide bridge formation with other thiol groups. To overcome this issue, an amine-based bifunctional linker was investigated. After a successful synthesis, the linker was used for EPL with MBP as a model protein. The EPL reaction conditions were optimized by variations in pH, reaction temperature and time to increase the total protein yield. However, the positive effects of these optimizations on the yield were also seen in the negative control samples. Hereby it is concluded that the higher protein yield was associated with a higher degree of hydrolysis of the thioester bond and not with a higher degree of MBP alkyne functionalization. Nevertheless, a click reaction between MBP that was alkynated by EPL using an amine-based bifunctional linker and azide functionalized biotin was proven by making use of western blotting. The absence of clear individual peaks on mass spectrometry indicates that only a minor percentage of the MBP was actually functionalized with an alkyne. Consequently, it is concluded that the tested amine-based bifunctional linker is not a fully-fledged alternative for thiol-based bifunctional linkers.

3.5 References

1. Sletten EM, Bertozzi CR. Bioorthogonal Chemistry: Fishing for Selectivity in a Sea of Functionality. Angew Chem Int Ed. 2009;48(38):6974-98.
2. Muir TW. Semisynthesis of proteins by expressed protein ligation. Annu Rev Biochem. 2003;72:249-89.
3. Muir TW, Sondhi D, Cole PA. Expressed protein ligation: a general method for protein engineering. Proc Natl Acad Sci U S A. 1998;95(12):6705-10.
4. Reulen SWA, Brusselaars WWT, Langereis S, Mulder WJM, Breurken M, Merkx M. Protein−Liposome Conjugates Using Cysteine-Lipids And Native Chemical Ligation. Bioconj Chem. 2007;18(2):590-6.
5. Reulen S, van Baal I, Raats J, Merkx M. Efficient, chemoselective synthesis of immunomicelles using single-domain antibodies with a C-terminal thioester. BMC Biotechnol. 2009;9(1):66-74.
6. Chattopadhaya S, Abu Bakar FB, Yao SQ. Use of Intein-Mediated Protein Ligation Strategies for the Fabrication of Functional Protein Arrays. Methods in Enzymology: Non-Natural Amino Acids. 2009;462:195-223.
7. Ghosh I, Considine N, Maunus E, Sun L, Zhang A, Buswell J, et al. Site-specific protein labeling by intein-mediated protein ligation. Methods Mol Biol. 2011;705:87-107.
8. Johnson ECB, Kent SBH. Insights into the Mechanism and Catalysis of the Native Chemical Ligation Reaction. J Am Chem Soc. 2006;128(20):6640-6.
9. Seyedsayamdost MR, Yee CS, Stubbe J. Site-specific incorporation of fluorotyrosines into the R2 subunit of E. coli ribonucleotide reductase by expressed protein ligation. Nat Protocols. 2007;2(5):1225-35.
10. Kalia J, Raines RT. Reactivity of Intein Thioesters: Appending a Functional Group to a Protein. ChemBioChem. 2006;7(9):1375-83.
11. Hall HK. Correlation of the Base Strengths of Amines1. J Am Chem Soc. 1957;79(20):5441-4.
12. Bonnet D, Ollivier N, Gras-Masse H, Melnyk O. Chemoselective Acylation of Fully Deprotected Hydrazino Acetyl Peptides. Application to the Synthesis of Lipopeptides. The Journal of Organic Chemistry. 2001;66(2):443-9.
13. Hinman R. Notes - Base Strengths of Some Alkylhydrazines. The Journal of Organic Chemistry. 1958;23(10):1587-8.
14. Edwards JO, Pearson RG. The Factors Determining Nucleophilic Reactivities. J Am Chem Soc. 1962;84(1):16-24.
15. Buncel E, Um I-H. The α-effect and its modulation by solvent. Tetrahedron. 2004;60(36):7801-25.
16. Evans TC, Jr., Benner J, Xu MQ. Semisynthesis of cytotoxic proteins using a modified protein splicing element. Protein Sci. 1998;7(11):2256-64.
17. Evans TC, Xu MQ. Intein-mediated protein ligation of expressed proteins. Google Patents; 2000.

18. Chong S, Mersha FB, Comb DG, Scott ME, Landry D, Vence LM, et al. Single-column purification of free recombinant proteins using a self-cleavable affinity tag derived from a protein splicing element. Gene. 1997;192(2):271-81.

19. Lin P-C, Ueng S-H, Tseng M-C, Ko J-L, Huang K-T, Yu S-C, et al. Site-Specific Protein Modification through CuI-Catalyzed 1,2,3-Triazole Formation and Its Implementation in Protein Microarray Fabrication. Angew Chem Int Ed. 2006;45(26):4286-90.

20. Bracher PJ, Snyder PW, Bohall BR, Whitesides GM. The relative rates of thiol-thioester exchange and hydrolysis for alkyl and aryl thioalkanoates in water. Orig Life Evol Biosph. 2011;41(5):399-412.

21. Hauser PS, Ryan RO. Expressed protein ligation using an N-terminal cysteine containing fragment generated in vivo from a pelB fusion protein. Protein Expression Purif. 2007;54(2):227-33.

22. Zourob M. Recognition Receptors in Biosensors: Springer New York; 2010.

23. Evans TC, Benner J, Xu M-Q. The in Vitro Ligation of Bacterially Expressed Proteins Using an Intein from Methanobacterium thermoautotrophicum. J Biol Chem. 1999;274(7):3923-6.

24. Yu H-H, Nakase I, Pujals S, Hirose H, Tanaka G, Katayama S, et al. Expressed protein ligation for the preparation of fusion proteins with cell penetrating peptides for endotoxin removal and intracellular delivery. Biochim Biophys Acta. 2010;1798(12):2249-57.

25. Marshall CJ, Agarwal N, Kalia J, Grosskopf VA, McGrath NA, Abbott NL, et al. Facile Chemical Functionalization of Proteins through Intein-Linked Yeast Display. Bioconj Chem. 2013;24(9):1634-44.

Chapter 4

Cytoplasmic versus periplasmic expression of site-specifically and bioorthogonally functionalized nanobodies using expressed protein ligation

---

Published as: **Billen B**, Vincke C, Hansen R, Devoogdt N, Muyldermans S, Adriaensens P, Guedens W. Cytoplasmic versus periplasmic expression of site-specifically and bioorthogonally functionalized nanobodies using expressed protein ligation. Protein Expression Purif. 2017;133:25-34. (IF:1.351)

Author contributions: The experimental work in this chapter was mainly performed by Billen B. Hansen R. developed the control vector as used for the experiments showed in Figure 4.2. The SPR experiments were performed in close collaboration with Vincke C. and Muyldermans S.

Site-specific functionalization of nanobodies after introducing bioorthogonal groups offers the possibility to biofunctionalize surfaces with a uniformly oriented layer of nanobodies. In this paper, expressed protein ligation (EPL) was used for site-specific alkynation of the model nanobody NbBcII10. In contrast to EPL constructs, which are typically expressed in the cytoplasm, nanobodies are expressed in the periplasm, where its oxidizing environment ensures a correct folding and disulfide bond formation. Different pathways were explored to express the EPL constructs in the periplasm, but simultaneously the effect of cytoplasmic expression on the functionality of NbBcII10 was also evaluated. By using *Escherichia coli* SHuffle®T7 cells, it was demonstrated that expression of the EPL complex in the cytoplasm was readily established and that site-specifically mono-alkynated nanobodies can be produced with the same binding properties as the non-modified NbBcII10 expressed in the periplasm. In conclusion, this paper shows that periplasmic expression of the EPL complex is quite challenging, but cytoplasmic expression has proven to be a valuable alternative.

4.1 Introduction

The oriented and covalent coupling of proteins to functionalized surfaces is a crucial step in the production of bioactive surfaces as found in biosensors (1). Nowadays, immobilization is mostly based on physical adsorption, resulting in a weak, non-covalent and non-oriented coupling of these proteins (2-4). To strengthen the coupling, covalent attachments involving endogenous reactive groups (from lysines) are often used (e.g. EDC/NHS couplings) (5, 6). However, these couplings still result in a non-oriented immobilization because the endogenous groups occur at multiple locations spread over the protein's surface. Alternatively, a site-specifically introduced affinity tag (e.g. His_6-tag) on the protein can be used to associate with a properly functionalized biosensor surface (e.g. Ni-NTA), but this interaction is weak and easily disrupted (7, 8).

Therefore, the site-specific introduction in the protein of a single bioorthogonal group to react covalently with a complementary group on the biosensor surface, seems an attractive approach for a robust and directed protein immobilization. Such a site-specific functionalization and immobilization on a sensor surface will result in a higher specificity and selectivity of the envisaged antigen-protein interaction. In this chapter, expressed protein ligation (EPL) is used for the introduction of an alkyne click functionality onto a single-domain antibody fragment, i.e. a nanobody (Nb), to develop site-specific functionalized probes for subsequent generation of oriented and covalently coupled protein layers onto a solid carrier.

EPL is a technique that involves the recombinant expression of a protein of interest fused with a mutated Mxe GyrA intein and a chitin-binding domain (CBD). The mutant intein will facilitate an N,S-acyl shift in the peptide bond between the protein of interest and the intein, resulting in a thioester bond. Moreover, the CBD enables purification of the expressed protein on a chitin column. The protein of interest can subsequently be disconnected from the protein complex via a reaction between the newly formed thioester bond in the protein and a thiol group containing nucleophile (9, 10). Through careful design of so-called bifunctional linkers containing both a thiol group as nucleophile and a bioorthogonal group such as an alkyne, the protein can readily be site-specifically functionalized at its C-terminus (11, 12).

Nbs, also known as single-domain antibody fragments (sdAbs) or VHHs, are the recombinant autonomous antigen-binding domains of heavy-chain-only antibodies that occur in species of the *Camelidae* family (13, 14). They are an interesting alternative for monoclonal antibodies in diagnostic applications due to their small size (~ 15 kDa) and their high specificity and affinity for their antigen (15). Furthermore, they have a well-conserved structure, are relatively easy to express in *Escherichia coli* (*E. coli)*, they are encoded by only one gene (which facilitates an easy genetic manipulation) and they remain soluble and stable at elevated temperatures (15-17).

In general, Nbs are expressed in the periplasm of *E.coli* (18, 19). The oxidizing environment of the periplasm facilitates protein folding and the periplasmic extracts enriched with the recombinant Nb facilitate subsequent purification. The periplasmic transport of the Nb is provoked by the N-terminal pelB leader sequence of the Sec pathway, which enables transport through the inner membrane of bacteria (Figure 4.1). EPL-based constructs, however, are preferentially expressed in the cytoplasm (20-22) and previous reports already indicated that the pelB leader sequence is not practical for the Nb-intein-CBD fusion protein (23). We therefore explored alternative strategies to produce Nb-intein-CBD fusion proteins.

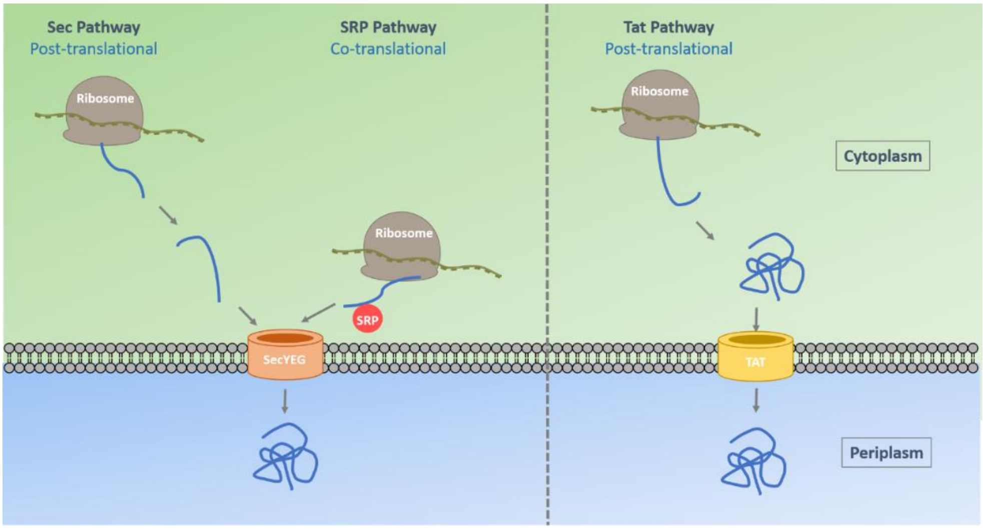

Figure 4.1: Three periplasmic secretion pathways for proteins in E. coli. The Sec pathway is a post-translational pathway in which the protein is fully secreted by ribosomes. Afterwards, the leader sequence enables correct folding of the protein by transporting it to the periplasm via the SecYEG translocon. The SRP pathway uses the same translocon as the Sec pathway but here SRP is binding to the leader sequence, and translocates the protein-ribosome complex to the SecYEG translocon during the protein synthesis. The Tat pathway uses a different approach since it is transporting folded proteins from the cytoplasm to the periplasm using the Tat translocon.

Three pathways allowing periplasmic transport of recombinant proteins in *E.coli* are known: the Sec pathway, the signal recognition particle (SRP) pathway, and the twin-arginine translocation (Tat) pathway (Figure 4.1). The Sec pathway is a post-translational pathway in which the protein is synthesized completely, i.e. with a leader sequence, and released from the ribosome after which it is directed to the Sec-translocase (24). Common leader sequences used for this pathway are pelB, ompA, ompF and malE (25). The efficacy of these four Sec leader signals was evaluated to produce the Nb-intein-CBD fusion in the periplasm. The second pathway for periplasmic transport is the SRP pathway. This pathway also targets the Sec-translocase but it is a co-translational pathway. SRP binds to the leader sequence after its translation from the ribosomes and the entire complex of SRP-ribosome-nascent protein is targeted to the Sec-translocase (24). Commonly used leader sequences dedicated to the SRP pathway are DsbA and TolB (26). These two leader sequences were also tested in this study on their ability to produce Nb-intein-CBD fusions in the bacterial periplasm. The third pathway, the Tat pathway is not interesting for Nb transport because this pathway transports folded proteins into the periplasm using Tat translocons (27).

In the present study, a nanobody against *Bacillus cereus* β-lactamase (BcII) (19, 28, 29), NbBcII10, is used as a model to evaluate various approaches for the periplasmic transport of the Nb-intein-CBD fusion protein. Furthermore, the requirement for periplasmic expression of Nbs alkynated by EPL was investigated by comparing the functionality of Nb-intein-CBD fusion protein expressed in the cytoplasm and native non-functionalized NbBcII10 expressed in the periplasm. To this end, the binding capacities of both formats were analyzed using ELISA and surface plasmon resonance (SPR).

4.2 Materials and Methods

4.2.1 Materials

The primers were synthesized by Integrated DNA technologies (IDT). Materials for the PCR and molecular cloning were purchased from Thermo Scientific. Sanger sequencing was performed by LGC Genomics Germany. Growth media components were purchased from Becton Dickinson (BD) Biosciences. The BcII antigen was kindly provided by Prof. André Matagne (Université de Liège, Belgium). The pTXB1 vector, chitin resin, *E.coli* BL21(DE3) and SHuffle®T7 competent cells were purchased from New England Biolabs. Materials and chemicals for the SPR experiments were purchased from GE Healthcare. All other chemicals were purchased from Sigma, unless stated otherwise.

4.2.2 Molecular cloning

The pTXB1 vector was used to express the Nb-intein-CBD fusion protein. The different leader sequences used for the different constructs are summarized in Table 4.1.

Table 4.1: Overview of the DNA sequences of the different leader sequences used for the periplasmic expression of NbBcII10 (25, 26).

Construct	Leader	DNA sequence leader	Pathway	Accession no.
A	pelB	5’ ATG AAA TAC CTA TTG CCT ACG GCA GCC GCT GGA TTG TTA TTA CTC GCG GCC CAG CCG GCC ATG GCC 3’	Sec	P11431°
B	ompA	5’ ATG AAA AAG ACA GCT ATC GCG ATT GCA GTG GCA CTG GCT GGT TTC GCT ACC GTA GCG CAG GCC 3’	Sec	V00307*
C	ompF	5’ ATG ATG AAG CGC AAT ATT CGT GCA GTG ATC GTC CCT GCT CTG TTA GTA GCA GGT ACT GCA AAC GCT 3’	Sec	J01655*
D	malE	5’ ATG AAA ATA ACA GGT GCA CGC ATC CTC GCA TTA TCC GCA TTA ACG ACG ATG ATG TTT TCC GCC TCG GCT CTC GCC 3’	Sec	V00303*
E	DsbA	5’ ATG AAA AAA ATT TGG CTG GCG CTG GCG GGC CTG GTG CTG GCG TTT AGC GCG AGC GCG 3’	SRP	P0AEG4°
F	TolB	5’ ATG AAA CAG GCG CTG CGT GTG GCG TTT GGC TTT CTG ATT CTG TGG GCG AGC GTG CTG CAT GCG 3’	SRP	P0A855°
G	None	None	N.A.	N.A.

*** GenBank, ° Uniprot**

The *NbBcII10* gene was amplified from the pHEN6:*pelB*-NbBcII10-His$_6$ vector (19) using different primers to generate different amplicons to clone in the pTXB1 vector. The pelB-NbBcII10 insert was made using the *pelB_fw* forward primer (5′-GGTGGTCATATGATGAAATACCTATTGCCTACGGCAGCCG-3′) and *pelB_rv* reverse primer (5′-GGTGGTTGCTCTTCGCATGAGGAGACGGTGA-3′). The gene of the other leader sequences was not available, so these leader sequences were added to the Nb by two subsequent PCR reactions. The forward primers are summarized in Table 4.2, the reverse primer, *leader_rv* (5‵-GGTGGTTGCTCTTCCGCATGAGGAGACGGTGA-3′) was the same for all the reactions.

Table 4.2: Overview of the different forward primers used for the attachment of different leader sequences to NbBcII10 in order to direct the periplasmic expression of the Nb-intein-CBD fusion protein.

Leader	Primer sequence
OmpA_1	5′-TGCAGTGGCACTGGCTGGTTTCGCTACCGTAGCGCAGGCCCAGGTGCAGCTGGTGGAGTC-3′
OmpA_2	5′-GGTGGTCATATGATGAAAAAGACAGCTATCGCGATTGCAGTGGCACTGGCTGGTT-3′
OmpF_1	5′-GATCGTCCCTGCTCTGTTAGTAGCAGGTACTGCAAACGCTCAGGTGCAGCTGGTGGAGTC-3′
OmpF_2	5′-GGTGGTCATATGATGATGAAGCGCAATATTCGTGCAGTGATCGTCCCTGCTCTGTTAG-3′
malE_1	5′-CGCATTAACGACGATGATGTTTTCCGCCTCGGCTCTCGCCCAGGTGCAGCTGGTGGAGTC-3′
malE_2	5′-GGTGGTCATATGATGAAAATAACAGGTGCACGCATCCTCGCATTATCCGCATTAACGACGATGATGT-3′
DsbA_1	5′-CCTGGTGCTGGCGTTTAGCGCGAGCGCGCAGGTGCAGCTGGTGGAGTC-3′
DsbA_2	5′-GGTGGTCATATGATGAAAAAAATTTGGCTGGCGCTGGCGGGCCTGGTGCTGGCGTTTAG-3′
TolB_1	5′-GGCTTTCTGATTCTGTGGGCGAGCGTGCTGCATGCGCAGGTGCAGCTGGTGGAGTC-3′
TolB_2	5′-GGTGGTCATATGATGAAACAGGCGCTGCGTGTGGCGTTTGGCTTTCTGATTCTGTGGGC-3′
None	5′-GGTGGTCATATGCAGGTGCAGCTGGTGGAGTCTGGGGGAGGCTCGGTG-3′

As a positive control, a variant of construct (a) was made containing two stop codons (TAA-TGA) downstream of the pelB-NbBcII10 gene (construct (a′)). This pelB-NbBcII10-TAA-TGA insert was made using the pelB_stop_fw primer (5'-GGTCACGGTCACGGTGGTCATATGATGAAATACCTATTGCCTACGGCAGCCGCTG-3') and the pelB_stop_rv primer (5'-GGTGGTTGCTCTTCCGCATCATTATG AGGAGACGGTGACCTGGG-3'). For cytoplasmic expression, no leader sequence is needed and the insert only consists of NbBcII10 (last primer of Table 4.2). In contrast to the other constructs, a different reverse primer (5'-GGTGGTTGCTCTTCCGCAGTACTCGAGTGAGGAGACGGTGACCTGGGT-3') was used to add three amino acids (LEY) at the C-terminus of the Nb.

All PCRs were performed using Phusion Hot Start II high-fidelity DNA polymerase for 30 sec at 98°C, followed by 30 cycles of 8 sec at 98°C and 15 sec at 72°C. The final elongation step was performed for 8 minutes at 72°C resulting in the final inserts. Next, the Nb constructs and pTXB1 vector were digested using Fastdigest *NdeI* and *SapI* restriction enzymes using a standard protocol as provided by the supplier, and purified using PCR cleanup or gel extraction kits. After purification, the vector and insert were ligated using T4 ligase according to the manufacturer's protocol. The ligated constructs were subsequently transformed into chemically competent TOP10F' cells using the heat shock method, plated on Luria-Bertani (LB) agar containing 100 µg/mL Ampicillin (LB^{amp}) and incubated for 16 h at 37°C. Afterwards, individual colonies were randomly selected, cultured and DNA was extracted to check the constructs by means of Sanger sequencing.

4.2.3 Expression and extraction of the Nb-intein-CBD fusion protein

4.2.3.1 Periplasmic expression in E. coli BL21(DE3)

Constructs (a)-(d) and (a') were transformed into chemically competent *E. coli* BL21(DE3) cells and cultured in 50 mL LB^{amp} medium until an optical density OD_{600} between 0.6 and 0.9 was reached. Next, expression for 16 h at 28°C was induced by adding isopropyl β-D-1-thiogalactopyranoside (IPTG) to a final concentration of 1 mM. The cells were harvested by centrifugation and a periplasmic extraction was performed using an osmotic shock. To this end, the cell pellet was resuspended in Tris-EDTA-Sucrose (TES) solution and incubated on ice for 1 hour while shaking. Next, an osmotic shock was achieved by adding a double amount of TES diluted 1:4 with Milli-Q water and the cell suspension was shaken on ice during 2 hours. Afterwards, $MgCl_2$ was added to a final concentration of 10-15 mM. After centrifugation, the supernatant was collected for further use.

4.2.3.2 Periplasmic expression in E. coli Lemo21(DE3)

To increase the periplasmic extraction yield, a BL21(DE3) variant, *E.coli* Lemo21(DE3), was used. This strain is especially designed for the expression of poorly soluble proteins. The strain contains an additional plasmid, i.e. pLemo that can produce T7 lysozyme, a natural inhibitor of T7 RNA polymerase. The expression of T7 lysozyme is under control of a rhamnose inducible promotor. By varying the concentration of rhamnose, and consequently the concentration of T7 lysozyme, the activity of T7 RNA polymerase can be modulated, resulting in a controlled regulation of the target protein expression (30, 31). Constructs (a)-(f), the negative control (g) and positive control (a') were transformed into chemically competent Lemo21(DE3) cells and expression was performed in the same way as for normal BL21(DE3) except that only 400 µM IPTG was used to induce the expression and 100 µg/mL chloramphenicol was added to the medium to preserve the pLemo vector. In addition, to regulate the expression level of T7 lysozyme, varying concentrations of rhamnose (final concentration between 0 and 2000 µM) were tested. Periplasmic extraction was performed as described for BL21(DE3) or as described by Schlegel et al. (31).

4.2.3.3 Cytoplasmic expression in E. coli SHuffle®T7

Construct (g) was transformed into chemically competent *E. Coli* SHuffle®T7 cells. These cells are derived from the *E.coli* K12 strain and are especially developed to facilitate disulfide formation in the cytoplasm. The *NbBcII10*-gene containing SHuffle®T7 cells were cultured in 300 mL LB^{amp} medium until an OD_{600} between 0.6 and 0.9 was reached. Expression was induced by adding IPTG to a final concentration of 1 mM during 3 hours at 37°C. Afterwards, the cells of a 300 mL culture were harvested using centrifugation and extracted by resuspending the cell pellet in 6 mL B-PER solution (Thermo Scientific), supplemented with 6 U DNAseI (Thermo Scientific), and incubated for 15 minutes at room temperature. After centrifugation for 30 minutes at 20 000 g and 4°C, the supernatant was collected for further use.

4.2.3.4 Periplasmic expression in E. coli WK6

Non-modified NbBcII10-His_6 (pHEN6 vector) was expressed in *E.coli* WK6 cells (5 mg/L culture) as described by Conrath et al. (19). NbBcII10-HLC (pHEN25 vector) is expressed following the same protocol. This expressed protein contains at its C terminal end a spacer of 14 amino acids, a hexahistidine tag and a cysteine, which will cause a dimerization of the Nb (32).

4.2.4 Synthesis of the 2-amino-3-mercapto-*N*-(prop-2-yn-1-yl)propanamide bifunctional linker

2-Amino-3-mercapto-*N*-(prop-2-yn-1-yl)propanamide was synthesized by dissolving 2 mmol (0.9272 g) *N*-(tert-butoxycarbonyl)-S-trityl-L-cysteine, 2.2

mmol (0.4217 g) of *N*-(3-dimethylaminopropyl)-*N′*-ethylcarbodiimide hydrochloride (EDC) and 2.2 mmol (0.2532 g) N-hydroxysuccinimide (NHS) in 30 mL dichloromethane (DCM) and stirring for 16 h at room temperature. After extraction with water, the DCM phase was dried over $MgSO_4$ and evaporated under reduced pressure. 1 mmol (0.5607 g) of the resulting white powder was dissolved in 20 mL dry DCM together with 2 mmol (0.137 mL) propargylamine and 2 mmol triethylamine (0.279 mL) and stirred continuously for 16 h under N_2 atmosphere at room temperature. The resulting product was purified using column chromatography over silica with ethyl acetate/DCM (1/24) as eluent. The solvent was removed under reduced pressure. To remove the protective Boc and trityl groups, 100 mg of the dry purified product was dissolved in 3 mL trifluoroacetic acid (TFA), 100 µL water and 100 µL triisopropylsilane. After 30 minutes of stirring at room temperature, the TFA was removed under reduced pressure and the product was dissolved in 20 mL DCM. The mixture was extracted 5 times with water and the water phase was lyophilized.

4.2.5 Site-specific alkynation of NbBcII10 by expressed protein ligation

After a cytoplasmic extraction, expressed in *E. coli* SHuffle®T7, the supernatant was slowly added to columns containing chitin beads that were equilibrated with running buffer (20 mM HEPES, 500 mM NaCl and 1 mM EDTA at pH 8.5). After extensive washing with running buffer, the columns were incubated overnight at 4°C with cleavage buffer (CB; 20 mM HEPES, 500 mM NaCl, 1 mM EDTA, 1 mM tris(2-carboxyethyl)phosphine (TCEP) at pH 8.5). While one column was incubated with CB supplemented with 30 mM 2-mercaptoethane sulfonate Na (MESNA), another column was incubated with CB supplemented with 30 mM MESNA and 1 mM of the bifunctional linker 2-amino-3-mercapto-*N*-(prop-2-yn-1-yl)propanamide. After overnight incubation, the columns were eluted using 1.5 column volumes of running buffer and immediately dialyzed against PBS using an Amicon Ultra-15 Centrifugal Filter Unit with Ultracel-3 membrane having a molecular weight cut-off of 3 kDa (Merck Millipore).

4.2.6 SDS-PAGE and electrospray ionization mass spectrometry

All protein extracts were analyzed using sodium dodecyl sulfate-polyacrylamide gel electrophoresis (SDS-PAGE). The samples were boiled in a 2x or 5x SDS sample buffer containing β-mercaptoethanol for 5 minutes and analyzed by 12% SDS-PAGE.

The cytoplasmic extracts were, after alkynation using EPL and dialysis, analyzed by electrospray ionization mass spectrometry (ESI-MS), as described by Ta et al. (23).

4.2.7 Clickability of NbBcII10-LEY-alkyne using western blot

To test the clickability of the EPL-functionalized NbBcII10, a copper-catalyzed azide-alkyne cycloaddition (CuAAC) was performed in solution. In 200 µl phosphate buffered saline (pH 7.4), containing purified NbBcII10-LEY-alkyne, an excess of the azide functionalized biotin derivative *N*-(3-azidopropyl)-5-(2-oxohexahydro-1*H*-thieno[3,4-*d*]imidazol-4-yl)pentanamide (11) (180 µM, dissolved in DMSO) was added together with 900 µM TCEP, 90 µM tris(benzyltriazolylmethyl)amine (TBTA, dissolved in DMSO) and 900 µM $CuSO_4$. As a negative control, non-alkynated NbBcII10 was used. After 2 hours of shaking at 21°C, the reaction products were, without any further purification, boiled with 2x SDS sample buffer. Afterwards, gel electrophoresis was performed using a 12% SDS-PAGE gel with a molecular weight marker. Subsequently, the proteins were transferred to a polyvinylidene fluoride (pvdf) membrane by diffusion overnight. The next day, the membrane was blocked in 5% (w/v) Bovine Serum Albumin (BSA) solution in Tris Buffered Saline Tween (TBST: 25 mM Tris, 150 mM NaCl, 0.05% (v/v) Tween-20, pH 8.0) for 2 hours. To detect the presence of biotin, the membrane was incubated with streptavidin alkaline phosphatase (1/1000) in TBST for 1 hour. Finally, visualization of the biotinylated sample was performed by soaking the membrane for a few seconds in a bromo-4-chloro-3-indolyl-phosphate/nitro blue tetrazolium (BCIP/NTB) solution that will react with the alkaline phosphate on the protein, resulting in a purple precipitate visible on the membrane.

4.2.8 Enzyme-linked immunosorbent assay

To test the capacity of alkynated NbBcII10 to bind to its cognate BcII antigen, a competitive enzyme-linked immunosorbent assay (ELISA) was performed. Non-modified NbBcII10-His_6 was used as a control. A 96-well microplate (Thermo scientific Nunc Maxisorp^{TM}) was coated with 200 µl of a 1 µg/mL BcII antigen solution in ELISA coating buffer (0.1 M $NaHCO_3$, pH 8.2) and incubated overnight at 4°C while shaking. Next, the microplate was rinsed 5 times using TBST buffer, incubated for 7 hours with a 2% (w/v) skimmed milk powder in TBST solution at 4°C while shaking and again washed 5 times using TBST buffer. The NbBcII10-His_6 was then added in a concentration range between 5 and 250 ng/mL to one part of the plate, a combination of NbBcII10-LEY-alkyne (concentration range 250 - 49750 ng/mL) and NbBcII10-His_6 (fixed concentration of 250 ng/mL) was added to the other part. After overnight incubation at 4°C while shaking, the plate was washed 5 times with TBST buffer. Next, the plate was incubated with a monoclonal mouse anti-histidine antibody (1 µg/mL) for 3 hours at 21°C, rinsed again 3 times with TBST and incubated with anti-mouse IgG-alkaline phosphate antibody (0.1 µg/mL) for 2 hours at 21°C. Finally, the plate was rinsed 3 times with TBST and 200 µl of a ready-to-use *p*-nitrophenylphosphate (pNPP) solution was added. After

6.5 minutes, the reaction was blocked with 50 µL NaOH solution (3 M) and the absorbance was measured at 405 nM (OD_{405}) using a FLUOStarOmega Reader (BMG Labtech).

4.2.9 Surface plasmon resonance analysis

Surface plasmon resonance (SPR) affinity measurements were performed using a Biacore T200 (GE Healthcare). A CM5 SPR chip was coated with 348 RU of BcII antigen (MW 24 962 Da) by means of an EDC/NHS coupling. A kinetic study was performed as described in the manufacturer's protocol using a 2-fold serial dilution (500 - 1.95 nM) of NbBcII10-His_6, NbBcII10-HLC and four different batches of NbBcII10-LEY-alkyne. A flow rate of 30 µl/min in HBS (10 mM HEPES, 150 mM NaCl, 3.4 mM EDTA; 0.005 % (v/v) Tween20; pH 7.4) was used, combined with an association phase of 120 sec and a dissociation phase of 600 sec. For regeneration after binding, 100 mM glycine-HCl (pH 2.5) was used. The data were fitted using a 1:1 binding stoichiometry with drift and RI2 kinetic model (Biacore T200 evaluation software).

4.3 Results and discussion

4.3.1 Periplasmic expression

Nbs, including NbBcII10, are generally expressed with a pelB leader signal sequence for secretion in the bacterial periplasm (19). In 2009, Reulen et al. (33) reported the possibility to express a Nb-intein-CBD fusion protein in the periplasm using this N-terminal pelB leader sequence. However, this approach failed for a broad panel of antibody fusion partners and the periplasmic expression of antibody-intein fusions in prokaryotes seems to have its limitations (20). Recent experiments further supported the difficulties to reproduce this strategy for other Nb-intein-CBD fusion proteins (23).

In our study the contribution of the leader signal and the corresponding targeted translocation pathway in the expression level of this fusion was primarily assessed. To this end, NbBcII10 preceded by the pelB (a and a'), ompA (b), ompF (c) or malE (d) signal sequences was cloned between the *NdeI* and *SapI* restriction sites in the pTXB1 vector and transformed in the *E.coli* strain BL21(DE3), expressing T7 RNA polymerase (6, 34, 35). The ability of these four constructs (a)-(d) to export the NbBcII10-intein-CBD fusion protein to the periplasm using the Sec pathway was assessed by monitoring the SDS-PAGE band pattern for the presence of a 43 kDa protein band in the different periplasmic fractions. The absence of any significant protein band corresponding to the NbBcII10-intein-CBD fusion protein, even after enrichment on chitin beads confirmed the previously reported practical problems to transport the Nb-intein-CBD fusion protein through the inner membrane of BL21(DE3) cells via the Sec pathway (23). As a positive control, construct (a') was cloned in the pTXB1 vector in the same way as construct (a-d) but due to the two stop codons between the pelB-NbBcII10 gene and the intein gene, only pelB-NbBcII10 was expressed and transported to the periplasm. As shown in Figure 4.2 (right Lane 1), NbBcII10 was clearly present in the periplasmic extract, indicating that the intein-CBD part prevents the transport of the NbBcII10-intein-CBD fusion protein to the periplasm.

Wagner et al. (30) noted that BL21(DE3) cells are sensitive to the toxic effect of overexpressing membrane proteins by the formation of inclusion bodies in the cytoplasm. Similarly to our Nb-intein-CBD fusion proteins, the same translocation pathways, Sec and SRP, are used by membrane proteins (36). However, expression of NbBcII10-intein-CBD fusion proteins is difficult to control in BL21(DE3) cells as it is driven by the T7 RNA polymerase, both under control of IPTG, and poorly adjustable (37). To solve these issues, Wagner et al. developed the Lemo21(DE3) cell line, derived from BL21(DE3), where the activity of the T7 RNA polymerase is precisely controlled using its natural inhibitor, T7 lysozyme. Following this approach, overexpression of the recombinant target protein can be avoided. The pLemo vector expresses T7 lysozyme, which is under control of a rhamnose inducible promotor, allowing full control of its expression by varying the rhamnose concentration.

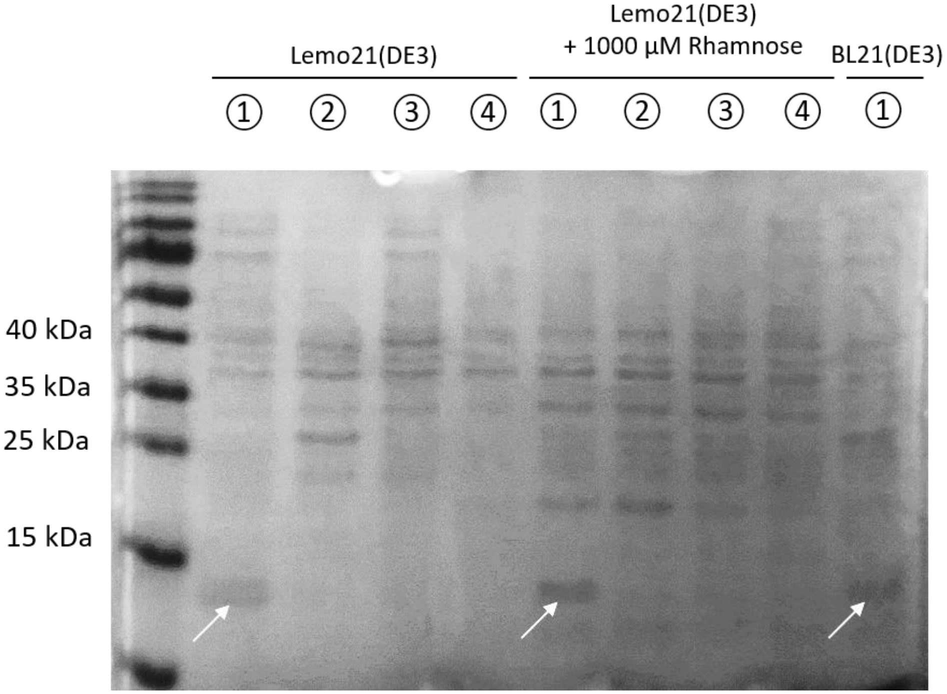

Figure 4.2: SDS-page profile of the unpurified periplasmic extract after expression of constructs (a), (a’), (e) and (g) in the pTXB1 vector using Lemo21DE3 and BL21DE3 cells. Lane ① represents the expression of the positive control (construct (a’)) in the pTXB1 vector in respectively Lemo21(DE3), Lemo21(DE3) enriched with 1000 µM rhamose and BL21(DE3) cells. Due to the two stop codons between the pelB-NbBcII10 gene and the intein-CBD gene, pelB-NbBcII10 was present in the extract as indicated by the white arrow. This means that it is possible to transport NbBcII10 into the periplasm using respectively Lemo21(DE3) and BL21(DE3) cells. Lane ② is the negative control (construct (g)) with no leader sequence and shows no additional bands of the NbBcII10-intein-CBD protein complex (~ 43 kDa) in the periplasm. Note that between 35 kDa and 40 kDa some native proteins are visible, which are present in all extracts, including the positive and negative control. Lane ③ and ④ are respectively constructs (a) and (e) which show no significant difference compared to the negative control. After enrichment using chitin beads, no protein could be detected in any of the samples, meaning that the extracts lack any CBD (and consequently also NbBcII10-intein-CBD is absent) (data not shown).

For this experiment, seven different constructs were transformed into competent Lemo21(DE3) cells: the previously tested constructs (a)-(d) preceded by leader sequences targeting the Sec pathway, two additional constructs incorporating the SRP-pathway targeting signal sequences DsbA (e) and TolB (f) and finally one construct devoid of any signal sequence as negative control (g). Different rhamnose concentrations were tested during expression, ranging from 0 to 2000 µM, and two extraction methods were evaluated (osmotic shock and snap-freezing/vortexing). Of note, in absence of rhamnose there is no functional difference between BL21(DE3) and Lemo21(DE3) cells. For all tested rhamnose concentrations and with both extraction methods, no protein band corresponding to the NbBcII10-intein-CBD fusion protein (43 kDa) could be detected in the periplasmic fraction by SDS-PAGE (Figure 4.2). Here again, we observe that the positive control (a’) was expressed and successfully transported to the periplasm. Consequently, in absence (corresponding to the BL21(DE3) system) or presence of rhamnose in Lemo21(DE3) cells, the periplasmic transport of the nanobody complex is blocked by the intein-CBD part.

These results confirm the difficulties reported by Ta et al. (23) and Marshall et al. (20) regarding the periplasmic expression of antibody fusion proteins, and therefore raise the question about the need for periplasmic expression of Nbs.

4.3.2 Cytoplasmic expression

Periplasmic extraction might have advantages in terms of protein folding, but there are also a number of disadvantages such as a decreased yield due to saturation of the secretion systems, protein aggregation in the cytoplasm (inclusion bodies) as well as a more time consuming expression process (38).

To circumvent these drawbacks, an increasing amount of research has been performed on the cytoplasmic expression of Nbs (23, 39-41). Zarschler et al. (41), for example, reported a strategy for the cytoplasmic expression of Nbs using SHuffle®T7 cells, with proper intradomain disulfide bridge formation. Conversely, Ta et al. (23) reported no affinity loss after cytoplasmic extraction of NbVCAM1 using SHuffle®T7 cells. Consequently, we also transformed our pTXB1 construct (g) in SHuffle®T7 cells to evaluate cytoplasmic expression of our NbBcII10-intein-CBD fusion protein. To guarantee an optimal EPL efficiency, three amino acids, leucine (L), glutamine (E) and tyrosine (Y), were also added downstream of the NbBcII10 protein. Firstly, tyrosine is one of the preferred amino acids at the cleavage site for EPL (35) and secondly, the addition of a peptide spacer between the NbBcII10 and the intein enhances the independent folding of both proteins (23). After expression in SHuffle®T7 cells, the Nb-fusion was extracted from the cytoplasm with B-PER solution containing DNAseI, followed by purification on a chitin column. EPL was then subsequently performed on this column (Figure 4.3).

4.3.3 Expressed protein ligation

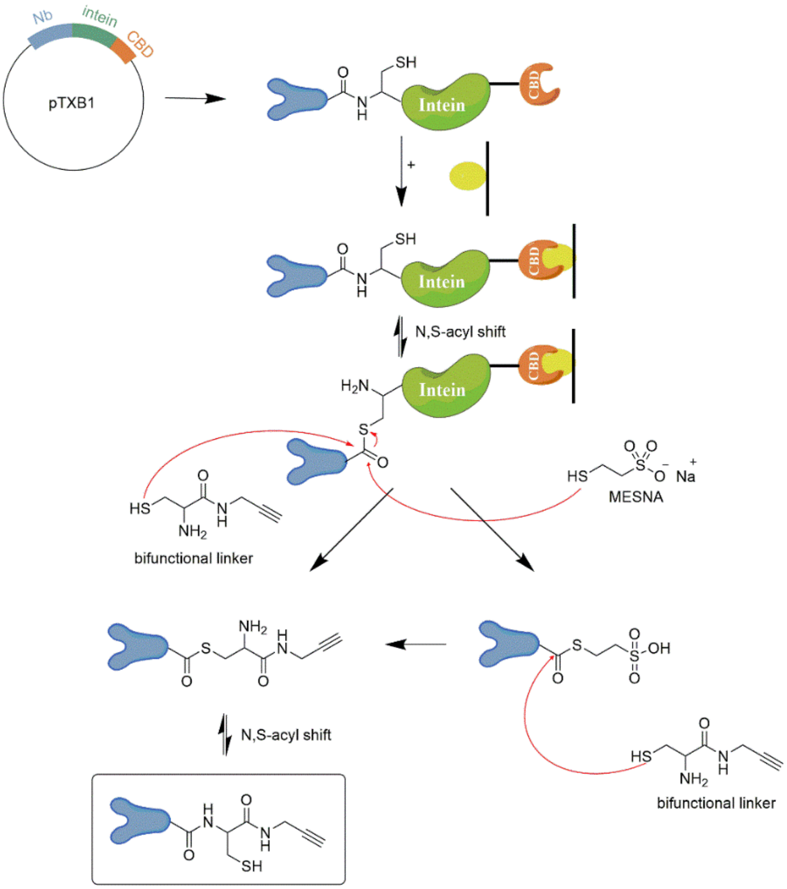

Figure 4.3: Scheme of the expressed protein ligation strategy. For the site-specific alkynation of NbBcII10, the NbBcII10-intein-CBD fusion protein was expressed in SHuffle®T7 cells using the pTXB1 vector. After expression, the fusion protein was purified from the protein extract using a chitin column that binds the CBD present in the fusion protein. Next, the intein will facilitate an N,S-acyl shift of the amide bond between the NbBcII10 (C-terminally) and the intein. The bifunctional linker 2-amino-3-mercapto-*N*-(prop-2-yn-1-yl)propanamide reacts with the thioester bond, resulting in the splicing of NbBcII10 from the column (*left*), and the alkynation of the NbBcII10. In order to increase the yield of the reaction, 2-mercaptoethane sulfonate Na (MESNA) was added at high concentration to facilitate splicing from the column by a nucleophilic attack followed by an exchange of MESNA for the bifunctional linker (*right*).

As illustrated in Figure 4.3, the NbBcII10-intein-CBD fusion protein first binds to an affinity matrix composed of chitin resin. Subsequently, an N,S-acyl shift, facilitated by the intein, will alter the amide bond between the NbBcII10 and the intein into a less stable thioester bond. The thiol functionality of the bifunctional linker 2-amino-3-mercapto-*N*-(prop-2-yn-1-yl)propanamide will act as a nucleophile and will break the thioester bond, resulting in a 2-amino-3-mercapto-*N*-(prop-2-yn-1-yl)propanamide functionalized NbBcII10. A second N,S-acyl shift then turns the formed thioester bond back into a stable amide bond, leaving a C-terminal alkynated NbBcII10.

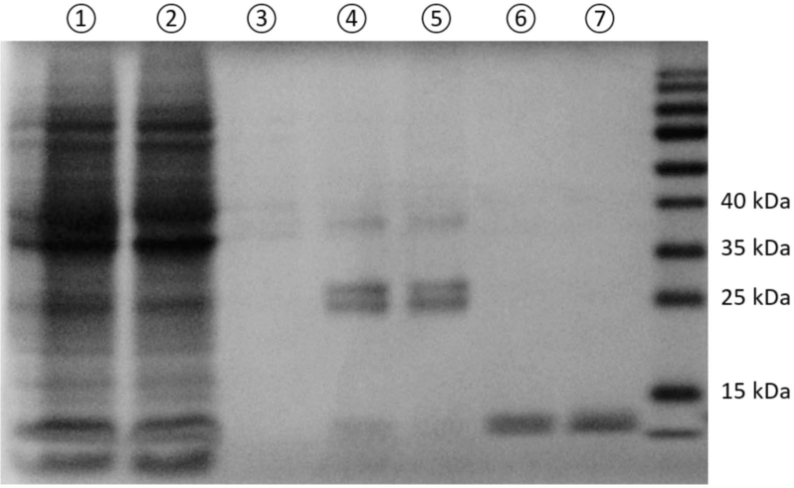

Figure 4.4: SDS-page profile of the EPL process. Lane ① represents the cytoplasmic extract, lane ② and ③ are respectively the first and the last washing step after binding of the Nb-intein-CBD fusion protein on the chitin column. Lane ④ and ⑤ are extraction samples of the chitin beads after the EPL reaction with respectively MESNA and MESNA + bifunctional linker, showing a mass of 28 kDa which corresponds to the molecular mass of the intein-CDB complex, and a faint band of 43 kDa which corresponds to the mass of remaining total NbBcII10-intein-CBD fusion. Finally, lane ⑥ is the eluate of the column after incubation in cleavage buffer containing only MESNA, resulting in non-alkynated, MESNA functionalized NbBcII10, and lane ⑦ is the eluate after incubation with cleavage buffer containing MESNA and bifunctional linker, resulting in alkynated NbBcII10.

To increase the yield of this process, 2-mercaptoethane sulfonate Na (MESNA) was added to the reaction with the bifunctional linker. MESNA will also react via the thioester bond between the NbBcII10 and the intein, resulting in a thioester intermediate that is spliced from the column (35). This MESNA intermediate can afterwards undergo a nucleophilic attack by the 2-amino-3-mercapto-*N*-(prop-2-yn-1-yl)propanamide, thereby exchanging MESNA for the bifunctional linker. The characteristics of the final alkynated protein, NbBcII10-LEY-alkyne (yield of 3.5 mg/L culture), were evaluated on SDS-PAGE (Figure 4.4) and by electrospray ionization mass spectrometry (ESI-MS) (Figure 4.5). Both assays confirmed the theoretically calculated mass of 14506 Da of the mono-alkynated NbBcII10-LEY.

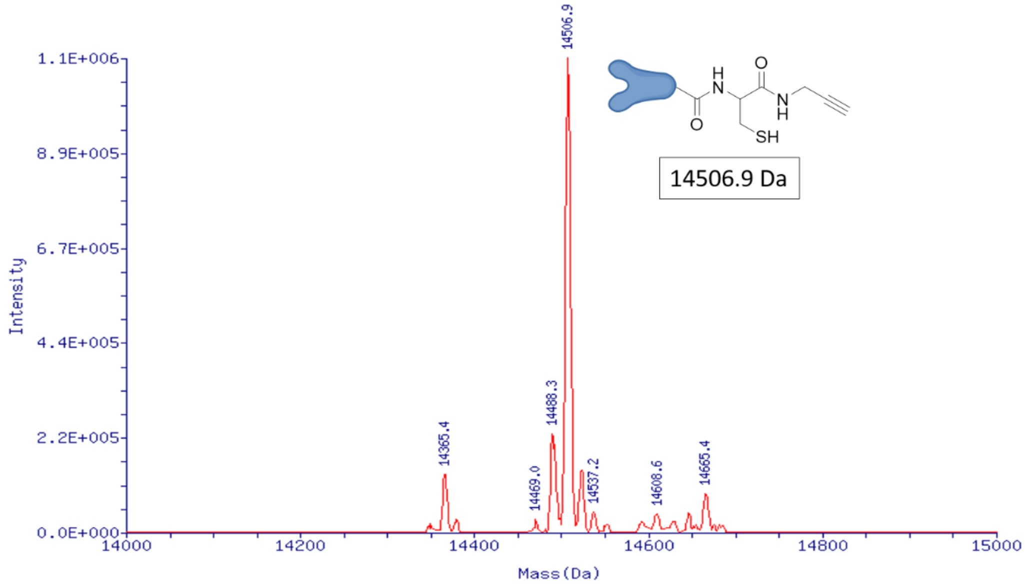

Figure 4.5: Electrospray ionization mass spectrometry (ESI-MS) spectrum of C-terminally, mono-alkynated NbBcII10-LEY. The theoretical mass is 14506 Da.

In order to test the ability of the alkynated NbBcII10 to click on an azide functional group, a click reaction was performed in solution with a biotin-azide derivative. The biotinylated Nb was subsequently visualized in western blot with a streptavidin alkaline phosphatase conjugate. As shown in Figure 4.6, a color reaction appeared at 14.5 kDa in lane 1 and 2, confirming the presence of biotin on the Nb as a result of a successful click reaction. The negative control, lane 3, that contains non-alkynated NbBcII10, showed no reaction. Of note, due to the absence of reducing agent in the sample, dimers are also visible around 29 kDa.

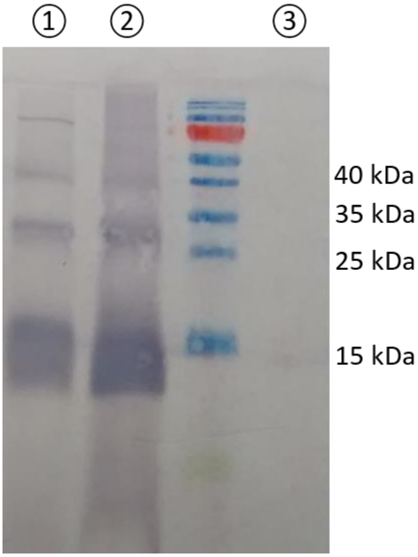

Figure 4.6: Western blot of the click reaction product between NbBcII10-LEY-alkyne and a biotin-azide derivate. Lanes ① and ② contain the reaction product (amount applied in lane ② is 10 times higher than lane ①), while lane ③, the negative control, contains non-alkynated NbBcII10.

4.3.4 Functionality test of NbBcII10-LEY-alkyne

Finally, the functionality of NbBcII10 after cytoplasmic extraction of the Nb-intein-CBD complex and after alkynation using EPL remains to be demonstrated. To this end, the affinity of NbBcII10-LEY-alkyne for its antigen BcII was evaluated in a competitive enzyme-linked immunosorbent assay (ELISA). First, the unmodified, native NbBcII10-His$_6$ at a concentration range between 0 and 250 ng/mL was used as a reference. The ELISA showed a clear logarithmic correlation between the OD$_{405}$ signal and the concentration of NbBcII10-His$_6$ (Figure 4.7a). Next, in addition to 250 ng/mL NbBcII10-His$_{6,}$ a concentration range between 250 and 49.750 ng/mL NbBcII10-LEY-alkyne was added to BcII coated wells and the antigen captured NbBcII10-His$_6$ was detected. As shown in Figure 4.7, the OD$_{405}$ signal decreases with higher NbBcII10-LEY-alkyne concentrations indicating that NbBcII10-LEY-alkyne competes with NbBcII10-His$_6$ for binding the BcII antigen, thereby reducing the amount of detectable His$_6$-tag.

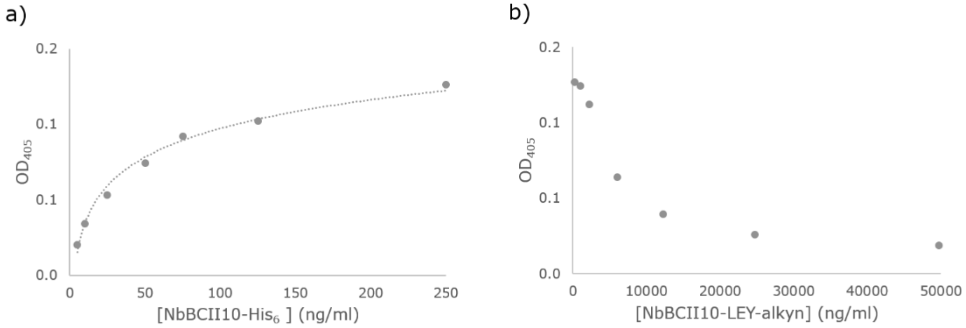

Figure 4.7: Enzyme-linked immunosorbent assay (ELISA) results (a) showing the binding of NbBcII10-His$_6$ to the BcII antigen and (b) competitive ELISA results showing the decrease in binding of NbBcII10-His$_6$ (250 µg/mL) after adding an increasing concentration of the NbBcII10-LEY-alkyne (250-49750 ng/mL).

In order to compare the affinity of NbBcII10-LEY-alkyne for BcII lactamase with that of NbBcII10-His$_6$, an antigen binding study using SPR was performed. The association (k_{on}) and dissociation (k_{off}) rate constants between NbBcII10-LEY-alkyne and BcII were measured, from which the dissociation equilibrium constant (K_D) can be calculated. Of note, due to the use of a cysteine-based bifunctional linker during the EPL process, i.e. 2-amino-3-mercapto-*N*-(prop-2-yn-1-yl)propanamide, a cysteine is incorporated at the C-terminus of the Nb, as shown in Figure 4.3. As a result, spontaneous dimerization of the Nbs is expected to occur, which could potentially influence the SPR experiment. Indeed, under these circumstances a 1:1 binding model can no longer be assumed and therefore an additional control measurement was included. This control is the NbBcII10-HLC having an additional cysteine at its C-terminus and which is expressed in the periplasm and isolated in the same way as the unmodified NbBcII10-His$_6$ (32). Table 4.3 reveals the improvement of the K_D for the NbBcII10-LEY-alkyne recognition of BcII, compared with that of the non-modified NbBcII10-His$_6$. This K_D decrease is mainly caused by a 10-fold drop in the k_{off}-value, as observed for the four independent batches of NbBcII10-LEY-alkyne. The variation in k_{on}-values between NbBcII10-His$_6$ and the alkynated Nbs is marginal, whereas the k_{off} values differ by nearly a factor 10. Note that a similar effect on the k_{off} is observed for the dimerized NbBcII10-HLC.

Table 4.3: Affinity constants (association rate constant k_{on}, dissociation rate constant k_{off}, and dissociation equilibrium constant K_D) of the binding between NbBcII10 variants and BcII.

Nanobody	k_{on} (1/M.s)	k_{off} (1/s)	K_D (M)*
NbBcII10-His$_6$	1.24 x10^{6}	2.23 x10^{-2}	1.78 x10^{-8}
NbBcII10-LEY-alkyne-1	9.67 x10^{5}	1.35 x10^{-3}	1.39 x10^{-9}
NbBcII10-LEY-alkyne-2	4.44 x10^{5}	1.26 x10^{-3}	2.82 x10^{-9}
NbBcII10-LEY-alkyne-3	5.16 x10^{5}	1.32 x10^{-3}	2.57 x10^{-9}
NbBcII10-LEY-alkyne-4	3.70 x10^{6}	1.70 x10^{-3}	4.60 x10^{-10}
NbBcII10-HLC	2.85 x10^{7}	2.56 x10^{-3}	8.99 x10^{-11}

*$K_D = k_{off}/k_{on}$

When construing the sensorgram of NbBcII10-LEY-alkyne in Figure 4.8b, however, it is clear that the dissociation phase of NbBcII10-LEY-alkyne deviates from that of the unmodified NbBcII10-His$_6$ (Figure 4.8a). After an initial rapid drop in signal during the washing phase, the further release from the antigen apparently slows down and eventually stops to reach a (nearly) constant signal. Likewise, the sensorgram of NbBcII10-HLC (Figure 4.8c) shows a very similar pattern. Clearly, this emphasizes the contribution of a fraction of Nb proteins that are dimerized Nbs through their C-terminal cysteine residues within these samples. Of note, after every association-dissociation cycle, full regeneration of the surface was achieved with 100 mM glycine-HCl (pH 2.5).

In conclusion, neither the cytoplasmic extraction nor the site-specific alkynation of the NbBcII10-LEY-alkyne had any effect on the association rate constant relative to the native Nb. The dissociation rate constant, however, and consequently the dissociation equilibrium constant (K_D) showed an improvement by almost a factor 10, most likely due to dimerization of the probe. This clearly demonstrates that the functionality of the antigen-recognizing moiety is not affected by the C-terminal functionalization.

Nonetheless, for diagnostic applications, where the Nb is immobilized to the surface rather than the antigen, this fractional dimerization should not raise any concerns.

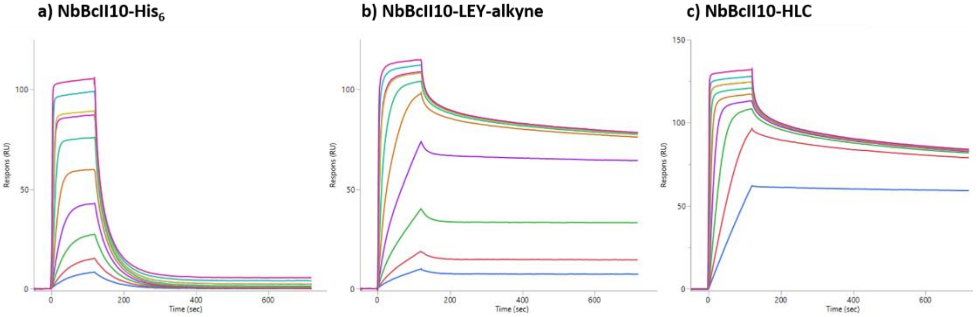

Figure 4.8: SPR sensorgrams of the BcII antigen binding study of NbBcII10-His$_6$ (a), NbBcII10-LEY-alkyne (b) and NbBcII10-HLC (c). NbBcII10-LEY-alkyne and NbBcII10-HLC have a similar pattern with an improved k_{off} in comparison with NbBcII10-His$_6$.

To summarize, in this study, an alkyne was site-specifically introduced as a bioorthogonal group on a single-domain antigen binding fragment without compromising its functionality. Through a copper(I)-catalyzed alkyne-azide cycloaddition (CuAAC) (42) these probes can subsequently uniformly be immobilized in an oriented fashion on azide functionalized surfaces (43). This strategy can also easily be extended to alternative click chemistries, using other bioorthogonal groups, such as the strain-promoted alkyne-azide cycloaddition (SPAAC) (44), Staudinger ligation (45), Diels-Alder cycloaddition (1) or the more recently developed strain-promoted inverse electron-demand Diels–Alder cycloaddition (SPIEDAC) (46) by simple adjustment of the bifunctional linker.

4.4 Conclusions

In this study, it was proven that it is possible to site-specifically alkynate NbBcII10 using EPL and couple the alkynated Nb to an azide functionality. With respect to the periplasmic expression of the Nb-intein-CBD complex, several leader sequences were evaluated, but none of them was successful. Nevertheless, by using SHuffle®T7 cells and appending a small peptide spacer (LEY) to the C-terminus of the Nb, fully functional Nb-LEY-alkyne was produced through cytoplasmic expression and alkynation by EPL. This demonstrates that Nb-intein-CBD fusion complexes, prepared for alkynation by EPL, do not necessarily need to be expressed in the periplasm to remain active and that post-translation alkynation using EPL has no influence on the binding activity of NbBcII10.

4.5 References

1. Rusmini F, Zhong Z, Feijen J. Protein Immobilization Strategies for Protein Biochips. Biomacromolecules. 2007;8(6):1775-89.
2. Barbosa O, Torres R, Ortiz C, Berenguer-Murcia Á, Rodrigues RC, Fernandez-Lafuente R. Heterofunctional Supports in Enzyme Immobilization: From Traditional Immobilization Protocols to Opportunities in Tuning Enzyme Properties. Biomacromolecules. 2013;14(8):2433-62.
3. Grieten L, Janssens SD, Ethirajan A, Bon NV, Ameloot M, Michiels L, et al. Real-time study of protein adsorption on thin nanocrystalline diamond. Phys Status Solidi A. 2011;208(9):2093-8.
4. Steen Redeker E, Ta DT, Cortens D, Billen B, Guedens W, Adriaensens P. Protein Engineering For Directed Immobilization. Bioconj Chem. 2013;24(11):1761-77.
5. Fischer ME. Amine Coupling Through EDC/NHS: A Practical Approach. In: Mol NJ, Fischer MJE, editors. Surface Plasmon Resonance. Methods in Molecular Biology. 627: Humana Press; 2010. p. 55-73.
6. Lempens EHM, Helms BA, Merkx M. Chemoselective Protein and Peptide Immobilization on Biosensor Surfaces. In: Mark SS, editor. Bioconjugation Protocols: Strategies and Methods. Totowa, NJ: Humana Press; 2011. p. 401-20.
7. Porath J, Carlsson JAN, Olsson I, Belfrage G. Metal chelate affinity chromatography, a new approach to protein fractionation. Nature. 1975;258(5536):598-9.
8. Ganesana M, Istarnboulie G, Marty J-L, Noguer T, Andreescu S. Site-specific immobilization of a (His)6-tagged acetylcholinesterase on nickel nanoparticles for highly sensitive toxicity biosensors. Biosensors Bioelectron. 2011;30(1):43-8.
9. Chong S, Mersha FB, Comb DG, Scott ME, Landry D, Vence LM, et al. Single-column purification of free recombinant proteins using a self-cleavable affinity tag derived from a protein splicing element. Gene. 1997;192(2):271-81.
10. Berrade L, Camarero JA. Expressed protein ligation: a resourceful tool to study protein structure and function. Cell Mol Life Sci. 2009;66(24):3909-22.
11. Lin P-C, Ueng S-H, Tseng M-C, Ko J-L, Huang K-T, Yu S-C, et al. Site-Specific Protein Modification through CuI-Catalyzed 1,2,3-Triazole Formation and Its Implementation in Protein Microarray Fabrication. Angew Chem Int Ed. 2006;45(26):4286-90.
12. Sletten EM, Bertozzi CR. Bioorthogonal Chemistry: Fishing for Selectivity in a Sea of Functionality. Angew Chem Int Ed. 2009;48(38):6974-98.
13. Hamers-Casterman C, Atarhouch T, Muyldermans S, Robinson G, Hamers C, Songa EB, et al. Naturally occurring antibodies devoid of light chains. Nature. 1993;363(6428):446-8.

14. Vanlandschoot P, Stortelers C, Beirnaert E, Ibañez LI, Schepens B, Depla E, et al. Nanobodies®: New ammunition to battle viruses. Antiviral Res. 2011;92(3):389-407.

15. Huang L, Muyldermans S, Saerens D. Nanobodies®: proficient tools in diagnostics. Expert Rev Mol Diagn. 2010;10(6):777-85.

16. Muyldermans S, Baral TN, Retamozzo VC, De Baetselier P, De Genst E, Kinne J, et al. Camelid immunoglobulins and nanobody technology. Vet Immunol Immunopathol. 2009;128(1–3):178-83.

17. Hassanzadeh-Ghassabeh G, Devoogdt N, De Pauw P, Vincke C, Muyldermans S. Nanobodies and their potential applications. Nanomedicine. 2013;8(6):1013-26.

18. Muyldermans S. Single domain camel antibodies: current status. Rev Mol Biotechnol. 2001;74(4):277-302.

19. Conrath KE, Lauwereys M, Galleni M, Matagne A, Frère J-M, Kinne J, et al. β-Lactamase Inhibitors Derived from Single-Domain Antibody Fragments Elicited in the Camelidae. Antimicrob Agents Chemother. 2001;45(10):2807-12.

20. Marshall CJ, Grosskopf VA, Moehling TJ, Tillotson BJ, Wiepz GJ, Abbott NL, et al. An Evolved Mxe GyrA Intein for Enhanced Production of Fusion Proteins. ACS Chem Biol. 2015;10(2):527-38.

21. Ghosh I, Considine N, Maunus E, Sun L, Zhang A, Buswell J, et al. Site-specific protein labeling by intein-mediated protein ligation. Methods Mol Biol. 2011;705:87-107.

22. Muir TW, Sondhi D, Cole PA. Expressed protein ligation: a general method for protein engineering. Proc Natl Acad Sci U S A. 1998;95(12):6705-10.

23. Ta DT, Steen Redeker E, Billen B, Reekmans G, Sikulu J, Noben J-P, et al. An efficient protocol towards site-specifically clickable nanobodies in high yield: cytoplasmic expression in Escherichia coli combined with intein-mediated protein ligation. Protein Eng Des Sel. 2015;28(10):351-63.

24. Natale P, Brüser T, Driessen AJM. Sec- and Tat-mediated protein secretion across the bacterial cytoplasmic membrane—Distinct translocases and mechanisms. Biochim Biophys Acta. 2008;1778(9):1735-56.

25. Voss T, Falkner E, Ahorn H, Krystek E, Maurer-Fogy I, Bodo G, et al. Periplasmic expression of human interferon-ɑ 2c in Escherichia coli results in a correctly folded molecule. Biochem J. 1994;298(3):719-25.

26. Steiner D, Forrer P, Stumpp MT, Pluckthun A. Signal sequences directing cotranslational translocation expand the range of proteins amenable to phage display. Nat Biotech. 2006;24(7):823-31.

27. Nangola S, Minard P, Tayapiwatana C. Appraisal of translocation pathways for displaying ankyrin repeat protein on phage particles. Protein Expression Purif. 2010;74(2):156-61.

28. Vincke C, Loris R, Saerens D, Martinez-Rodriguez S, Muyldermans S, Conrath K. General Strategy to Humanize a Camelid Single-domain Antibody and

Identification of a Universal Humanized Nanobody Scaffold. J Biol Chem. 2009;284(5):3273-84.

29. Saerens D, Pellis M, Loris R, Pardon E, Dumoulin M, Matagne A, et al. Identification of a Universal VHH Framework to Graft Non-canonical Antigen-binding Loops of Camel Single-domain Antibodies. J Mol Biol. 2005;352(3):597-607.

30. Wagner S, Klepsch MM, Schlegel S, Appel A, Draheim R, Tarry M, et al. Tuning Escherichia coli for membrane protein overexpression. Proc Natl Acad Sci U S A. 2008;105(38):14371-6.

31. Schlegel S, Rujas E, Ytterberg AJ, Zubarev R, Luirink J, de Gier J-W. Optimizing heterologous protein production in the periplasm of E. coli by regulating gene expression levels. Microb Cell Fact. 2013;12(1):24.

32. Massa S, Xavier C, De Vos J, Caveliers V, Lahoutte T, Muyldermans S, et al. Site-Specific Labeling of Cysteine-Tagged Camelid Single-Domain Antibody-Fragments for Use in Molecular Imaging. Bioconj Chem. 2014;25(5):979-88.

33. Reulen S, van Baal I, Raats J, Merkx M. Efficient, chemoselective synthesis of immunomicelles using single-domain antibodies with a C-terminal thioester. BMC Biotechnol. 2009;9(1):66-74.

34. Sydor JR, Mariano M, Sideris S, Nock S. Establishment of Intein-Mediated Protein Ligation under Denaturing Conditions: C-Terminal Labeling of a Single-Chain Antibody for Biochip Screening. Bioconj Chem. 2002;13(4):707-12.

35. Xu M-Q, Evans Jr TC. Intein-Mediated Ligation and Cyclization of Expressed Proteins. Methods. 2001;24(3):257-77.

36. Wagner S, Bader ML, Drew D, de Gier J-W. Rationalizing membrane protein overexpression. Trends Biotechnol. 2006;24(8):364-71.

37. Wanner BL, Kodaira R, Neidhart FC. Physiological regulation of a decontrolled lac operon. J Bacteriol. 1977;130(1):212-22.

38. Pleiner T, Bates M, Trakhanov S, Lee C-T, Schliep JE, Chug H, et al. Nanobodies: site-specific labeling for super-resolution imaging, rapid epitope-mapping and native protein complex isolation. eLife. 2015;4:e11349.

39. Djender S, Schneider A, Beugnet A, Crepin R, Desrumeaux KE, Romani C, et al. Bacterial cytoplasm as an effective cell compartment for producing functional VHH-based affinity reagents and Camelidae IgG-like recombinant antibodies. Microb Cell Fact. 2014;13(1):1-10.

40. Olichon A, Surrey T. Selection of genetically encoded fluorescent single-domain antibodies engineered for efficient expression in Escherichia coli. J Biol Chem. 2007;282(50):36314-20.

41. Zarschler K, Witecy S, Kapplusch F, Foerster C, Stephan H. High-yield production of functional soluble single-domain antibodies in the cytoplasm of Escherichia coli. Microb Cell Fact. 2013;12(1):1-13.

42. Huisgen R. Proceedings of the Chemical Society. October 1961. Proc Chem Soc. 1961(October):357-96.

43. Vranken T, Steen Redeker E, Miszta A, Billen B, Hermens W, de Laat B, et al. In situ monitoring and optimization of CuAAC-mediated protein functionalization of biosurfaces. Sens Actuators B Chem. 2017;238:992-1000.
44. Mbua NE, Guo J, Wolfert MA, Steet R, Boons G-J. Strain-Promoted Alkyne–Azide Cycloadditions (SPAAC) Reveal New Features of Glycoconjugate Biosynthesis. ChemBioChem. 2011;12(12):1912-21.
45. Staudinger H, Meyer J. Über neue organische Phosphorverbindungen III. Phosphinmethylenderivate und Phosphinimine. Helv Chim Acta. 1919;2(1):635-46.
46. Horner KA, Valette NM, Webb ME. Strain-Promoted Reaction of 1,2,4-Triazines with Bicyclononynes. Chem Eur J. 2015;21(41):14376-81.

Chapter 5

Experimental details

5.1 Introduction

This chapter focusses on the experimental framework used during this thesis.

First, methods used for random and site-specific functionalization of proteins are described. For the random protein functionalization, the EDC/NHS coupling was used. For the site-specific protein functionalization, this thesis makes use of expressed protein ligation (EPL). The EPL strategy is explained in detail, starting with the vector design (including an overview of the used constructs), the different expression hosts, the synthesis of the bifunctional linkers and the expression and purification.

Secondly, the molecular cloning techniques that are necessary for the vector design of the EPL vectors are presented.

Finally, the experimental details of the characterization techniques to evaluate the expressed proteins and the immobilization of the proteins on functionalized surfaces are explained.

5.2 Random versus site-specific protein functionalization

In Chapter 1, a detailed overview is presented of the different protein functionalization and subsequent immobilization methods. In this thesis, the EDC/NHS reaction is used for the random functionalization of proteins or for the direct coupling of proteins on a surface plasmon resonance (SPR) chip. Secondly, EPL is used for the site-specific functionalization of maltose binding protein (MBP) and nanobody BcII10 (NbBcII10).

5.2.1 Random protein functionalization via an EDC/NHS coupling reaction

As already mentioned in the introduction, the EDC/NHS reaction is based on the coupling between an amine group and an NHS activated carboxyl group. The EDC/NHS reaction is one of the most commonly used random protein functionalization methods because of its simplicity, relative fast reaction and the possibility to perform it in physiological conditions (1-3). This reaction is applied in two experimental set-ups, namely the random alkynation of MBP as discussed in Chapter 2, and the coupling of the BcII antigen to the CM5 SPR chip in Chapter 4.

For the random alkynation of MBP, 2,5-dioxopyrrolidin-1-yl-hex-5-ynoate was used. The synthesis of this alkynated NHS-ester was described by Jagadish et al. (4). The NHS-ester reacts with the ε-amine of one of the available lysines on the surface of MBP (in total, MBP contains 37 lysines). The reaction mechanism is shown in Figure 5.1. The reaction conditions were described in Chapter 2.

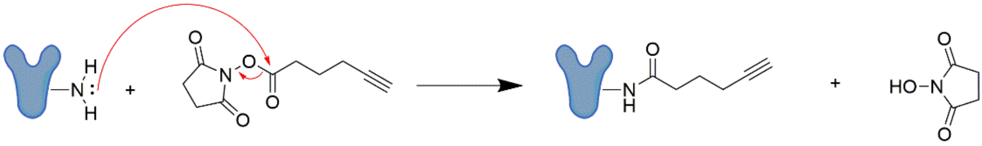

Figure 5.1: The ECS/NHS mechanism of the reaction between the ε-amine of a lysine side chain and 2,5-dioxopyrrolidin-1-yl-hex-5-ynoate.

A similar reaction is used for the SPR experiments with NbBcII10 in Chapter 4. Here, the protein is not functionalized in advance but directly coupled to the CM5 chip surface, which contains a carboxymethylated dextran layer on a gold surface. The reaction mechanism of the EDC/NHS reaction on a carboxylated surface is already discussed in Chapter 1.

5.2.2 Site-specific protein functionalization via expressed protein ligation

The general idea of the EPL strategy is already discussed in Chapter 1. This part will discuss EPL specifically applied on MBP and NbBcII10, including the used vector constructs and bacterial cell lines. The molecular cloning techniques for the EPL constructs are discussed in section 2.3.

5.2.2.1 Vector design

The first step in the functionalization protocol of MBP or NbBcII10 is the development of a suitable vector. This vector needs to contain the protein of interest (POI), the mutated Mxe GyrA intein and a chitin binding domain (CBD). For MBP, this vector, pMXB10, is commercially available (New Engeland Biolabs) and requires no modifications of the genetic code. Further details concerning the components of the vector are discussed at the end of this section.

With regard to NbBcII10, the encoding gene has to be isolated from the pHEN6:*pelB*-NbBcII10-His$_6$ vector (5) as originally developed at the Vrije Universiteit Brussel (VUB). Besides the genetic code for the expression of NbBcII10, this vector also contains the pelB-leader sequence. This sequence was added to facilitate the periplasmic transport during the expression of the NbBcII10 in *E. coli* WK6 cells. Nanobodies are expressed in the periplasm because its oxidizing environment facilitates protein folding and the purification afterwards is easier (5, 6). As will be discussed in Chapter 4, there are difficulties with the periplasmic transport of the NbBcII10-intein-CBD fusion protein using the pelB leader sequence. Since there are multiple leader sequences and pathways possible for periplasmic transport, different gene fragments were developed using different leader sequences as shown in Figure 5.2. These constructs were developed using PCR, as described further in section 5.3.

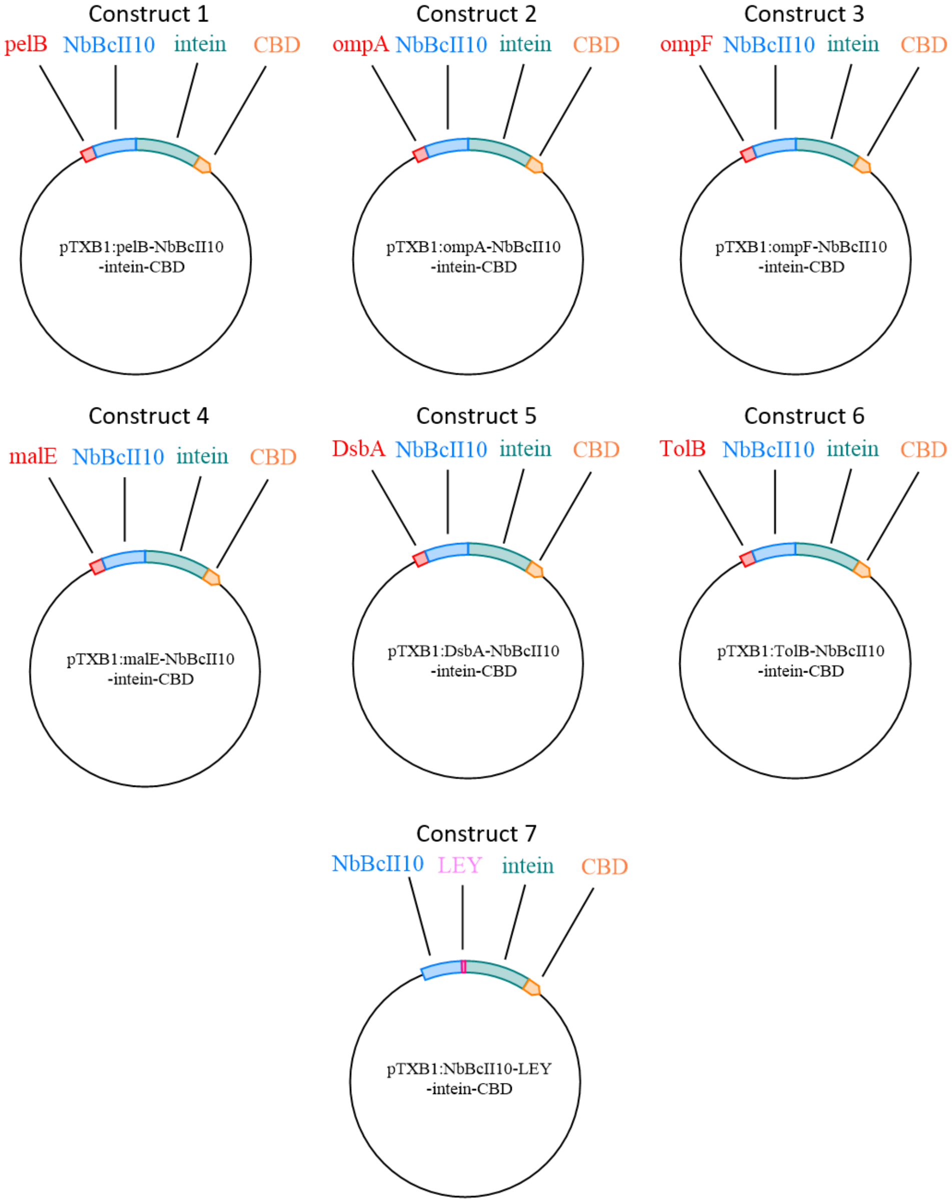
Construct 1
pelB
NbBcII10
intein
CBD
pTXB1:pelB-NbBcII10 -intein-CBD
Construct 2
ompA
NbBcII10
intein
CBD
pTXB1:ompA-NbBcII10 -intein-CBD
Construct 3
ompF
NbBcII10
intein
CBD
pTXB1:ompF-NbBcII10 -intein-CBD
Construct 4
malE
NbBcII10
intein
CBD
pTXB1:malE-NbBcII10 -intein-CBD
Construct 5
DsbA
NbBcII10
intein
CBD
pTXB1:DsbA-NbBcII10 -intein-CBD
Construct 6
TolB
NbBcII10
intein
CBD
pTXB1:TolB-NbBcII10 -intein-CBD
Construct 7
NbBcII10
LEY
intein
CBD
pTXB1:NbBcII10-LEY -intein-CBD

Figure 5.2: Overview of the different vector constructs used for EPL.

Besides the POI, a vector is necessary containing the mutated intein and the CBD. Here, the pTXB1 vector was used as shown in Figure 5.3. The vector is designed for the in-frame insertion of a target gene into the polylinker upstream of the Mxe intein/chitin-binding domain. The details about vector preparation are discussed in section 5.3.2.

Besides the genetic code for the intein and CBD, the vector contains other components, necessary for the successful protein expression as shown in Figure 5.3.

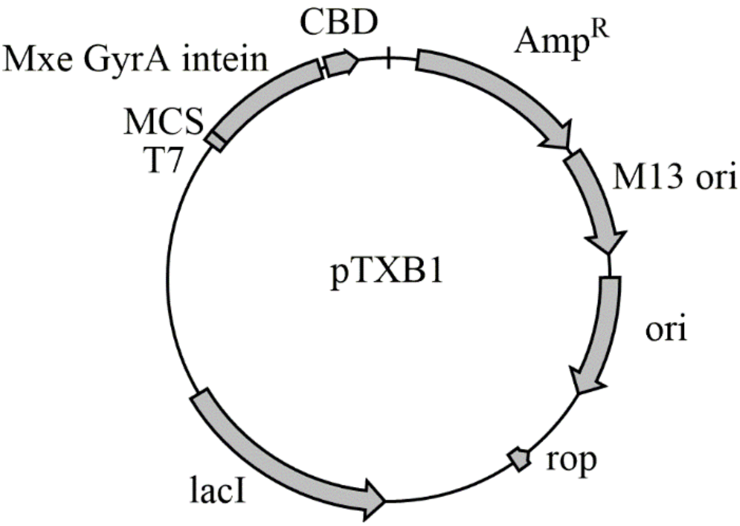

Feature	Location in vector
Ampicillin resistance gene (Amp^R)	140-1000
M13 origin	1042-1555
Origine of replication (ori)	1666-2254
rop	2714-2623
lacI	4453-3371
T7 promotor	5637-5654
Multiple cloning site (MCS)	5722-5775
Mxe GyrA intein	5776-6369
CBD	6400-6558

Figure 5.3: Schematic overview of the components of the pTXB1 vector.

The pTXB1 vector is under control of the T7 promotor as shown in Figure 5.3. This promotor needs to be activated by T7 RNA polymerase. Note that the vector also contains the lacI gene, which is encoding for the tetrameric lac repressor. The lac repressor is responsible for the constant inactivation of the T7 promotor by binding to the lac operon. This means that there are two crucial factors for the expression of the NbBcII10-intein-CBD complex. First, the lac repressor has to be inhibited, and secondly the T7 RNA polymerase has to be added. Inhibition of the lac repressor is done by using a molecular mimic of allactose, in this case isopropyl β-D-1-thiogalactopyranoside (IPTG). IPTG binds to the lac repressor and releases the tetrameric repressor from the lac operator in an allosteric manner, thereby allowing the transcription of genes in the lac operon. The T7 RNA polymerase is produced by the host *E. coli* genome. T7 RNA polymerase is highly selective for initiation at its own promoter sequences and it does not initiate transcription from any sequences on *E. coli* DNA (7). All expression hosts used in this thesis for EPL are (derivatives of) BL21(DE3) except for the E. coli SHuffle® T7 cells. The detailed mechanism of each expression system is discussed in the next section.

Note that the pMXB10 vector, for the expression of the MBP-intein-CBD complex is exactly the same as the pTXB1 vector, except for the genetic code of MBP which is already build in upstream from the Mxe GyrA intein (Figure 5.4).

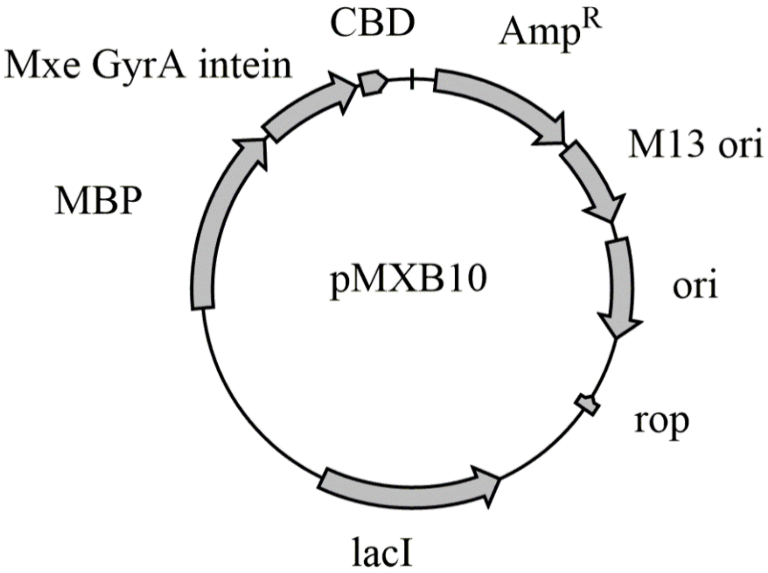

Figure 5.4: Schematic overview of the components of the pMXB10 vector. Except for the MBP gene, all the components are the same as in the pXB1 vector.

5.2.2.2 Expression hosts

For the expression of the protein-intein-CDB complex, three different expression hosts, with different properties, were evaluated.

BL21(DE3). The *E. coli* BL21(DE3) cells are developed for protein expression and can be optimally used with bacteriophage T7 promoter-based expression systems. BL21 strains originate from the *E. coli* B strain and have been specifically constructed for high-level expression of recombinant proteins. These strains have two important attributes that make them ideal for protein expression: key genetic markers and inducibility of protein expression. The most important genetic markers help recombinant RNA and/or protein accumulation to high levels without degradation. Inducibility helps to minimize the toxic effects of some recombinant proteins (8). BL21(DE3) cells contain the lambda DE3 lysogen, which carries the gene for T7 RNA polymerase under control of the lacUV5 promoter. IPTG is required to maximally induce expression of the T7 RNA polymerase in order to express recombinant genes cloned downstream of a T7 promoter (9, 10). The molecular process is shown in Figure 5.5. In natural circumstances, the lac promotor (DE3) is blocked by the lac repressor, coded by the lac I gene. By adding IPTG, the repression of the T7 gene is removed and the *E. coli* RNA polymerase can bind to the lac promotor resulting in the expression of T7 RNA polymerase. IPTG will also replace the lac repressor on the T7 promotor, resulting in the binding of T7 RNA polymerase to the T7 promotor which induced the expression of the protein-intein-CDB complex.

Lemo21(DE3). An interesting derivative of BL21(DE3) cells are *E. coli* Lemo21(DE3) cells. They are developed for the fine-tuning of T7 expression in order to control inclusion body formation or growth inhibitory effects from toxic proteins. Often, by decreasing the expression levels, more protein is produced. This is particularly true for membrane protein expression and periplasmic protein expression (11). Membrane protein expression and protein export in *E. coli* are both limited by the throughput capacity of the Sec translocase and in some cases the Tat translocase. T7 expression of proteins targeted to the Sec translocase often leads to accumulation of inclusion bodies or inhibition of cell division if expression is not regulated (12). Lemo21(DE3) cells offer the same properties as BL21(DE3) but allow tunable expression of difficult clones (Figure 5.5). They contain an additional vector, pLemo, that expresses lysozyme lysY, which is the natural inhibitor of T7 RNA polymerase. The expression of lysY is under control of a L-rhamnose inducible promoter (rhaBAD). This results in a tunable expression dependent on the concentration of rhamnose that is added to the culture media (10, 12, 13).

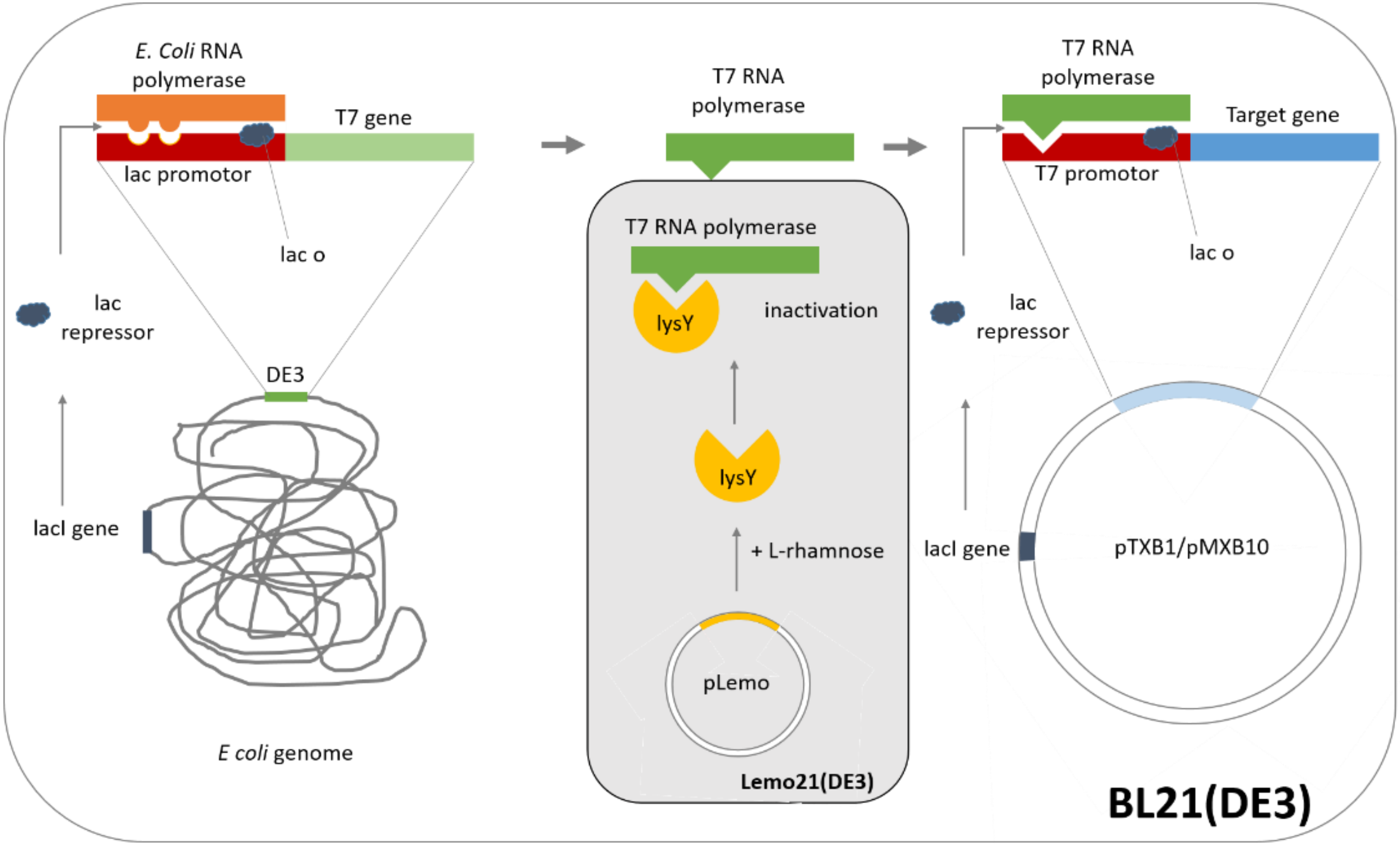
E. Coli RNA polymerase
T7 gene
lac promotor
lac o
lac repressor
DE3
lacI gene
E coli genome
T7 RNA polymerase
T7 RNA polymerase
lysY
inactivation
lysY
+ L-rhamnose
pLemo
Lemo21(DE3)
T7 RNA polymerase
Target gene
T7 promotor
lac o
lac repressor
lacI gene
pTXB1/pMXB10
BL21(DE3)

Figure 5.5: Induction of protein expression in BL21(DE3) and Lemo21(DE3) *E. coli* cells

SHuffle®T7*.* Nbs need an oxidizing environment for their correct folding and disulfide bond formation. SHuffle®T7 cells are an *E. coli* K12 strain that promotes disulfide bond formation in the cytoplasm. As discussed in Chapter 4, this gives the possibility to express Nbs in the cytoplasm (14). (15-17). Besides DsbC, SHuffle®T7 also expresses a chromosomal copy of T7 RNA polymerase, making it possible to use it in combination with T7 promoter-based vectors.

5.2.2.3 Expression, extraction and purification of the proteins

For the expression of the protein-intein-CBD complex, the different constructs need to be transformed into the different bacterial hosts. This is done by a process known as transformation. In order to use this approach, the bacteria need to be competent, meaning that the outer membrane is slightly damaged so that the DNA can cross the membrane, but still can recover after the transformation. The transformation process and the subsequent steps in molecular cloning are discussed in section 5.3.3.

Once the bacteria are transformed with the vector constructs, the expression takes places. This is done using Luria-Bertani (LB) medium. As mentioned before, the pTXB1 and pMXB10 vectors contain an ampicillin resistance gene, meaning that ampicillin (amp) can be added to all growth media to avoid any contamination with other bacteria. First, the bacteria are grown to an optical density between 0.6 and 0.9 at 600 nm (OD_{600}). At this stage, the bacteria are in their exponential growth phase and are ready for expression. When induction takes place below an optical density of 0.6, the high expression of recombinant protein will inhibit bacterial growth and reduce the final protein yield.

The induction of the protein expression is done by the addition of IPTG which causes the expression of T7 RNA polymerase, which activates the T7 promotor as discussed in section 5.2.2.2.

Constructs 1-6 (Figure 5.2) contain a leader sequence that transports the protein-intein-CBD complex to the periplasm using the Sec pathway (construct 1-4) or the signal recognition particle (SRP) pathway (construct 5-6) during the expression. These pathways are discussed more elaborately in Chapter 5. After the expression, the proteins need to be collected from the bacterial periplasm or cytoplasm, dependent on the presence or absence of a leader sequence as schematically represented in Figure 5.6.

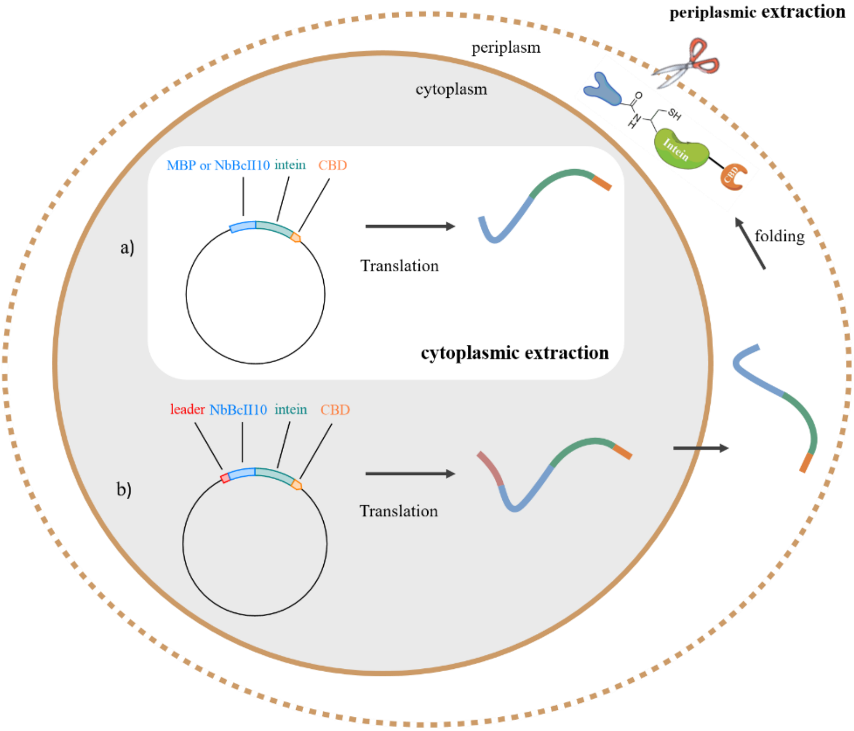
periplasmic extraction
periplasm
cytoplasm
MBP or NbBcII10 intein CBD
a)
Translation
cytoplasmic extraction
Intein
CBD
SH
folding
leader NbBcII10 intein CBD
b)
Translation

Figure 5.6: Cytoplasmic (a) versus periplasmic (b) extraction of proteins.

For a cytoplasmic extraction (MBP and NbBcII10 without leader sequence), cell lysis is necessary to get the proteins out of the cytoplasm. To do this, a commercial solution, B-PER™ (ThermoFisher) is used. B-PER™ contains a mild nonionic detergent that disrupts the cell membranes and solubilizes the recombinant proteins without denaturation. For a periplasmic extraction, only the outer membrane of the bacteria is damaged, without disrupting the inner membrane. This can be done by means of an osmotic shock using a Tris-EDTA-Sucrose (TES) buffer (13, 18). Further details about periplasmic extractions were discussed in Chapter 4.

Last but not least, the protein complex needs to be separated from other endogenous proteins. Therefore, the cytoplasmic or periplasmic extract is purified using a chitin column. The Nb-intein-CBD complex will bind to this column due to the CBD present in the complex. Subsequent functionalization experiments are performed after the immobilization on this column as discussed in the next section.

5.2.2.4 Site-specific Functionalization of MBP and NbBcII10

As mentioned in the general introduction, the EPL method makes use of an intein that facilitates an N,S-acyl shift between the protein and the intein. Consequently, the amide bond between the POI and the intein is replaced by a thioester bond. This thioester bond is vulnerable to a nucleophilic attack. By adding so-called bifunctional linkers containing a nucleophile at one end and a bioorthogonal functionality at the other end, a nucleophilic reaction takes place resulting in a site-specifically modified protein.

Two types of bifunctional linkers are synthesized and tested in this thesis. One linker contains a thiol-based nucleophile and the other one an amine-based nucleophile. As a bioorthogonal functionality, an alkyne is built-in in both linkers. In Chapter 2, the use of both linkers was investigated in detail.

Synthesis of the thiol-based bifunctional linker (Figure 5.7). Bifunctional linker 2-amino-3-mercapto-*N*-(prop-2-yn-1-yl)propanamide (**4**) was synthesized by dissolving 2 mmol (0.9272 g) *N*-(*tert*-butoxycarbonyl)-*S*-trityl-L-cysteine (**1**), 2.2 mmol (0.4217 g) of *N*-(3-dimethylaminopropyl)-*N′*-ethylcarbodiimide hydrochloride (EDC) and 2.2 mmol (0.2532 g) N-hydroxysuccinimide (NHS) in 30 mL dichloromethane (DCM) and stirring for 16h at room temperature. After washing with water, the DCM phase was dried over $MgSO_4$ and evaporated under reduced pressure. 1 mmol (0.5607 g) of the resulting white powder (**2**) was dissolved in 20 mL dry DCM together with 2 mmol (0.1372 mL) propargylamine and 2 mmol triethylamine (0.279 mL) and stirred continuously for 16 h under N_2 atmosphere at room temperature. The resulting product (**3**) was purified using column chromatography over silica with ethyl acetate/DCM (1/24) as eluent. The solvent was removed under reduced pressure. To remove the protective Boc and trityl groups, 100 mg of the dry purified product (**3**) was dissolved in 3 mL trifluoroacetic acid (TFA), 100 µL extra pure water and 100 µL triisopropylsilane. After 30 minutes of stirring at room temperature, the TFA was removed under reduced pressure and 20 mL of fresh DCM was added to the product. The mixture was extracted 5 times with water and the water phase was lyophilized, resulting in 2-amino-3-mercapto-*N*-(prop-2-yn-1-yl)propanamide.

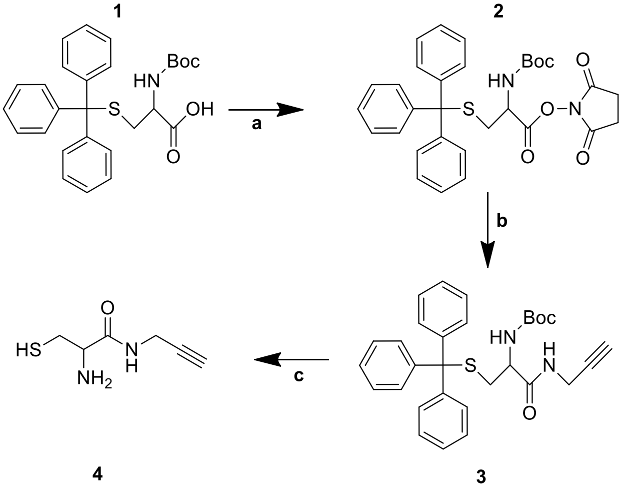

Figure 5.7: Synthetic pathway towards 2-amino-3-mercapto-*N*-(prop-2-yn-1-yl)propanamide (**4**). (**a**) EDC, NHS, DCM; (**b**) propargylamine, triethylamine, DCM; (**c**) TFA, water, triisopropylsilane.

Synthesis of the amine-based bifunctional linker (Figure 5.8) The amine-based bifunctional linker 2-hydrazinyl-N-(prop-2-yn-1-yl)acetamide (**8**) was synthesised similar to the thiol-based bifunctional linker. Tri-Boc-hydrazinoacetic acid (**5**) (1.28 mmol, 0.5g) was dissolved in 30 mL DCM and 1.408 mmol (0.2698 g) EDC and 1.408 mmol (0.081 g) NHS was added. After overnight stirring at room temperature, the mixture was extracted with water and the DCM was dried over $MgSO_4$ and evaporated under reduced pressure. The resulting oily product (**6**) was dissolved in 40 mL dry DCM and 2.56 mmol (0.3568 mL) triethylamine and 2.56 mmol (0.1756 mL) propargylamine were added under N_2 atmosphere. The mixture was stirred overnight at room temperature and the resulting product (**7**) was purified by column chromatography over silica using an ethyl acetate/hexane (50/50) mixture as eluent. The resulting viscous product (**7**) was deprotected in the same way as described for the thiol-based bifunctional linker.

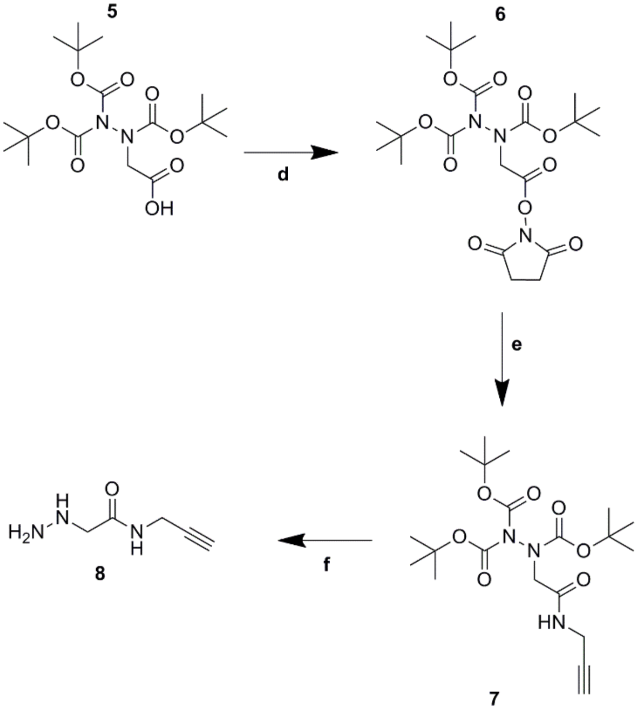

Figure 5.8: Synthetic pathway towards 2-hydrazinyl-*N*-(prop-2-yn-1-yl)acetamide (**8**). (d) EDC, NHS, DCM (**e**) triethylamine, propargylamine, DCM (**f**) TFA, water, triisopropylsilane.

In addition to the bifunctional linkers, also 2-mercaptoethane sulfonate Na (MESNA) is added as a nucleophile. The exact function and mechanism of this reaction is discussed in Chapter 4.

After the alkynation, the proteins were purified using dialysis and characterized using the techniques discussed in section 5.4.

5.2.3 Native nanobody expression

Besides the expression of the NbBcII10-intein-CBD complex as discussed in the previous section, also the native NbBcII10 (pHEN6 vector, (5)) further noted as NbBcII10-His$_6$ was expressed to use as a control protein in different analysis experiments such as ELISA and SPR. The site-specific alkynation of NbBcII10 using a thiol-based bifunctional linker has as consequence that an additional thiol group is introduced at the C-terminus. This can result in possible dimer formation. For this reason, a modified NbBcII10 containing an additional cysteine (pHEN25 vector, (19)), further noted as NbBcII10-HLC, was also expressed as a reference.

Besides the addition of a cysteine, this nanobody also contains a His6 tag and a 14 amino acid linker derived from the hinge sequence of a human IgA1. Both vectors are depicted in Figure 5.9.

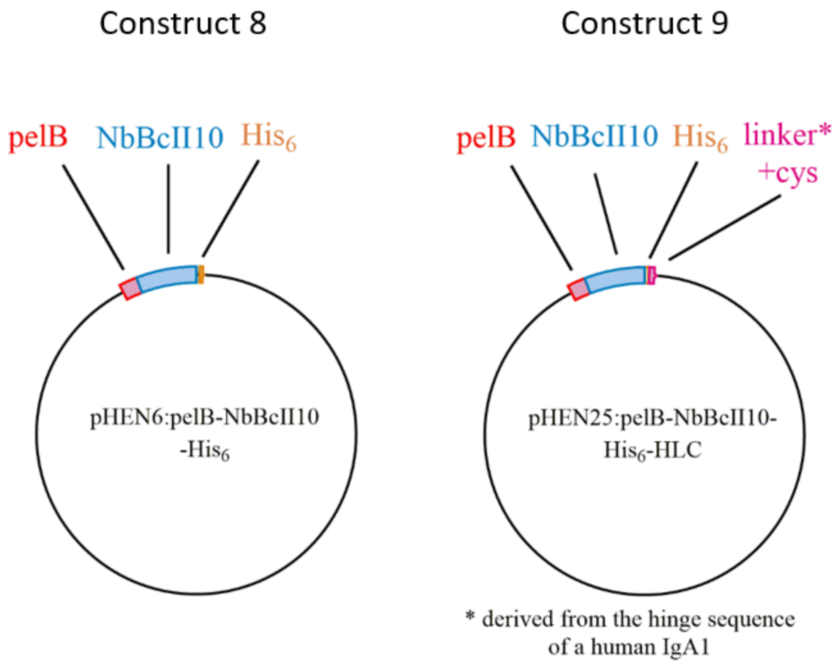
Construct 8
Construct 9
pelB
NbBcII10
His6
pHEN6:pelB-NbBcII10-His6
pelB
NbBcII10
His6
linker*
+cys
pHEN25:pelB-NbBcII10-His6-HLC
* derived from the hinge sequence of a human IgA1

Figure 5.9: Overview of the different vectors used for native NbBcII10 expression in this thesis.

Both vectors were transformed into competent WK6 *E. coli* and expressed and purified as described in literature (5). Both vectors and/or purified proteins were a kind gift of the lab of Prof. Serge Muyldermans (Vrije Universiteit Brussel).

5.3 Molecular cloning techniques

5.3.1 Two-step polymerase chain reaction

The polymerase chain reaction (PCR) is a commonly used technique in biotechnological research to amplify DNA fragments. To perform PCR, one needs the original DNA template, a forward and reverse primer flanking the target that needs to be amplified, all four deoxyribonucleoside triphosphates (dNTPs) and a heat-stable DNA polymerase. A PCR is a multi-step reaction were after denaturation of the DNA template, the primers anneal and the DNA is elongated by making use of DNA polymerase (Figure 5.10).

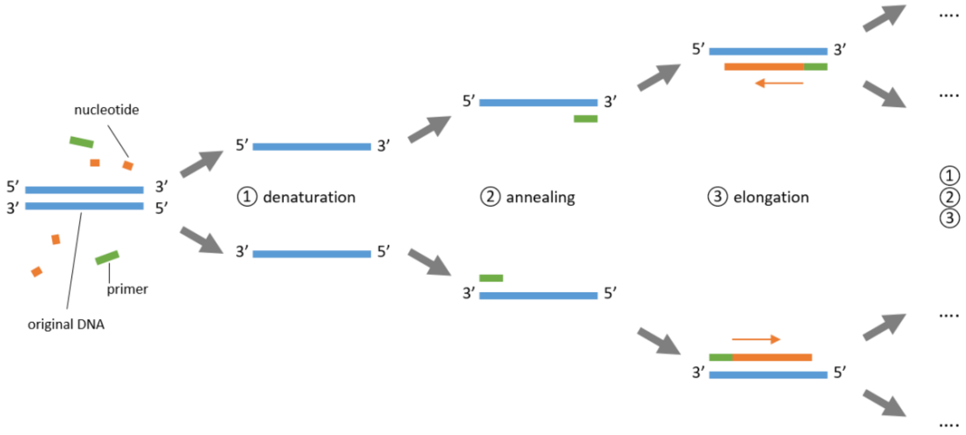

Figure 5.10: Polymerase chain reaction. After the denaturation of the DNA template, the primers anneal with the complementary target strand. Next, the DNA polymerase synthesizes new complementary DNA to the template. This process is repeated multiple times.

Besides of the classic PCR reactions, this thesis makes use of two-step PCR. In a PCR reaction, it is not necessary that the primers are 100% compatible with the ssDNA for hybridization. This means that it is possible to add additional nucleotides to the original DNA template. This technique is commonly used to add restriction sites for easy ligation into a vector as discussed in section 5.3.2.

In Chapter 5, the addition of leader sequences to NbBcII10 is discussed. The DNA of these leader sequences was not available in our lab (except for pelB) and was added to the original NbBcII10 by using 2 consecutive PCRs. Figure 5.11 shows a schematic overview of this process.

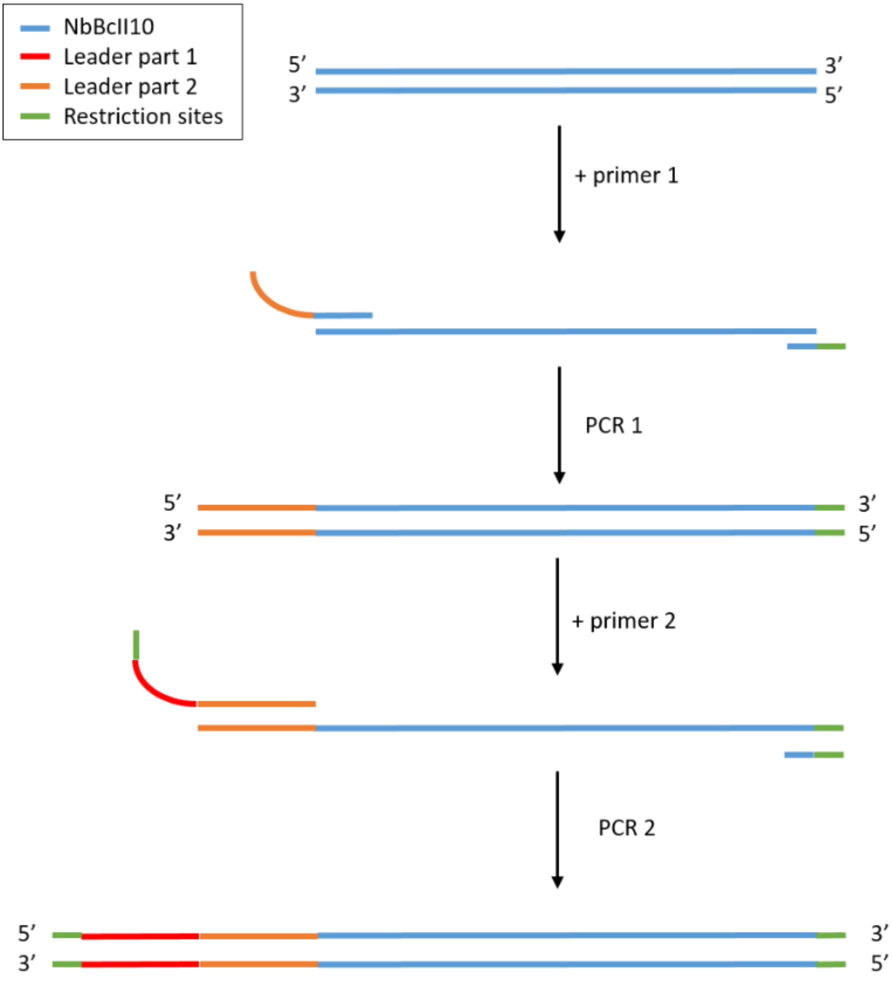

Figure 5.11: Attachment of the leader sequence to NbBcII10 using two-step PCRs.

First, a forward primer was designed containing 20 nucleotides that were compatible with the original DNA and the 40 last nucleotides of the leader sequence. The reverse primer was a normal primer complementary to the original DNA with the addition of a few nucleotides for the *LguI* restriction site. After the PCR reaction, the mixture was purified using a commercial PCR cleanup kit (Qiagen). Next, a second PCR was performed using a forward primer containing the first nucleotides from the leader sequence with an overlap to the previously attached nucleotides and extra nucleotides for the *NdeI* restriction site. This finally results in a construct containing *NdeI*-leadersequence-NbBcII10-*LguI*.

5.3.2 Vector preparation

In order to get the NbBcII10 sequence, whether or not with a leader sequence, into the pTXB1 vector, a process called ligation is used. First, the NbBcII10 DNA and the vector are digested using restriction enzymes. Restriction enzymes, also called restriction endonucleases, are able to recognize specific base sequences in dsDNA and cut both strands of the DNA at specific locations.

As discussed in section 5.2.2.1, the pTXB1 contains a multiple cloning site. This multiple cloning site contains multiple (unique) restriction enzyme cleavage sites that correspond to specific restriction enzymes. Using PCR, restriction sites are also added at the 5' and 3' terminus of the NbBcII10 DNA. For the ligation of NbBcII10 into the pTXB1 vector, the *NdeI* and *LguI* (a.k.a. *SapI*) were used as shown in Figure 5.12.

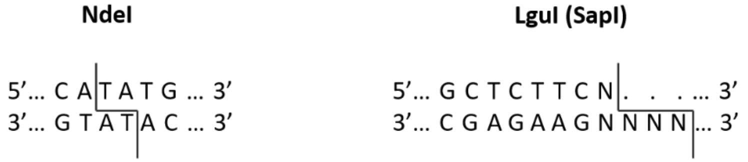
NdeI
5'… C A T A T G … 3'
3'… G T A T A C … 3'
LguI (SapI)
5'… G C T C T T C N . . . … 3'
3'… C G A G A A G N N N N … 3'

Figure 5.12: Restriction sites *NdeI* and *LguI* (*SapI*).

The DNA fragment and the vector were digested separately, the restricted parts were removed from the rest of the DNA using PCR cleanup or gel extraction (Qiagen) after a agarose gel. Next, the fragments were brought together and T4 DNA ligase (Thermofisher) was added. T4 DNA ligase promotes the formation of a phosphodiester bond between the 5'-phosphate and 3'-hydroxyl termini. Note that the *LguI* restriction site disappears after ligation because the recognition site of *LguI* is located downstream from the cleavage site. The digestion/ligation process is schematically represented in Figure 5.13.

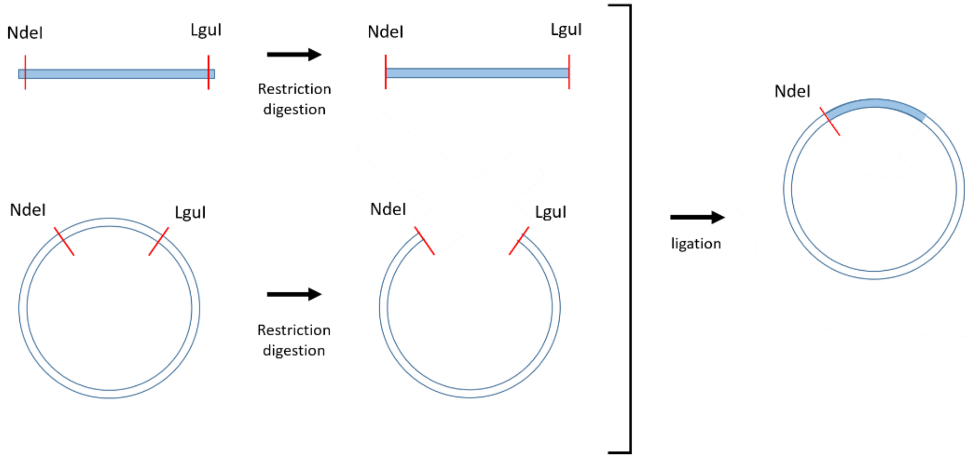

Figure 5.13: Schematic representation of the digestion and ligation process.

5.3.3 Transformation and selection

After ligation, the vector constructs were transformed into competent Top10 *E. coli*. These cells are highly-efficient for cloning and plasmid propagation and allow stable replication of high-copy number plasmids. In this experimental set-up, the cells are only used for vector replication.

There are two kinds of competent cells: chemically competent cells and electrocompetent cells. Chemically competent cells are calcium chloride treated to facilitate attachment of the plasmid DNA to the competent cell membrane. By heating the competent cell to 42°C, the pores of the cell membrane open, allowing entry of the plasmid. Electrocompetent cells use a process called electroporation. Electrical pulses create pores that allow genetic material to permeate the bacterial membrane. After the electric shock, the holes are rapidly closed by the cells membrane-repair mechanisms.

After transformation into Top10 cells, the cells are plated on a LB^{amp} agar plate. As mentioned before, the vector contains an ampicillin resistance gene, so only the successfully transformed Top10 cells grow on this plate. To increase the amount of vector for testing, the bacteria that have grown on the plate are inoculated into a 5 mL liquid LB^{amp} culture grown overnight at 37°C. Next, the vectors are extracted from the bacteria using a commercial miniprep kit (GeneJET Plasmid miniprep kit, Thermofisher).

5.3.4 Restriction analysis and sequencing

To test if the transformation process was successful, a restriction analysis is performed. The vector is digested with restriction enzymes and analyzed using an agarose gel. The digestion results in linear DNA fragments and the size of these fragments can be predicted. To ensure the absence of small mutations, the samples that seem successful after restriction analysis are further analyzed using Sanger sequencing (20, 21) by LGC genomics Germany.

After a positive evaluation by Sanger sequencing, the vector is again transformed but this time in one of the previously mentioned expression hosts BL21(DE3), Lemo21(DE3) and SHuffle®T7.

5.4 Protein characterization techniques

5.4.1 Western blotting

Western blotting is an extension of the polyacrylamide gel electrophoresis (PAGE) technique. After separation, the proteins are transferred from the polyacrylamide gel onto a polyvinylidene fluoride (PVDF) or nitrocellulose membrane. In this thesis, PVDF membranes are used. This transfer is realized by immersing both the polyacrylamide gel and PVDF membrane into Towbin buffer (192 mM glycine, 25 mM Tris, 20% methanol (v/v), pH8.3). Since the pH of this buffer is higher than the isoelectric point (pI) of most proteins, it will cause the migration of the negatively charged proteins towards the anode (+) (22) (Figure 5.14).

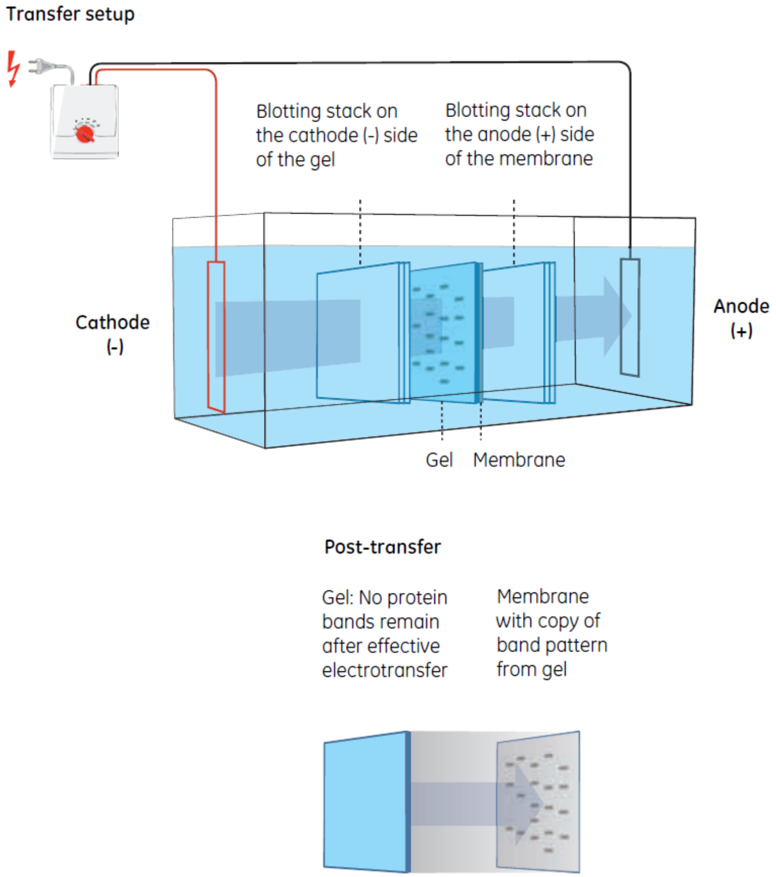
Transfer setup
Blotting stack on the cathode (-) side of the gel
Blotting stack on the anode (+) side of the membrane
Cathode (-)
Anode (+)
Gel
Membrane
Post-transfer
Gel: No protein bands remain after effective electrotransfer
Membrane with copy of band pattern from gel

Figure 5.14: Western blotting: protein transfer from the gel to the PVDF membrane. The proteins on the gel (negatively charged) will migrate into the direction of the anode onto the membrane (GE Healthcare - western blotting: principles and methods).

After the transfer to the PVDF membrane, the proteins can be detected by immunodetection. First, the areas on the membrane that do not contain any protein need to be blocked in order to avoid non-specific binding of the applied antibodies to the membrane. The blocking is mostly done by a 5% (w/v) milk powder or BSA solution in TBST (Tris-Buffered Saline supplemented with 0.1% (v/v) Tween 20). Secondly, a primary antibody is added to the membrane. This antibody is specific for the protein that needs to be detected. Next, a secondary antibody directed against the primary antibody is added. This secondary antibody contains a label e.g. the enzyme alkaline phosphatase (AP). AP converts several substrates such as 5-bromo-4-chloro-3-indolyl phosphate/nitroblue tetrazolium (BCIP/NTB) to a colored precipitate allowing colorimetric detection (Figure 5.15). The alkaline phosphatase will dephosphorylate the BCIP resulting in an indoxyl intermediate. The NBT will oxidize the indoxyl yielding an indigoid dye (purple). The NBT was reduced by the indoxyl resulting in the opening of the tetrazole ring, which produces an insoluble NTB formazan (blue).

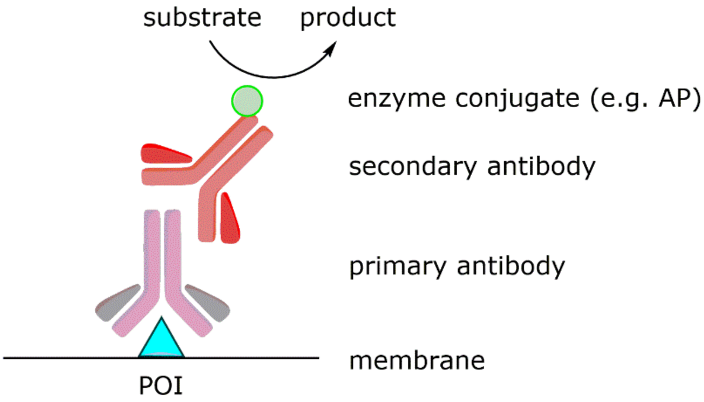

Figure 5.15: Colorimetric protein detection using western blotting. The primary antibody binds to the protein of interest (POI). The secondary antibody binds to the primary antibody and contains an enzyme such as alkaline phosphatase (AP). As a result, the enzyme converts its substrate (NBT-BCIP) to a colored precipitate

Note that in this thesis, a slightly modified version of the classic western blotting process is used. As described in the following chapters, the POI is first coupled to an azide functionalized biotin molecule by means of a click reaction. Next, a streptavidin-AP derivate is added to the membrane that will bind to the biotin on the target protein (Figure 5.16).

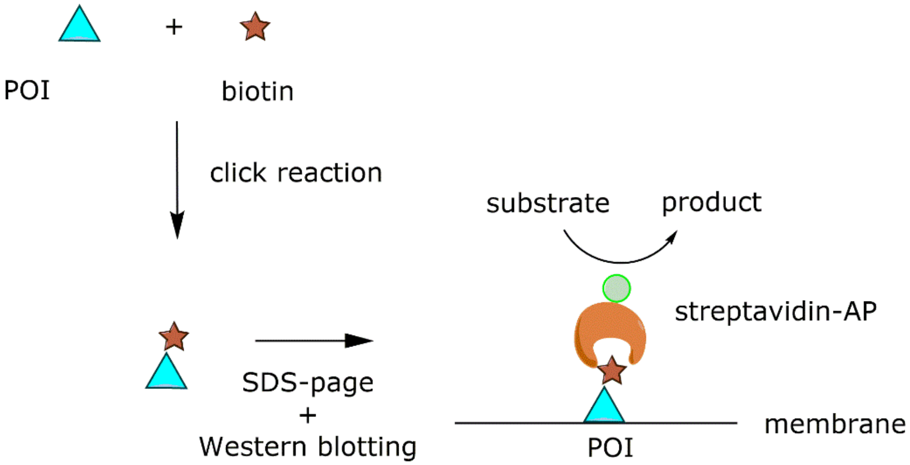

Figure 5.16: Western blotting using biotin. First, a click reaction is performed between the POI and azide functionalized biotin. Next, the biotinylated POI is analyzed using western blotting by making use of streptavidin-alkaline phosphatase instead of the classical primary and secondary antibody.

5.4.2 Enzyme-Linked Immuno-Sorbent Assay (ELISA)

Enzyme-linked immunosorbent assay (ELISA), also known as an enzyme immunoassay (EIA), is a biochemical technique used mainly in immunology to detect and quantify the presence of an antibody or an antigen in a sample. There are different types of ELISA experiments. This thesis makes use of the standard ELISA and the competitive ELISA.

In a standard ELISA, the POI is coupled to a polystyrene microtiter-plate and the plate is blocked, usually with skim milk to avoid further protein attachment to the plate. In a direct approach (Figure 5.17a), an enzyme-conjugated antibody (e.g. alkaline phosphatase conjugated) is added to the microwell, which will bind to the POI. By adding a substrate, in case of alkaline phosphatase this can be p-nitrophenol phosphate, the enzyme will hydrolyze the substrate to form the yellow-colored p-nitrophenol. The absorbance of the final solution, measured with a spectrophotometer, is then proportional to the concentration of the POI. Besides the direct approach, an indirect approach (Figure 5.17b) is also possible. Here, the antibody is not enzyme-conjugated and a conjugated secondary antibody, targeted against the primary antibody is needed.

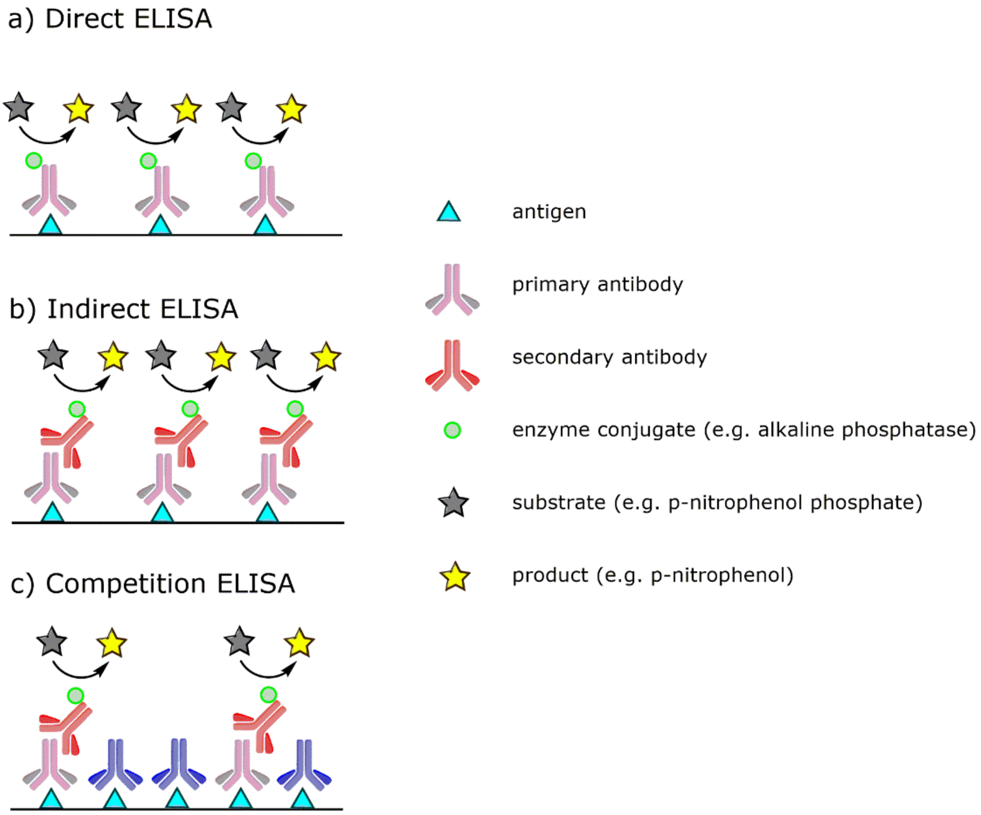
a) Direct ELISA
b) Indirect ELISA
c) Competition ELISA
antigen
primary antibody
secondary antibody
enzyme conjugate (e.g. alkaline phosphatase)
substrate (e.g. p-nitrophenol phosphate)
product (e.g. p-nitrophenol)

Figure 5.17: Schematic representation of the direct ELISA (a), indirect ELISA (b) and competition ELISA (c) concept.

When testing antibody properties, the standard approach is not always applicable. Sometimes, a competitive ELISA (Figure 5.17c) can be helpful in this situation. In this case, two different antibodies are added to the microplate, resulting in a competition between the antibodies. By labeling one of the two antibodies (direct approach) or by using a secondary antibody that is only directed against one of the two antibodies (indirect approach), affinity information can be gathered about the unlabeled antibody because the measured absorbance is indirectly proportional to the concentration of the unlabeled protein.

In this thesis, competitive ELISA is used to control the affinity of the alkynated NbBcII10. A standard ELISA is not possible because the alkynated NbBcII10 is not labeled. As discussed in Chapter 5, the BcII antigen is immobilized onto the polystyrene microtiter plate and a concentration range of alkynated NbBcII10 is added to the different micro wells, combined with a fixed concentration of native NbBcII10 that contains a His$_6$ tail. Next, an enzyme-conjugated secondary antibody against His_6 is added. When the measured absorbance is inversely proportional to the concentration of alkynated NbBcII10, this proves that the alkynated NbBcII10 still has a binding activity towards its antigen. This method is only qualitative. For a quantitative test of binding activity, surface plasmon resonance (SPR) is more appropriate as discussed in the next section.

5.4.3 Mass spectrometry

For the MS analyses in this thesis, the ThermoFisher Orbitrap Velos Pro was used. This device contains a dual cell linear ion trap for sample ionization, selection fragmentation and automatic gain control, a curved linear trap as intermediate storage device, an orbitrap analyzer for Fourier transformation based analysis and a collision cell to perform high energy collision-induced dissociation experiments.

In an orbitrap mass analyzer, ions are trapped in an electrostatic field between an inner and outer electrode. The frequency of the rotation of the ions around the inner electrode is a characteristic of their mass-to-charge (m/z) ratio. Acquisition of transients and the Fourier transformation of that signal yields frequencies and their intensities. These frequencies and intensities can be converted into m/z values. (23-25)

For all experiments, following experimental procedures were used. Two buffers were prepared, buffer 1 (solvent A) contained 0.1% formic acid in acetonitrile and buffer 2 (solvent B) 0.1% formic acid in MilliQ water. All samples (with a concentration of at least 50 µM) were ½ diluted in solvent A. The samples were loaded on a 5 mm Guard C18 column (sample volume = 30 µL) with a flow of 5 µL/sec and a maximum pressure of 200 bar. Afterwards, following gradient for HPLC chromatography (ThermoFisher Ultimate 3000) was used:

Table 5.1: Gradient for HPCL chomatograpy used for the ESI-MS experiments.

Time (min)	Duration	Solvent B	Flow (µl/min)
0	-	100%	500
5.0	5	100%	500
5.1	0.1	50%	100
12.0	6.9	50%	100
12.1	0.1	10%	100
15.0	0.1	10%	100
15.1	0.5	100%	500
20	0.5	100%	500

The HPCL device was controlled by the Chromeleon XPress software (v6.80), the Orbitrap Velos Pro by the Xcalibur software (v2.2) and deconvolution of the spectra was performed using Promass software for Xcalibur (v2.8).

5.4.4 Ellipsometry

Ellipsometry is a very accurate, non-invasive and non-destructive method for the characterization of thin films. It is an optical technique which allows the determination of the thickness and refraction index of thin films deposited on light-reflective surfaces like silicon. Based on these parameters, it is possible to calculate the mass per unit surface area on the film. Ellipsometry uses the fact that linearly polarized light at an oblique incidence to a surface changes polarization state when it is reflected. It becomes elliptically polarized, therefore the name ”ellipsometry” (26).

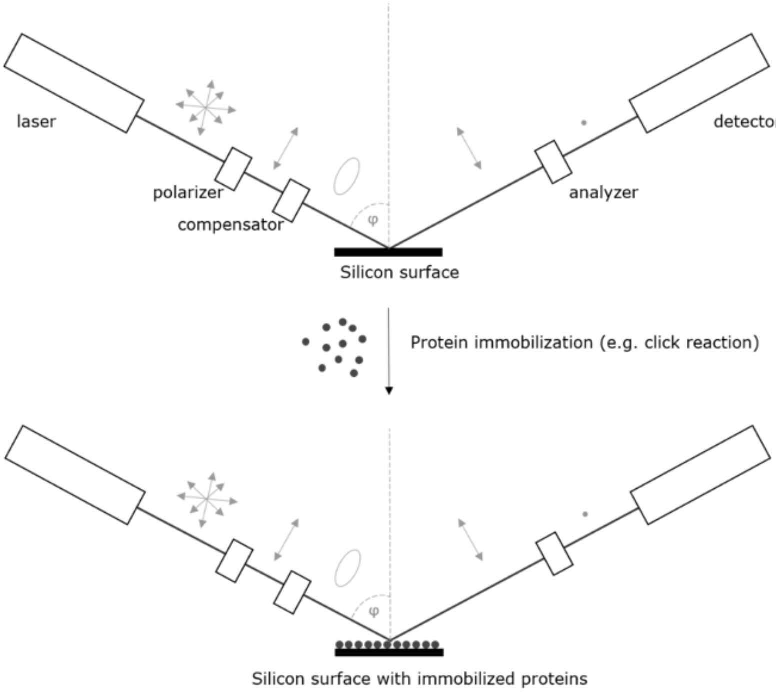
laser
detector
polarizer
compensator
analyzer
φ
Silicon surface
Protein immobilization (e.g. click reaction)
φ
Silicon surface with immobilized proteins

Figure 5.18: Schematic representation of the ellipsometry principle. The laser light beam passes through a polarizer and a compensator before reaching the reflecting sample (φ = angle of incidence). The reflected beam then passes through a second prism, the analyzer, and is detected by a detector (photodiode). The change in polarization is correlated to the thickness of the adsorbed biolayer.

The basic principles are shown in Figure 5.18. A light beam is sent through a polarizer, resulting in polarized light. Next, a compensator will convert this polarized light beam into an elliptical polarized light. The resulting elliptically polarized light is then reflected against the surface and passed through a second polarizing prism, the analyzer. Finally, the light intensity is detected by a photodiode detector. By determining the state of polarization on both the uncovered surface and on the biofunctionalized surface, it becomes possible to convert the change in polarization into a thickness of the adsorbed biolayer with a high precision and reproducibility. Several configurations for an ellipsometer are possible, but the most important is the null ellipsometry that is also used in Chapter 3. Here, the polarizer and compensator are rotational. When the layers on the surface are changed, for example by the coupling of proteins on the surface, the angles of the polarizer and analyzer are adjusted in order to minimize (null) the light intensity at the detector. This change in angle of the polarizer and analyzer can be translated into a net mass change on the surface (27-29).

In this thesis, the same custom made ellipsometer was used as used by Damen et al. (27). A schematic representation of the device is shown in Figure 5.19.

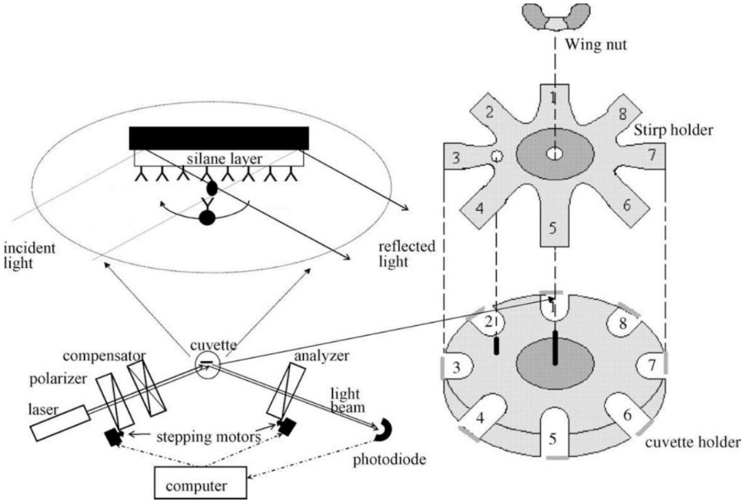

Figure 5.19: Schematic representation of the ellipsometer as used in this thesis (27).

The device is equipped with a carousel containing mounting for eight silicon slides (0.3x3.2 cm) and a cuvette holder for eight 400 µl cuvettes for the reaction mixture. The device is software controlled. The polarizer and analyzer are controlled by motors and the angles are automatically altered by the software to achieve the null status. The binding of proteins on the surface will result in the shift in angle of the polarizer to maintain the null status (ΔP, degrees). This value can be used to calculate the surface mass density (Γ, ng protein/cm²) by using a simplified Lorents-Lorenz relation $\Gamma = 85 \times \Delta P$ (3, 29, 30).

5.4.5 Surface Plasmon Resonance (SPR)

Surface plasmon resonance (SPR) is an optical technique for measuring the refractive index of very thin layers of material adsorbed on a metal (e.g. gold). When a light beam impinges onto the metal film at a specific (resonance) angle, the surface plasmons are set to resonate with the light. This resonance results in the absorption of light. In the widely used Kretschmann configuration (Figure 5.20), were the metal film is evaporated onto a glass block and a light beam is focused onto the metal film, the plasmons are excited at the outer side of the film. The focused light provides a range of incident angles using a prism placed at the backside of the metal film, and the metal surface reflects all the light except for the ray at a certain angle from which the light energy is adsorbed and not reflected due to surface plasmon resonance. This angle is called the SPR angle and it changes by the deposition of materials on the surface. The change in SPR angle is proportional to the change in mass on the metal layer (31-34).

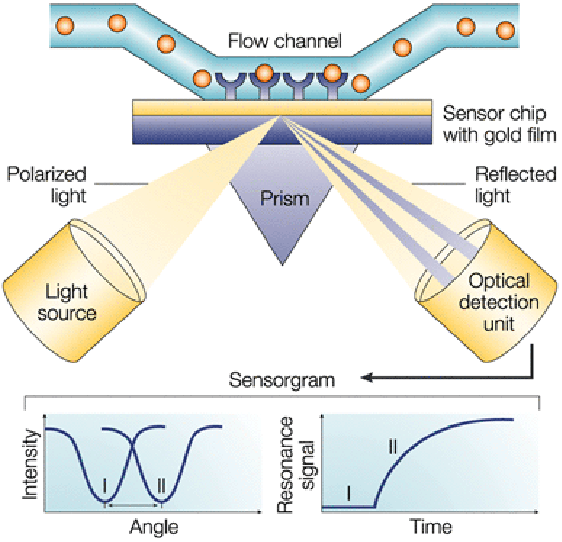

Figure 5.20: The principle of surface plasmon resonance (31). Polarized light passes through a prism and is refracted to reach the surface at different incident angles. When the light impinges at a specific resonance angle (SPR angle), the light is absorbed by the surface, resulting in the disappearance of the reflected light. When proteins bind to the surface, the SPR angle shifts from position I to position II. The change in this angle corresponds to the surface mass change.

In this thesis SPR is used to test the binding affinity of NbBcII10 and the influence of alkynation using EPL on the binding affinity. As shown in Figure 5.20, biomolecules are immobilized on the sensor chip. In our case, a CM5 chip containing a carboxymethylated dextran layer covalently attached to a gold surface. The chip contains microfluidic tubing and four independent flow paths that can be controlled separately. To test the binding specificity of NbBcII10, the BcII antigen was covalently immobilized using an amide coupling (EDC/NHS). After immobilization of the antigen, the SPR angle is determined (position I in Figure 5.20). Next, after the addition of NbBcII10, the SPR angle will increase if the NbBcII10 is still capable to bind to the BcII antigen (position II in Figure 5.20). The more bound NbBcII10, the higher the SPR angle. The shift in SPR angle is recorded in real time by the SPR apparatus (e.g. Biacore T200) and converted into response units (RU) whereby 1 RU is approximately 1pg/mm^2.

5.5 References

1. Fischer ME. Amine Coupling Through EDC/NHS: A Practical Approach. In: Mol NJ, Fischer MJE, editors. Surface Plasmon Resonance. Methods in Molecular Biology. 627: Humana Press; 2010. p. 55-73.
2. Gao Y, Kyratzis I. Covalent Immobilization of Proteins on Carbon Nanotubes Using the Cross-Linker 1-Ethyl-3-(3-dimethylaminopropyl)carbodiimide—a Critical Assessment. Bioconj Chem. 2008;19(10):1945-50.
3. Vranken T, Steen Redeker E, Miszta A, Billen B, Hermens W, de Laat B, et al. In situ monitoring and optimization of CuAAC-mediated protein functionalization of biosurfaces. Sens Actuators B Chem. 2017;238:992-1000.
4. Jagadish B, Sankaranarayanan R, Xu L, Richards R, Vagner J, Hruby VJ, et al. Squalene-derived flexible linkers for bioactive peptides. Bioorg Med Chem Lett. 2007;17(12):3310-3.
5. Conrath KE, Lauwereys M, Galleni M, Matagne A, Frère J-M, Kinne J, et al. β-Lactamase Inhibitors Derived from Single-Domain Antibody Fragments Elicited in the Camelidae. Antimicrob Agents Chemother. 2001;45(10):2807-12.
6. Muyldermans S. Single domain camel antibodies: current status. Rev Mol Biotechnol. 2001;74(4):277-302.
7. Tabor S. Expression Using the T7 RNA Polymerase/Promoter System. Curr Protoc Mol Biol: John Wiley & Sons, Inc.; 2001.
8. Studier FW, Moffatt BA. Use of bacteriophage T7 RNA polymerase to direct selective high-level expression of cloned genes. J Mol Biol. 1986;189(1):113-30.
9. (NEB) NEB. What is the difference between BL21 and BL21(DE3) competent E.coli cells? 2016. Available from: https://www.neb.com/faqs/2016/01/21/what-is-the-difference-between-bl21-and-bl21-de3-competent-e-coli-cells2.
10. Rosano GL, Ceccarelli EA. Recombinant protein expression in Escherichia coli: advances and challenges. Front Microbiol. 2014;5:172.
11. Wagner S, Bader ML, Drew D, de Gier J-W. Rationalizing membrane protein overexpression. Trends Biotechnol. 2006;24(8):364-71.
12. Wagner S, Klepsch MM, Schlegel S, Appel A, Draheim R, Tarry M, et al. Tuning Escherichia coli for membrane protein overexpression. Proc Natl Acad Sci U S A. 2008;105(38):14371-6.
13. Schlegel S, Rujas E, Ytterberg AJ, Zubarev R, Luirink J, de Gier J-W. Optimizing heterologous protein production in the periplasm of E. coli by regulating gene expression levels. Microb Cell Fact. 2013;12(1):24.
14. Zarschler K, Witecy S, Kapplusch F, Foerster C, Stephan H. High-yield production of functional soluble single-domain antibodies in the cytoplasm of Escherichia coli. Microb Cell Fact. 2013;12(1):1-13.
15. Chen J, Song J-l, Zhang S, Wang Y, Cui D-f, Wang C-c. Chaperone Activity of DsbC. J Biol Chem. 1999;274(28):19601-5.

16. Bessette PH, Åslund F, Beckwith J, Georgiou G. Efficient folding of proteins with multiple disulfide bonds in the Escherichia coli cytoplasm. Proceedings of the National Academy of Sciences. 1999;96(24):13703-8.
17. Lobstein J, Emrich CA, Jeans C, Faulkner M, Riggs P, Berkmen M. SHuffle, a novel Escherichia coli protein expression strain capable of correctly folding disulfide bonded proteins in its cytoplasm. Microb Cell Fact. 2012;11(1):1-16.
18. Skerra A, Pluckthun A. Assembly of a functional immunoglobulin Fv fragment in Escherichia coli. Science. 1988;240(4855):1038-41.
19. Massa S, Xavier C, De Vos J, Caveliers V, Lahoutte T, Muyldermans S, et al. Site-Specific Labeling of Cysteine-Tagged Camelid Single-Domain Antibody-Fragments for Use in Molecular Imaging. Bioconj Chem. 2014;25(5):979-88.
20. Sanger F, Coulson AR. A rapid method for determining sequences in DNA by primed synthesis with DNA polymerase. J Mol Biol. 1975;94(3):441-8.
21. Sanger F, Nicklen S, Coulson AR. DNA sequencing with chain-terminating inhibitors. Proceedings of the National Academy of Sciences. 1977;74(12):5463-7.
22. Towbin H, Staehelin T, Gordon J. Electrophoretic transfer of proteins from polyacrylamide gels to nitrocellulose sheets: procedure and some applications. Proceedings of the National Academy of Sciences. 1979;76(9):4350-4.
23. Makarov A. Electrostatic Axially Harmonic Orbital Trapping: A High-Performance Technique of Mass Analysis. Anal Chem. 2000;72(6):1156-62.
24. Makarov A, Denisov E, Kholomeev A, Balschun W, Lange O, Strupat K, et al. Performance Evaluation of a Hybrid Linear Ion Trap/Orbitrap Mass Spectrometer. Anal Chem. 2006;78(7):2113-20.
25. Makarov A, Denisov E, Lange O, Horning S. Dynamic range of mass accuracy in LTQ orbitrap hybrid mass spectrometer. J Am Soc Mass Spectrom. 2006;17(7):977-82.
26. Jung J, Holmgaard T, Kortbek NA. Ellipsometry. Aalborg: Aalborg University; 2004.
27. Damen CWN, Speijer H, Hermens WT, Schellens JHM, Rosing H, Beijnen JH. The bioanalysis of trastuzumab in human serum using precipitate-enhanced ellipsometry. Anal Biochem. 2009;393(1):73-9.
28. Elwing H. Protein absorption and ellipsometry in biomaterial research. Biomaterials. 1998;19(4–5):397-406.
29. Giesen PLA, Willems GM, Hemker HC, Stuart MCA, Hermens WT. Monitoring of unbound protein in vesicle suspensions with off-null ellipsometry. Biochim Biophys Acta. 1993;1147(1):125-31.
30. Robers M, Rensink IJ, Hack CE, Aarden LA, Reutelingsperger CP, Glatz JF, et al. A new principle for rapid immunoassay of proteins based on in situ precipitate-enhanced ellipsometry. Biophys J. 1999;76(5):2769-76.
31. Cooper MA. Optical biosensors in drug discovery. Nat Rev Drug Discov. 2002;1(7):515-28.

32. Nguyen H, Park J, Kang S, Kim M. Surface Plasmon Resonance: A Versatile Technique for Biosensor Applications. Sensors. 2015;15(5):10481.

33. Nirschl M, Reuter F, Vörös J. Review of Transducer Principles for Label-Free Biomolecular Interaction Analysis. Biosensors. 2011;1(3):70-92.

34. Pattnaik P. Surface plasmon resonance. Appl Biochem Biotechnol. 2005;126(2):79-92.

Chapter 6

General discussion, conclusions and future perspectives

The aim of this thesis was to design and synthesize site-specifically functionalized nanobodies for their covalent and oriented coupling onto complementary functionalized surfaces to obtain a uniform layer of nanobodies for the development of next generation biosensors with an increased sensitivity, selectivity and reproducibility. To achieve this, the expressed protein ligation (EPL) protein engineering technique was used in combination with copper (I)-catalyzed azide alkyne cycloaddition (CuAAC) click chemistry. This approach was applied to maltose binding protein (MBP) and later on to the β-lactamase targeting nanobody BcII10 (NbBcII10), by introducing a bioorthogonal alkyne functionality at the C-terminus of the protein in order to allow for a covalent conjugation to an azide-functionalized surface/molecule.

This chapter highlights the research performed to achieve these goals and its outcome. In addition, the limitations of these approaches, as well as some remaining issues are discussed.

6.1 Site-specific functionalization of MBP for covalent and oriented coupling to an azide-functionalized surface

EPL is a well-known technique for the C- or N-terminal modification of proteins. The required expression vectors pTXB1 and pMXB10 are commercially available, as well as a basic protocol for cloning and expression of proteins. MBP is the ideal model protein for EPL because it i) is already cloned into the pMXB10 vector, ii) has a high expression yield and iii) is very well described in literature. Therefore, it is often used as a proof-of-concept protein in EPL.

In order to perform the EPL-based alkynation, a bifunctional linker containing a thiol functionality (for the nucleophilic attack on the thioester function between MBP and intein) and an alkyne functionality was synthesized. More specifically, 2-amino-3-mercapto-*N*-(prop-2-yn-1-yl)propanamide was successfully synthesized as proven by NMR spectroscopy. Using this linker, site-specifically alkynated MBP (ssA-MBP) was produced in a high yield (21.6 mg/mL) in the presence of MESNA in order to increase the reaction yield. To demonstrate the presence of the alkyne functionality at the C-terminus of MBP, a CuAAC click reaction in solution was performed with azide-functionalized biotin. This reaction in solution is the most straightforward way of click chemistry because of the reduced influence of steric hindrance and surface preconcentration in comparison to reactions on a surface. After the reaction, the biotin was visualized using western blotting. To quantify the degree of alkynation of MBP, electrospray ionisation mass spectrometry (ESI-MS) was performed. Because of the presence of MESNA in the reaction mixture, MESNA functionalized MBP is produced in addition to the desired ssA-MBP. Unfortunately, the mass difference between these two end products is low (only 16 Da), resulting in one single large peak, making it impossible to quantify the degree of alkynation.

In addition to ssA-MBP, randomly alkynated MBP (rA-MBP) was also produced through EDC/NHS coupling chemistry by utilizing the amino groups of the internal lysines of MBP and an alkyne NHS linker. MBP contains 37 lysines. Theoretically speaking, the use of a six-fold molar excess of alkyne NHS ester would effectuate the functionalization of maximum 16% of all lysines. In order to alkynate all (accessible) lysines, a larger excess of alkyne NHS ester is necessary. In this thesis, a 54-fold molar excess was used to produce fully alkynated MBP (fA-MBP). After analysis of rA-MBP and fA-MBP using mass spectrometry, it was clear that in case of rA-MBP up to four lysines were alkynated. In case of fA-MBP, only four to nine alkyne functionalities were detected. It can thus be concluded that only nine lysines are accessible at the surface of MBP for functionalization, and that the remainder cannot be functionalized due to sterical hindrance, polarity differences, secondary structure elements and electrostatic interactions in the protein structure.

After site-specific and random alkynation of MBP, its clickability on a solid surface was evaluated using *in situ* ellipsometry. In order to achieve this, silicon surfaces were functionalized with an azide functionality. More specifically, the surface was first hydroxylated, carboxylated by silanization using N-(trimethoxysilylpropyl)-ethylenediaminetriacetate trisodium salt (TMS-EDTA) and finally azidified using 3-azido-1-aminopropane (AAP). Subsequently, the alkynated MBP species were placed in an ellipsometer to monitor the click reaction *in situ*. Analysis pointed out that the CuAAC-coupled MBP (ssA-MBP, rA-MBP and fA-MBP) could not be removed from the surface using washing buffers or a 0.5% (w/v) SDS solution, meaning that MBP was covalently coupled to the surface. Since this functionalization approach requires a large amount of protein (the surface is dipped into an alkynated MBP solution i.e. DIP-method), an alternative approach was developed where a drop of MBP solution is added on top of the surface, i.e. the so-called DROP method. By optimizing the click reaction mix, i.e. by varying the concentration of the copper catalyst and the corresponding concentrations of sodium ascorbate and THPTA, almost the same surface mass increase could be achieved using the DROP method as compared to the DIP method. As functionalization of proteins is often very labor intensive, makes use of custom-made chemical components and as a consequence, is very expensive, the DROP method is an interesting alternative approach for surface functionalization.

In conclusion, alkynated MBP can be coupled in a reasonable amount to silicon surfaces. Furthermore, ssA-MBP is coupled in an oriented way and, by using the DROP method, in a very cost-efficient way, which opens up new possibilities for the development of uniformly oriented biosurfaces.

6.2 The site-specific functionalization of MBP using alternative nucleophiles in the EPL process

In the previously described proof-of-concept study, evaluating the clickablility of MBP, ssA-MBP was produced by EPL using the thiol-based bifunctional linker 2-amino-3-mercapto-*N*-(prop-2-yn-1-yl)propanamide. By making use of this linker, an additional cysteine is added to the C-terminus of the protein. The thiol group of this cysteine can form disulfide bridges with other modified or native proteins, or with other bifunctional linkers in the reaction mixture. These drawbacks raised the question whether other nucleophiles can be used instead of thiols for the nucleophilic attack of the internal thioester function during the EPL process. Therefore, the amine-based bifunctional linker 2-hydrazinyl-*N*-(prop-2-yn-1-yl)acetamide was synthesized. This nucleophile makes use of the α-effect that increases the nucleophilicity by the presence of an adjacent α-atom that contains a lone pair of electrons and no additional thiol groups. In theory, several amine-based nucleophiles are capable of reacting directly with the thioester function between the protein of interest (POI) and the intein-CBD complex due to their nucleophilicity at neutral pH. To assess the nucleophilicity of the synthesized linker, MBP was used again as a model protein. Furthermore, the necessity of MESNA, for both the thiol-based EPL process and the amine-based process, was evaluated. When applying the same standard EPL protocol as previously described for the classical thiol-based bifunctional linker, the protein yield after EPL was lower when using the amine-based linkers, even with a 10 times higher concentration of amine-based linker. Despite the lower yield, it was still possible to perform a click reaction in solution with azide-functionalized biotin, as shown by western blotting, demonstrating that the eluted protein was alkyne-functionalized using the amine-based linker. To increase the protein yield, the pH, the reaction temperature and the reaction time were varied. However, the yield increases that were accomplished in this way were also visible in the negative control (no bifunctional linker), meaning that these parameter variations only had an effect on the hydrolysis of the thioester bond between MBP and the intein, and not on the actual nucleophilic reaction. In addition, the need for MESNA in the EPL reaction was evaluated. The EPL reaction was performed using the same reaction conditions as before, for both the thiol-based and the amine-based bifunctional linker, without the addition of MESNA to the reaction mixture. The absence of MESNA had a large effect on the total reaction yield: both linkers led to a reaction yield of nearly 5 mg/L culture. This indicates that MESNA is indeed an important component to increase the yield of the EPL reaction. Nevertheless, western blotting showed that, even without the use of MESNA, alkyne functionalization is possible. On MS, no clear peak was visible for the alkynated MBP using the amine-based linker. The largest peak was the one for hydrolyzed MBP. This means that the percentage of alkynated MBP in the protein solution after EPL is low and the solution mainly consists of non-alkynated or MESNA-functionalized MBP. The same effect is visible when using NbBcII10 as a protein instead of MBP. In the end, it has to be concluded that amine-based bifunctional linkers are not really suitable for EPL. These results are confirmed in literature, as there are no new studies reporting the successful use of amine-based bifunctional linkers. Marshall et al. (2013) reported successful alkynation using an amine-based bifunctional linker but the authors only showed western blotting results in their paper. However, western blotting is a non-quantitative technique so it cannot be proven that all the eluted protein is actually alkynated as a blot also looks positive if only a minor percentage of the protein is alkynated. Furthermore, the authors applied a 200x higher concentration of amine-based bifunctional linker in comparison to the concentration used for a thiol-based bifunctional linker. According to the results obtained in this dissertation combined with the results of Marshall et al., it can be concluded that amine-based bifunctional linkers are not a valuable alternative for thiol-based bifunctional linkers to be used for site-specific protein alkynation by EPL.

6.3 Cytoplasmic versus periplasmic extraction of site-specifically and bio-orthogonally functionalized nanobodies using expressed protein ligation

The final goal of this dissertation was the site-specific functionalization of nanobodies using EPL. Nanobodies are an interesting alternative for classical monoclonal antibodies due to their relatively small size of ~ 15 kDa, well-conserved structure, high affinity and specificity for their antigen. They are expressed from a single gene, making them an ideal substrate for engineering purposes and expression in *Escherichia coli* (*E. coli).*

Nanobodies are generally extracted in the periplasm of *E.coli* because of the oxidizing environment that facilitates a correct protein folding. EPL-based constructs on the other hand are expressed in the cytoplasm. In this thesis, a strategy for the periplasmic extraction of nanobodies containing EPL constructs was investigated. Preliminary studies and literature already indicated that the pelB leader sequence, often used for the periplasmic transport of nanobody constructs, is not the preferred way for the periplasmic transport of the Nb-intein-CBD protein complex. As a solution for this issue, a broad array of different leader sequences for periplasmic transport using the Sec pathway (OmpA, OmpF, malE) was investigated. For the expression of these leader sequence containing constructs, *E. coli* BL21(DE3) cells were used and NbBcII10 was used as a model protein. Unfortunately, even after enrichment by means of chitin beads, the periplasmic extract did not contain any NbBcII10-intein-CBD, as shown by SDS-page. A pelB-NbBcII10-intein-CBD complex containing two stop codons between the pelB-NbBcII10 gene and the intein gene was included as a positive control. In this way, only pelB-NbBcII10 was expressed and transported to the periplasm. When using this construct, NbBcII10 was clearly present in the periplasmic extract, indicating that the intein-CBD part prevents the transport of the NbBcII10-intein-CBD fusion protein to the periplasm.

To overcome this issue, the *E. coli* Lemo21(DE3) cell line was included in this study. These cells allow a precise control of the T7 RNA polymerase activity by means of its natural inhibitor, T7 lysozyme, which will prevent the formation of inclusion bodies, which can have a toxic effect on the cells and results in a better regulation of the expression. In addition, two other constructs incorporating the SRP-pathway targeting signal sequences DsbA and TolB were evaluated. Unfortunately, similar results were found as when using BL21DE3 cells, raising questions regarding the need of periplasmic extraction of the Nb-intein-CBD complex. Periplasmic extraction also has some disadvantages such as a lower protein yield, more time consuming expression and formation of inclusion bodies. As a solution for these drawbacks, more and more research is performed regarding cytoplasmic expression and extraction of nanobodies. An excellent cell candidate for such application are *E. coli* SHuffle®T7 cells. SHuffle®T7 cells express a chromosomal copy of the DsbC-chaperone which isomerizes misoxidized proteins to their native state. To promote the correct protein folding even more, an additional spacer peptide was added between the NbBcII10 and the intein, containing the three amino acids leucine (L), glutamine (E) and tyrosine (Y). After expression, the NbBcII10-LEY-intein-CBD fusion protein was treated with the same thiol-based bifunctional linker as in the previous experiment using the same EPL protocol (including the use of MESNA). The final reaction yield after EPL was 3.5 mg/L culture. The successful alkynation of NbBcII10 was not only demonstrated by western blotting but also by a very clear peak on MS. The clickability was established using western blotting after a click reaction with biotin-azide. The main concern after cytoplasmic extraction of a Nb complex is the loss of binding activity of the Nb towards its antigen, which was evaluated by two different techniques. First, the affinity of NbBcII10-LEY-alkyne for its antigen BcII was evaluated in a competitive enzyme-linked immunosorbent assay (ELISA), showing a decrease in the amount of bound wild type NbBcII10-His$_6$ after adding an increasing concentration of the NbBcII10-LEY-alkyne. In order to obtain a more quantitative result for the binding activity of NbBcII10-LEY-alkyne, SPR was performed. The dissociation equilibrium constant (K_D) of the binding between NbBcII10-LEY-alkyne and BcII was compared with the K_D value of the binding between NbBcII10-His$_6$ and BcII. An additional control containing dimerized NbBcII10-HLC was included to evaluate the effect of dimerization, which is also expected in the NbBcII10-LEY-alkyne due to the additional thiol that is introduced during EPL. An improvement of the K_D value for the NbBcII10-LEY-alkyne recognition of BcII in comparison to the non-modified NbBcII10-His$_6$ was established, caused by a 10-fold decrease in the k_{off}-value for NbBcII10-LEY-alkyne. The same change in k_{off} was observed for the dimerized NbBcII10-HLC (meaning that NbBcII10-LEY-alkyne spontaneously dimerizes). When comparing the sensograms, NbBcII10-LEY-alkyne and NbBcII10-HLC have a similar pattern with an improved k_{off} in comparison with NbBcII10-His_6. Therefore, it is concluded that neither the cytoplasmic extraction nor the site-specific alkynation of the NbBcII10-LEY had an effect on the association rate constant relative to the native Nb.

6.4 Future perspectives

In the field of biosensing, nanobodies are very interesting proteins due to their small size (order 15 kDa) and stability. In this dissertation, NbBcII10 was used as a model Nb but the discussed techniques can also be applied for nanobodies in general. This results in a large panel of possible applications, not only for diagnostic purposes such as biosensing or imaging, but also for therapeutic applications like immunotherapy and targeted drug delivery. Furthermore, the click coupling optimizations obtained for MBP will also be valid for the coupling of other proteins, other than nanobodies.

In this thesis, a bifunctional linker was successfully synthesized that contains a thiol function as well as an alkyne functionality. By synthesizing other bifunctional linkers, it is possible to site-specifically functionalize nanobodies with other bioorthogonal functionalities. In this way, nanobodies can be coupled to substrates using other (copper-free) click chemistries, such as the strain-promoted alkyne-azide cycloaddition (SPAAC) or the strain-promoted inverse-electron-demand Diels-Alder cycloaddition (SPIEDAC), for e.g. *in vivo* applications.
In the past, nanobodies were mainly expressed in the periplasm. In this thesis we demonstrated that cytoplasmic expressed and extracted NbBcII10, using *Escherichia coli* SHuffle®T7 cells, still has the same target binding activity, and so folding of the active site region, as compared to periplasmic extracted NbBcII10. By using a cytoplasmic expression, a higher yield can be established. The number of studies reporting cytoplasmic expression of nanobodies also substantially increased since the start of this thesis, which means that the original concept of so-called indispensable periplasmic extraction may not always be necessary, and thus could lead to significant progress in nanobody research.

Summary

Nowadays, bioactive materials are mainly produced by the biofunctionalization of substrates based on non-specific coupling of proteins. The consequence of this approach is that due to the random orientation and the potentially associated structure disruption, part of the proteins will have an inaccessible active site. This has a negative effect on the sensitivity, selectivity and reproducibility of the final bioactive device. Site-specific modification of proteins circumvents these issues. This thesis describes the use of expressed protein ligation (EPL) as a protein engineering technique for the site-specific alkynation of maltose binding protein (MBP) and nanobody BcII10 (NbBcII10). The C-terminally attached alkyne functionality can then be further used for copper (I)-catalyzed azide alkyne cycloaddition click chemistry.

First, the site-specific alkynation of MBP was investigated as a proof of concept. Site-specific alkynation by means of EPL, requires a bifunctional linker that contains an alkyne group and a nucleophile that is able to react with the thioester function that is formed during the EPL process. As a bifunctional linker, 2-amino-3-mercapto-N-(prop-2-yn-1-yl)propanamide was synthesized containing an alkyne and thiol functionality. Using this linker, site-specifically alkynated MBP was produced with a yield of almost 22 mg/L culture. The presence of the alkyne functionality was successfully demonstrated by means of western blotting. In addition to the site-specific alkynation, random alkynation was also performed. For both alkynated MBP variants, the clickability was evaluated using *in situ* ellipsometry. Two different coupling protocols were investigated: the DIP method, where a silicon surface is submerged in a protein solution, and the DROP method where only one drop of protein solution is used for the functionalization of the surface. Both protocols resulted in the coupling of a reasonable amount of alkynated MBP to the surface, for both the site-specifically alkynated and the randomly alkynated MBP. By means of the the DROP method, combined with a high concentration of sodium ascorbate, THPTA and copper catalyst, site-specifically alkynated MBP was coupled in an oriented way with a minimum of protein waste resulting in a very cost-efficient immobilization protocol.

A disadvantage of using thiol-based bifunctional linkers, like 2-amino-3-mercapto-N-(prop-2-yn-1-yl)propanamide, is the subsequent introduction of a free thiol into the protein. This free thiol can cause unwanted side reactions, e.g. interference with endogenous cysteines and formation of disulphide bridges to form dimers. In this thesis, the synthesis and use of an amine-based bifunctional linker, 2-hydrazinyl-N-(prop-2-yn-1-yl)acetamide, was investigated for the site-specific alkynation of MBP. In this way the free thiol can be avoided. The first results, after a click reaction in solution with azide functionalized biotin were very promising and proved the clickability of MBP that was alkynated using the amine-based bifunctional linker. Nevertheless, ESI-MS showed that the main part consisted of hydrolyzed MBP instead of alkynated MBP. In other words, only a very minor part of the protein solution was actually alkynated. Attempts in protocol optimization did not result in an increase of the amount of alkynated MBP. The method was also evaluated on another protein, namely nanobody BcII10 (NbBcII10), but the results were similar.

The main goal of this thesis research was the site-specific modification of nanobodies, in particular NbBcII10. In general, nanobodies are expressed in the periplasm of *E.coli*. The periplasm has an oxidizing environment, which enables a correct protein folding. EPL constructs are generally expressed in the cytoplasm. In this thesis, various strategies for the periplasmic expression of EPL constructs were assessed. Therefore, several constructs were developed containing different leader sequences for periplasmic transport using two different pathways, i.e. the Sec pathway (leader sequences pelB, OmpA, OmpF and malE) and the SRP pathway (leader sequences DsbA and TolB). The constructs were expressed in *E. coli* BL21(DE3) and *E. coli* Lemo21(DE3) but even after enrichment of the protein extract, the expressed intein protein complex (NbBcII10-intein-CBD) could not be found in the periplasmic extract. As an alternative for periplasmic extraction, cytoplasmic expression and extraction was evaluated by using SHuffle®T7 cells and the addition of a small peptide spacer (LEY) at the C-terminus of the Nb, both of which promote a correct protein folding in the cytoplasm. ELISA and SPR experiments showed that fully functional NbBcII10-LEY-alkyne was produced through cytoplasmic expression and alkynation by EPL. This demonstrates that periplasmic extraction is not (always) a must for nanobodies to become/remain active (correctly folded) after expression and that post-translational alkynation by EPL does not influence the binding activity of the NbBcII10.

Finally, by strategic design of the bifunctional linker, every possible ‘click’ group can in principle be site-specifically attached to proteins. By doing this, a site-specifically modified protein can be coupled in a covalent and oriented way in order to improve the accessibility of the protein’s active region.

Samenvatting

Nog steeds worden bioactieve materialen voornamelijk geproduceerd door het biofunctionaliseren van substraten aan de hand van een niet-specifieke eiwit koppeling. Het gevolg van deze aanpak is een willekeurige oriëntatie en een potentiële structurele beschadiging van (delen van) het eiwit met een onbereikbare of niet-functionele actieve plaats als gevolg. Dit heeft een negatief effect op de sensitiviteit, selectiviteit en reproduceerbaarheid van de finale applicatie. Plaatsspecifieke modificatie van eiwitten kan deze problemen voorkomen. Deze thesis beschrijft het gebruik van de "expressed protein ligation" (EPL) methode als een eiwit modificatie techniek voor de plaatsspecifieke alkynering van "maltose binding protein" (MBP) en het nanobody BcII10 (NbBcII10). De C-terminaal gekoppelde alkyn functionaliteit kan dan vervolgens gebruikt worden in klik chemie, nl. voor koper(I) gekatalyseerde azide alkyn cycloadditie reacties.

Ter illustratie van bovengenoemd concept werd eerst de plaatsspecifieke alkynering van MBP onderzocht. Plaatsspecifieke alkynering met behulp van EPL vereist een bifunctionele linker die een alkyn groep en een nucleofiel bevat. Het nucleofiel kan dan reageren met de thioester functie die wordt gevormd tijdens het EPL proces. Als bifunctionele linker werd 2-amino-3-mercapto-N-(prop-2-yn-1-yl)propanamide gesynthetiseerd.

Door gebruik te maken van deze linker werd plaatsspecifiek gealkyneerd MBP via EPL geproduceerd met een opbrengst van 22 mg/L cultuur. De aanwezigheid van de alkyn functionaliteit werd succesvol aangetoond door middel van western blotting. Daarnaast werd ook willekeurig gealkyneerd MBP aangemaakt. Voor beide gealkyneerde MBP varianten werd de klikbaarheid geëvalueerd door middel van *in situ* ellipsometrie. Twee verschillende koppelingsprotocols werden onderzocht: de DIP methode waarbij het silicium substraat wordt ondergedompeld in een eiwitoplossing en de DROP methode waarbij slechts één druppel van de eiwitoplossing wordt gebruikt voor de functionalisatie van het oppervlak. Beide protocols resulteren in de covalente koppeling van een redelijke hoeveelheid gealkyneerd MBP aan het oppervlak voor zowel het plaatsspecifiek gealkyneerd als het willekeurig gealkyneerd MBP. Door gebruik te maken van de DROP methode, gecombineerd met een hoge concentratie van natriumascorbaat, THPTA en een koper katalysator, werd plaatsspecifiek gealkyneerd MBP op een georiënteerde manier gekoppeld met een minimum aan eiwitverlies resulterend in een zeer kostenefficiënte immobilisatie procedure.

Een nadeel van thiol-gebaseerde bifunctionele linkers zoals 2-amino-3-mercapto-N-(prop-2-yn-1-yl)propanamide is de introductie van een vrije thiol functie in het eiwit. Dit vrije thiol kan ongevraagde nevenreacties veroorzaken zoals interferentie met thiol groepen van endogene cysteines, de vorming van disulfide bruggen en dimeren. In deze thesis werd de synthese en het gebruik van de amine-gebaseerde bifunctionele linker 2-hydrazinyl-N-(prop-2-yn-1-yl)acetamide onderzocht voor de plaatsspecifieke alkynering van MBP. Op deze manier wordt de aanwezigheid van een vrije thiol na de alkynering voorkomen. De eerste resultaten van een klikreactie in oplossing met azide gefunctionaliseerd biotine waren veelbelovend en bewezen de klikbaarheid van MBP dat gealkyneerd werd door gebruik te maken van de amine-gebaseerde bifunctionele linker. Desalniettemin, toonde ESI-MS aan dat het grootste deel van het MBP gehydrolyseerd was in plaats van gealkyneerd. Met andere woorden, slechts een kleine fractie van de eiwitoplossing was daadwerkelijk gealkyneerd. Pogingen tot optimalisatie van de procedure resulteerde niet in een stijging van de hoeveelheid gealkyneerd MBP in de eiwitoplossing. Deze methodes werden eveneens geëvalueerd met een ander eiwit, het nanobody BcII10 (NbBcII10), maar de resultaten waren vergelijkbaar.

De voornaamste doelstelling van het onderzoek in deze thesis was de plaatsspecifieke modificatie van nanobodies, in het bijzonder NbBcII10. In het algemeen worden nanobodies gevouwen in en geëxtraheerd vanuit het periplasma van *E. coli*. Het periplasma heeft een oxiderende omgeving die een correcte eiwitvouwing mogelijk maakt. EPL constructen echter, worden normaal in het cytoplasma tot expressie gebracht en geëxtraheerd uit het cytoplasma. In deze thesis werden verschillende strategieën voor de periplasmatische expressie van EPL constructen onderzocht. Hiertoe werden meerdere constructen ontwikkeld die verschillende signaalsequenties bevatten voor periplasmatisch transport gebruikmakend van 2 pathways, namelijk de SEC pathway (signaalsequenties pelB, OmpA, OmpF and malE) en de SRP pathway (signaalsequenties DsbA and TolB). De constructen werden tot expressie gebracht in *E. coli* BL21(DE3) en *E. coli* Lemo21(DE3) maar zelfs na opzuivering van het eiwitextract, met behulp van chitine, werd het NbBcII10-inteine-CBD complex niet terug gevonden in het periplasmatisch extract. Als alternatief voor de periplasmatische extractie werd de cytoplasmatische expressie en extractie onderzocht. Hierbij werd gebruik gemaakt van SHuffle®T7 cellen en een kort LEY peptide fragment tussen de C-terminus van het nanobody en de alkyn linker, beide ter promotie van een correcte eiwitvouwing. ELISA en SPR experimenten toonden aan dat volledig functioneel NbBcII10-LEY-alkyn kon aangemaakt worden door een cytoplasmatische expressie, alkynering via EPL en extractie. Dit toont aan dat een periplasmatische extractie niet altijd een must is voor nanobodies om actief te blijven na expressie en dat post-translationele alkynering via EPL geen invloed heeft op de bindingsactiviteit van het NbBcII10.

Door het strategisch designen van de bifunctionele linker kan in principe elke mogelijke klik functie plaatsspecifiek op het eiwit gebonden worden. Door dit te doen kan het plaatsspecifiek gemodificeerd eiwit covalent en georiënteerd gekoppeld worden om op die manier de bereikbaarheid van de actieve regio te optimaliseren.

Publication list & conference contributions

Journal contributions

Steen Redeker E, Ta DT, Cortens D, **Billen B**, Guedens W, Adriaensens P. Protein Engineering For Directed Immobilization. Bioconjugate Chemistry. 2013;24(11):1761-77. (IF: 4.821)

Ta DT, Steen Redeker E, **Billen B**, Reekmans G, Sikulu J, Noben J, Guedens W, Adriaensens P. An efficient protocol towards site-specifically clickable nanobodies in high yield: cytoplasmic expression in Escherichia coli combined with intein-mediated protein ligation. Protein Engineering Design and Selection 2015;28(10): 351-363. (IF: 2.364)

Vranken T, Steen Redeker E, Miszta A, **Billen B**, Hermens W, de Laat B, Adriaensens P, Guedens W, Cleij T. In situ monitoring and optimization of CuAAC-mediated protein functionalization of biosurfaces. Sens Actuators B Chem. 2017;238:992-1000. (IF: 5.07)

Billen B, Vincke C, Hansen R, Devoogdt N, Muyldermans S, Adriaensens P, Guedens W. Cytoplasmic versus periplasmic expression of site-specifically and bioorthogonally functionalized nanobodies using expressed protein ligation. Protein Expression Purif. 2017;133:25-34. (IF:1.351)

Conferences with oral presentation

Billen B, Vranken T, Reekmans G, Steen Redeker E, Adriaensens P and Guedens W. Site-specific modification of maltose binding protein as a model for advanced biomaterials – Advanced Materials for Biomedical Applications (AMBA) 2014 – Gent

Conferences with poster presentation

Hydrazine-based expressed protein ligation for site-specific modification of maltose binding protein - **Billen B**, Vranken T, Reekmans G, Steen Redeker E, Adriaensens P and Guedens W – EnFi 2013, Hasselt

In vitro site-specific functionalization of proteins for advanced bioactive materials - **Billen B**, Reekmans G, Steen Redeker E, Adriaensens P and Guedens W – Chemcys 2014, Blankenberge

Hydrazine-based expressed protein ligation as a tool for the synthesis of site-specifically modified proteins, the building blocks towards advanced biomaterials - **Billen B**, Vranken T, Reekmans G, Steen Redeker E, Adriaensens P and Guedens W – IAP 2014 – Louvain-la-Neuve

Maltose binding protein as a model for site-specific modification by hydrazine-based expressed protein ligation for advanced biomaterials - **Billen B**, Vranken T, Reekmans G, Steen Redeker E, Adriaensens P and Guedens W – Biomedica 2014 – Maastricht (**Best poster presentation award**, **category: biomaterials)**

Dankwoord

Hier zitten we dan, op een druilerige zaterdagnamiddag even te reflecteren over mijn voorbije 11 jaar op de UHasselt. Na 6 jaar studeren (ja, dat eerste jaar was nu niet bepaald een succes te noemen) moest de beslissing genomen worden: gaan ik een job zoeken of ga ik een doctoraat starten. En als ik een doctoraat ga starten, welke richting ga ik dan uit? Ik heb biomedische wetenschappen gestudeerd maar die chemie stages hebben me toch meer zin gegeven in een chemie doctoraat. Dus, bedankt Hanne, Rafaël, Ans & Thomas om de chemie microbe aan mij door te geven!

En dan kom je op een dag een warrige Hollander op de gang tegen, beter gekend als Erik, die een geweldige combinatie van beide doet in zijn labo. Het duurde dan ook niet lang voor ik verkocht was en de beslissing nam om te solliciteren bij de BDG groep. Dus bij deze, Erik, bedankt om mij het licht te laten zien en de keuze wat eenvoudiger te maken. Ik moest thuis ook al jaren aanhoren: “uw broers zijn kinesist en verpleger, zou gij geen dokter worden dan hebben we alles in huis”. Ok, “not that kind of doctor” maar mama en papa, jullie zullen het er mee moeten doen :-) ! Mama, papa, Robbie & Maarten, bedankt voor alle steun.

1 augustus 2012 was het dan zo ver, mijn eerste dag bij de BDG groep. Aangezien ik toch al enige tijd in de chemie gangen rondspookte, en al heel wat was gaan stelen in het BDG lab tijdens mijn stage bij de PNB had ik mijn weg snel gevonden. Bedankt Erik & David om mij zo goed op te vangen. Er is hard gewerkt, maar verdomme toch ook veel gelachen! Niet lang erna vervoegde ook Tien ons dus ik was niet langer de enige nieuwe met de domme vragen. Nu, Erik & David, maar 1 zinnetje in mijn dankwoord aan jullie spenderen zou wat triestig zijn, bij deze zijn het er dus 2 :-) Een onderzoeksgroep is natuurlijk altijd een komen en gaan, en het enthousiasme wel groot toen we er zelfs een vrouw bij kregen. Wel eentje met meer ballen dan wij allemaal samen maar de BDG was niet langer een mannenclubje. Ik hoor Wanda het zo nog zeggen: nu er een vrouw in het lab bij komt gaat het zeker wat properder en opgeruimder zijn. Ik vrees dat ze op die woorden toch is moeten terug komen, nietwaar Rebekkka :-) ? Niet veel later hebben we afscheid moeten nemen van onze – weet ook echt alles – Erik. Een grote shock voor het BDG labo, maar Erik ging terug naar eigen land :-). En last but not least, op het einde van mijn rit kwam ook Sofie er nog bij. Na een jaar stage hebben we haar toch kunnen overtuigen om te blijven!

Ook een dikke merci aan alle andere doctoraatsstudenten van chemie. Het zijn er te veel om op te noemen, maar bedankt voor de leutige lunchpauzes en de “speciale” ervaringen op de congressen. Ook een speciale merci aan Hanne, ze was niet enkel tijdens mijn stage mijn steun en toeverlaat maar ook achteraf heb ik uren op haar bureau lopen klagen over mislukkende experimenten. De “mama van de bende” klinkt misschien een beetje oud, maar je was toch een leuke buurvrouw op onze gang :-) !

Doorheen de jaren zijn er ook nog heel wat stagairs gepasseerd. Eerst de korte stages, de ene al wat succesvoller dan de andere, maar toch hartelijk dank aan Jolien, Joeri, Richeek, Ardit, Wouter(ke). Altijd leuk om te zien dat jullie allemaal op jullie pootjes terecht gekomen zijn! Wel wat raar als je dan enkele jaren laten op een sollicitatiegesprek zit en een van je oude stagairs komt al wuivend aan het raam van de vergaderzaal voorbij waar je de ziel uit je lijf aan het zweten bent van de zenuwen. Maar Jolien, wel super dan we nu ook weer collega's zijn! Sommige stages duurden wat langer, bedankt Sander om mij (bijna) een volledig academiejaar te komen vergezellen. Ik weet dat het niet altijd makkelijk was, een stage waarin zo ongeveer niks heeft gewerkt zoals we het gehoopt hadden, maar ik hoop toch dat je er iets van geleerd hebt. Het feit dat je de R&D vaarwel gezegd hebt na je stage zal er wel iets mee te maken gehad hebben zeker ;-).

Je kan natuurlijk geen interdisciplinair onderzoek doen zonder af en toe eens naar een ander lab te trekken. Eerst en vooral, Tom en zijn ellipsometer. Uren hebben we aan dat ding doorgebracht, en nooit deed het wat we verwachtten. Het heeft dan ook veel tijd, geduld, en Si plaatjes gekost voor we hadden wat we wilden maar een van de hoofdstukken van deze thesis was toch nooit kunnen gebeuren zonder u. Dus Tom, een dikke merci, en niet alleen voor uwe onnozele zever over uw katten ;-) Ook Gunther, ook al had je de BGD groep vaarwel gezegd, onze "vroeg in de ochtend" en "laat in de avond" gesprekken hebben mij enorm geholpen. Je had nooit veel tijd, maar elk minuut info die ik uit je kon halen was waardevol. We hebben samen veel tijd doorgebracht om je oude nota's te ontcijferen en je SPR kennis op mijn bizarre resultaten los te laten. Daarbovenop ben je ook nog een fantastisch goeie mens en een voorbeeld voor vele wetenschappers! Twee mensen om zeker ook nooit te vergeten zijn Erik en Jean-Paul. Ook met deze fantastische mannen heb ik uren doorgebracht aan de MS, om dan meestal teleur gesteld te worden dat het toch niet was wat ik verwachtte te zien op deze spectra. Uren hebben we boven de spectra gehangen, 1000den keren in ons haar gekrabd maar uiteindelijk is het dan toch ongeveer allemaal goed gekomen. Ook mijn eerste SPR ervaringen waren op biomed, bedankt Luc en Baharak voor de goede zorgen daar. De toppertjes van de SPR bevonden zich echter een treinritje verder (als die treinen al reden, "dankjewel" NMBS) aan de VUB. Bedankt Cecile, Ema & Serge voor jullie hulp en expertise! Ook iedereen van didactiek, Gène, Hilde & Iris, bedankt voor het uitlenen van al het materiaal en het niet te fel klagen als ik weer eens in de weg liep omdat ik een zuurkast nodig heb.

En natuurlijk ook niet te vergeten, Peter & Wanda, bedankt voor de kans die jullie mij gegeven hebben en jullie kritisch blik op mijn onderzoek. Op deze manier hebben we toch het beste er kunnen uithalen! Ook mijn oprechte dank aan alle leden van de jury en doctoraatscommissie voor hun kritische blik op deze thesis.

Verder ook nog hartelijk dank aan iedereen van UgenTec. Het afgelopen jaar hebben jullie veel naar mijn gezaag over mijn doctoraat moeten luisteren, mijn slecht humeur moeten verdragen als ik weer avonden aan het verbeteren was geweest, of als weer eens niet alles ging zoals ik het wou. Bedankt om dit allemaal te verdragen, en om mij te steunen in deze laatste fase van mijn doctoraat.

Maar dan, last but not least, mijn allerliefste vrouwtje en moeder van onze topper Sepp, bedankt Petra (a.k.a. jappel, liefje, vrouw, …). Jou steun start al van in het begin van onze studententijd. Jij, de beste van de klas, ik …. (daar gaan we over zwijgen). Je hebt me altijd gesteund en er door getrokken in de moeilijke tijden, zowel tijdens mijn studies als tijdens mijn doctoraat. Ik wil de uren niet optellen dat ik tegen jou heb lopen klagen (en dan besefte je meestal dat jou onderzoek nog zo slecht niet gaat :-p). Samen hebben we in die periode ook nog eens een fantastisch huis gebouwd en dat was allemaal nooit gelukt als wij elkaar niet zo goed begrepen. Tot de laatste dag van mijn thesis heb je me gesteund, geholpen en 100den pagina’s nagelezen van onderzoek waar je zelf niets van snapte. Je bent zelfs gaan ruzie maken met de man van de drukkerij toen mijn thesis er niet op tijd was. Die man slaapt er nog slecht van… Dat zouden er niet veel je nadoen dus 1000x bedankt en ik zie je graag!